

NASA Contractor Report 175035

Influence of Large-Scale Motion on Turbulent Transport for Confined Coaxial Jets

Volume I—Analytical Analysis of the Experimental Data Using Conditional Sampling

N86-20395

(NASA-CR-175035) INFLUENCE OF LARGE-SCALE MOTION ON TURBULENT TRANSPORT FOR CONFINED COAXIAL JETS. VOLUME 1: ANALYTICAL ANALYSIS OF THE EXPERIMENTAL DATA USING CONDITIONAL SAMPLING Final (Connecticut

Unclas
G3/07 05601

David C. Brondum and John C. Bennett

*The University of Connecticut
Storrs, Connecticut*

January 1986



Prepared for
Lewis Research Center
Under Grant NAG 3-350



TABLE OF CONTENTS

<u>Title</u>	<u>Page</u>
Nomenclature.....	iii
INTRODUCTION.....	1
BACKGROUND.....	7
ANALYSIS.....	12
RESULTS.....	19
CONCLUSION.....	29
TABLES.....	32
ILLUSTRATIONS.....	33
REFERENCES.....	90
APPENDIX A: Computer Program Listings.....	93
APPENDIX B: Conditional Sampling Results.....	98

NOMENCLATURE

f = local fraction of inner jet fluid (ie., concentration)

k = turbulence energy [m^2/s^2]

m = mass flow rate [kg/s]

r = radius (mm)

R_0 = radius of sudden expansion (mm)

u = axial velocity (m/s)

v = radial velocity (m/s)

w = azimuthal velocity (m/s)

z = streamwise coordinate (mm)

ϵ = dissipation rate of turbulence [m^2/s^3]

ν_m = eddy diffusivity

Superscripts

$\bar{}$ = mean quantity

\prime = fluctuating quantity

PRECEDING PAGE BLANK NOT FILMED

INTRODUCTION

The outlet flow for a combustion chamber is determined by the complex pattern of the flow field through it. In order to perform parametric studies on the flow, it is necessary to have an accurate simulation program for prediction of the combustion process. Since combustors of practical interest are highly turbulent, understanding turbulent transport in this type of flow is critical to the development of computational procedures to be used in these simulations.

Modern combustion chambers typically have an annular configuration with fuel in a fine spray form being mixed into the airstream. This mixture is achieved with an array of fuel nozzles which ensure uniform fuel spray distribution. These nozzles may be of the swirl or non-swirl type, although the swirl type is usually used to promote rapid burning. The fuel-air mixture is burned in the combustion chamber and the resulting gases are delivered to the turbine inlet. A stabilized flame in the combustion process is necessary to achieve uniform burning, resulting in a desirable temperature profile at the turbine inlet (pattern factor). Other important parameters in the combustion process include burning length (flameout), noise production, pollutant emissions (reactant products), and engine performance (combustion efficiency).

Computational procedures for predicting the combustion process are being developed and improved by numerous researchers (1,2,3,). These procedures predict the velocity, species, temperature, and reaction rate distribution within the combustors which in turn are

used to calculate the previously named parameters. Because of the turbulent nature of the flow, mathematical models are used for the turbulent transport of mass (species), momentum, and heat. The data used to develop and verify these models have in the past been restricted to velocity and momentum transport measurements. Methods used prior to the mid-nineteen seventies for acquiring turbulent mass and momentum transport data have been indirect, requiring compromising assumptions or probes unsuitable for recirculating flows. Bennett & Johnson (4) have used new optical techniques to simultaneously measure a scalar quantity (mass) and velocity, and therefore mass transport.

Morganthaler (5) performed an

"assessment of the relative importance of turbulent mass, momentum, and energy transport, so that emphasis for the future could be directed to modeling the critical processes rather than merely continuing the historical trend of modelling turbulent momentum transport."

His results point out a critical need for the future in that

"turbulent transport of mass was demonstrated to be far more significant than the transport of either energy or momentum for a coaxial hydrogen jet reacting with an external high temperature air stream."

In order to provide an adequate data base for verifying computational procedures used for modeling mass transport, Bennett & Johnson (6) used laser velocimetry (LV) to obtain velocity measurements while simultaneously using laser-induced fluorescence

(LIF) to obtain concentration data for a coaxial jet geometry. In a companion paper, Syed & Sturgess (7) used the data of Bennett & Johnson for comparison with computational methods currently in use. While finding qualitative agreement of all variables, there were some significant quantitative discrepancies. Among their conclusions was that "prediction of mean quantities alone is not a sufficiently strict criterion" for evaluating the success of a turbulence model, but that "it is necessary to examine also the agreement obtained for fluctuating quantities and their cross correlations" (i.e., mass flux).

It should be pointed out that some of the difficulty encountered in accurately predicting the flow can be attributed to the lack of a set of good initial conditions. Another limiting factor - possibly the dominant one in certain situations - is the incomplete understanding of the mechanisms involved in the flow. One such mechanism is the influence of the large-scale motion on the turbulent transport. The understanding of this influence is the main thrust of this research effort.

Other comparison studies of turbulent flow in a coaxial jet have been done by Habib & Whitelaw, including experimental data obtained using hot wires (8) and using LV (9). In each study, the largest discrepancies were in the upstream region where the flow is developing and recirculation zones occur. They concluded that these errors were "associated with the inadequacy of the eddy-viscosity hypothesis." Again it is seen that a better understanding of the mechanisms involved is needed to improve the computational procedures currently in use.

The experimental efforts of Bennett & Johnson have also continued and produced some interesting results (10) which in some cases are contradictory to traditional thinking. Complete details of the experiments and data are found in the final NASA contractor reports of Bennett & Johnson (11) for a non-swirling flow and Roback & Johnson (12) for a swirling flow. These works were done on a coaxial jet configuration using water in both jets and fluorescein dye as a trace element. Bennett & Johnson show two distinct shear regions for the non-swirling flow (fig. 1a); one between the inner and annular jets and one between the annular jet and the recirculation region. The innermost shear layer develops as the annular fluid gradually fills the center jet, resulting in what has been called counter-gradient transport. Computational procedures for evaluating scalar (concentration) gradient and a transport diffusion coefficient, ϵ_m defined by

$$m = - \epsilon_m \left(\frac{\partial f}{\partial x} \right)$$

In many turbulent flows the scalar transport does not follow such a simple dimensional model and the traditional approach does not work.

The swirling flow results of Roback & Johnson (12) show a flow field (Fig. 1b) similar to that for the non-swirling case. they found a large eddy shear region between the inner and annular jets and one between the annular jet and outer recirculation zone. Unlike the non-swirling flow however, they found a large recirculation region on the centerline which gave the flow some different characteristics.

The multiple scale results of Bennett & Johnson are an example of a situation for which this simple gradient model is inadequate. Figure 2 shows regions of the flow field where this is the case. This region is qualitatively similar to the region where the inner jet fluid is being accelerated by the annular jet, although it is somewhat more extensive. Bennett & Johnson hypothesized that this was due to "response time or distance required to change the character of the turbulent structure". Another interesting finding was that the peak absolute values of the axial mass transport rates were higher than the values for the radial transport even though the peak radial concentration gradients were more than ten times the axial concentration gradients.

Observation of the concentration signal during the experiments showed much large-scale flow intermittency with the developing portion of the flow field. At axial locations within the upstream region (where the flow is developing), there were large-scale fluctuations in the signal: they were either negative (indicating a slug of annular jet fluid) or positive (suggesting a slug of inner jet fluid). No immediately recognizable periodicity in the occurrence of these fluctuations was found and no local peaks in the concentration autocorrelations were identified. It was believed that these excursions did identify the presence of a large-scale motion within the region.

This later work of Bennett & Johnson gives some justification for studying the influence of the large-scale motion on the turbulent transport. The comparisons of Syed & Sturgess, as well as Habib & Whitelaw, also support this in that, for both studies,

the region of greatest discrepancy is the upstream region where the flow is developing. Since this region is known to include large-scale motion, it seems reasonable to investigate the effects of that motion on the flow.

In addition, Schetz (13) has reviewed the mixing flows in terms of both experimental results and the implications for turbulence modeling. One of his basic conclusions was that large-scale structures are an essential aspect of future experimental and modeling studies for a wide variety of flows. Mathiew & Jeandel (14) point out that the large interacting eddies can have a time scale quite different from the dissipative time scale associated with the fine structure portion of the flow. Launder (15) has introduced multiple time scale models, chosen to give the best predictions. These scales could be chosen more appropriately from experimental data directly if the role of the large scale were identified. Finally Borghi (16) questions the importance of large coherent structures in combusting flow. His conclusion is that, for the upstream region, the numerical predictions are not close to observed data because either large structures or the redistribution of kinetic energy is badly calculated.

In summary, for the confined coaxial jet, the presence of large-scale structures has been identified in the region where computational predictions have shown to be least effective. Several researchers have hypothesized that the large-scale structures may be the source of these discrepancies. With this in mind, this study was undertaken to identify a way of detecting these structures and to determine the influence they have on the turbulent transport of the flow.

BACKGROUND

The notion of large-scale coherent structures in turbulent flow is not a new one. Several authors - including Roshko (17), Cantwell (18), and Davies & Yule (19) - have summarized many of the developments in this area. A starting point in any discussion must be a clear definition of the subject. Yule (20) defines coherent structures as large eddies which, (i) are repetitive in structure, (ii) remain coherent for distances downstream very much greater than their length scales, and (iii) contribute greatly to the properties of turbulence, in particular, turbulent energy and shear stress, entrainment and mixing.

The experimental work of Brown & Roshko (21) is considered classic in the study of large-scale motion in turbulent mixing layers. Their efforts (fig. 3) revealed the "presence of well-defined large structures", with the Reynolds number varying from a low value with no visible fine-scale turbulence to a higher value where it does exist. The significant point is that in each case "the measured mean properties of the flow, the velocity and density profiles, spreading rate, etc. are the same". They concluded that the "mean flow is controlled by the large organized structures which, it may be seen, are not affected by the small-scale turbulence appearing at the higher values of Reynolds number."

By observing the movement of the structures, Brown & Roshko (21) found that their spacing and diameter increased with increasing downstream distance. The large-scale structures move

at nearly constant streamwise velocity (equal to the mean flow velocity) which is independent of their size and location. Brown & Roshko conclude that they amalgamate into larger structures as they convect downstream. Winant & Browand (22) observed fluid rolling up into "discrete two-dimensional vortical structures" which periodically "interact by rolling around each other" eventually forming one larger vortex. Finally, Dimotakis & Brown (23) found similar large-scale coherent structures at a high Reynolds number (3×10^6). Their flow visualization study showed that these structures did exist and "appear to dominate in determining the overall characteristics of such flows".

Blackwelder & Kaplan (24) studied bursting in a turbulent boundary layer. They observed, using flow visualization, "a high degree of coherence over a considerable area in the direction normal to the wall", and found that bursts were associated with a high degree of velocity fluctuation. Their conditional averaging process showed the coherent structures to have turbulent transport properties an order of magnitude greater than the overall flow. This is in agreement with the work of Lu & Willmarth (25) who found large contributions to the turbulent transport from the coherent structures. Boundary layer flows have been studied more than any other type and are probably the best understood in terms of coherent structures. It is useful to apply this knowledge in developing a better understanding of other flows.

The experimental work of Bennett & Johnson (11) for non-swirling flow and Roback & Johnson (12) for swirling flow is the basis for the present study. The configuration they chose was a confined coaxial jet with a sudden expansion, a meaningful yet

geometrically simple case. It simulates the two-stream inlet and the diffuser (sudden expansion) similar to flow in combustors. Water was chosen for the experiments; the resultant capability for injecting dye into either stream was utilized for flow visualization and mass transport studies. The use of water limits the simulation in that it eliminates combustion and multiple species as variables to be considered. Water also reduces the effect of molecular diffusion to a negligible level. These limitations still resulted in a set of results useful in evaluating combustor design calculation codes; before the addition of combustion, the codes should be expected to accurately predict this more limited flow. To create this data base for comparison with models, the emphasis was on statistically repeatable data collection. As the emphasis was not on large-scale structures (i.e., conditional sampling), this limits the data's usefulness in studying large-scale structures somewhat. For example, it is not possible to trace the flow of a particular structure past a measurement location since the data collection rates needed for statistically steady data limit the number of samples within any one structure.

Bennett & Johnson (4, 11) and Roback & Johnson (12) documented the flow fields shown in figure 1a and 1b respectively. The ratios of jet diameters are approximately 0.25 for the inner jet and 0.50 for the annular jet (compared to the pipe diameter). The flow chosen for documentation has Reynolds numbers of 15,900 and 47,500 for the inner and annular streams respectively. These values are within the turbulent flow range and are typical of gas turbine combustors. The data base resulting from these

experiments consists of simultaneous two-component velocity data (u-v, u-w, v-w) and simultaneous concentration-velocity data (u-f, v-f, w-f) at numerous axial and radial locations on the flow field.

The comparison work of Syed & Sturgess (7), which utilized Bennett & Johnson's data base, was done with a two-dimensional k- ϵ model employed in the TEACH computer program. The largest of the discrepancies between experiment and predictions occurred in the upstream region where the flow was developing and included recirculation zones. For fluctuating velocity components, agreement was good qualitatively, but only fair quantitatively. Mean axial velocity profiles were found to be in better agreement. The centerline concentration growth is predicted to occur sooner than experiments indicated, while the subsequent decay is predicted later than found experimentally. Mass flux predictions exhibited similar discrepancies, as did limited momentum transport comparisons.

In the two Habib & Whitelaw studies (8, 9), their data is compared with predictions, again using the two-equation turbulence model in the TEACH code. Using hot-wire data, predictions of mean velocity distributions agreed well with the experimental data in the downstream regions. Shear stress distributions showed good agreement downstream but again had some trouble in the upstream flow developing region. Although the LV measurements in the second study were an improvement over the hot-wire data, errors were still found in the recirculation zone, reinforcing the need for modeling improvements in the prediction of turbulent transport.

In summary then, large-scale structures have been shown to contribute significantly to turbulent transport (at least in boundary layers). In addition, flow regions for which numerical predictions and experimental results differ the most are known to contain large-scale structures. It seems apparent that a better understanding of large-scale structures will be necessary for continued development of prediction methods. The present investigation represents an initial effort in this area for axisymmetric shear layers.

ANALYSIS

This study involved looking at the effects of the large-scale structures on the data collected by Johnson & Bennett (11) and Roback & Johnson (12). These data were used previously to study the overall flow characteristics. The present effort verified the overall properties; but the main thrust was on the large-scale structure properties and their influence on the overall flow.

In order to identify the role of large-scale structures in influencing turbulent transport, it is first necessary to separate these structures from the small-scale turbulent portion of the flow. A detector or trigger for the structure must be selected. Several potential detectors were identified based on other studies, including several done on turbulent boundary layers (24, 26). One possible detector is large velocity fluctuation compared to turbulence intensity, the rationale being that large-scale structures will involve blobs with larger velocity changes than for the overall flow. Another possible detector is concentration fluctuation. The entrainment and vortex pairing phenomena previously discussed led to this idea. Roshko (17) showed data from a concentration probe in a mixing layer where fluid from one stream penetrates deeply into the other stream, resulting in large concentration fluctuations. He states that information about the mixing can be obtained by measuring a scalar property such as temperature, density, or species concentration. The experiments of Bennett & Johnson and Roback & Johnson, previously discussed, also showed these large concentration fluctuations in regions

where the large-scale structures are known to exist.

Concentration fluctuation was chosen as the detector for this study.

The ultimate test of any detector is the completeness of the emerging pattern. Completeness refers in this case to a well-defined pattern, since a detector which yields randomly varying results cannot be a true detector. One way of testing a detector is to plot the relative frequency of each individual detection as a function of position. Relative frequency is the number of occurrences at each location ratioed by the complete set of data at that location. This can help identify the approximate size and most probable location of the large-scale region. These plots were done and will be discussed later.

Another useful plot is the scatter plot where the velocity fluctuation is plotted as a function of the concentration fluctuation or where fluctuation of one velocity component is plotted against the fluctuation of another velocity component. These types of plots help establish the existence of the large scale in the flow and assist in separating these structures from the general low level turbulence. They are also beneficial in determining if the large-scale correlation is significant.

An example of a plot with a zero correlation, shown in Figure 4, has almost all of the data concentrated uniformly near the center. A small amount of data has fairly large negative concentration fluctuations, but are equally distributed among positive and negative velocity fluctuations, yielding a zero correlation. Figure 5 shows data with much more scatter in both directions and a zero correlation. A situation where there is very little concentration fluctuation and very large positive and

negative velocity fluctuations in the flow can be seen in Figure 6. This data is taken in the recirculation zone where flow reversal occurs, but no large-scale motion is apparent. Data taken within the shear layer between the two jets is shown in Figure 7. Here there is much scatter in the data and a strongly negative correlation.

Once the detector was selected, a conditional sampling technique was used to determine the large-scale influence on the mass transport. Conditional sampling is a technique used to extract that portion of the data associated with the large-scale structures (as identified by the detector). One of the earliest uses of this experimental technique was that of Kovasznay, et al (27) in 1970 on a turbulent boundary layer. Mathieu & Charnay (28) have reviewed this sampling method and much of the work done utilizing it. They point out that the difficulties of conditional sampling "are not due to the detection of signals", but are "consequences of the delicate choice of an adequate criterion". Blackwelder & Kaplan (24) used conditional averaging to examine the effect of coherent structures on the Reynolds stress for a turbulent boundary layer. The idea of conditional sampling or averaging, again from Mathieu & Charnay, is simply "the observation of a property only when some criterion is satisfied". This basic idea has been adapted to an analytical technique, rather than an experimental one, for this study.

A computer program was written to perform conditional sampling on the simultaneous concentration-velocity data using concentration fluctuation as a trigger. A flow chart of this program is shown in Figure 8 and a program listing is included in

Appendix A. This program made it possible to quantitatively separate the effect of the large-scale motion from the overall turbulent motion on the mass transport. Figures 9, 10, and 11 show sample results from this program for the non-swirling flow. The section under DATA OUTPUT...includes various statistical parameters calculated using all of the data at that point (these results are those reported in Ref. 11, 12). The lower section under CONDITIONAL SAMPLING RESULTS contains statistical parameters based on conditional sampling of the data according to concentration fluctuation. The information shown includes the concentration fluctuation range and the number of data samples in the range. Also included are mean velocity, relative mean velocity, root mean square velocity fluctuation, mass transport coefficient, and transport ratio, all calculated using only the data in the range. The relative mean velocity is defined as the mean velocity for a given concentration fluctuation range minus the mean velocity for all the data samples at that point. The transport ratio is defined as the mass transport coefficient:

$$\frac{\overline{f u}}{f_{rms} u_{rms}}$$

for the data in a given concentration fluctuation range divided by the overall mass transport coefficient. The local fraction of inner jet fluid is used for concentration (f) and $\bar{f} = 1.0$ by definition at the sudden expansion (Fig. 1).

An example of data taken at a point on the inner edge of the shear layer is shown in Figure 9. The first interesting item is the negative overall mass transport coefficient. This combined with the fact that $\frac{\partial f}{\partial x} < 0$ leads to the following: $\frac{\overline{f u}}{\frac{\partial f}{\partial x}} > 0$

which is inconsistent with normal gradient transport models already discussed. Moving to the conditional sampling results, it is seen that the majority of the large concentration fluctuations are negative. This is to be expected here since the inner jet fluid contains the dye (Fig. 1) and thus has $\bar{f} \approx 1.0$. Any fluid swept into the region due to the large-scale motion will be outer jet fluid, with $\bar{f} \approx 0$, and will result in a negative concentration fluctuation. An examination of the conditional sampling results shows two distinct flow characteristics among the data. The first is for the data with $|f'| < 0.2$, where the gradient transport model seems to fit. This data has a positive (or slightly negative) mass transport coefficient and very small relative mean velocity, indicating this well-mixed fluid is moving almost uniformly in the axial direction. The second flow characteristic is for the data with large concentration fluctuations (in this case $|f'| \geq 0.2$). This data is seen to have orders of magnitude, larger relative mean velocities and transport coefficients than the other data. The larger relative mean velocity indicates this fluid is not well-mixed with the rest of the flow and is moving at a considerably different, in this case higher, velocity than the mean flow due to the large-scale motion. The much larger mass transport coefficient indicates that even though the number of data samples is small, this data is responsible for the majority of the axial mass transport at this point. This data has a negative transport coefficient which, as already shown, is contrary to gradient transport. These data appear to be part of large-scale structures not well mixed with the overall flow and exhibit characteristics inconsistent with gradient transport.

Figure 10 shows data from a point well inside the shear layer under the strong influence of the large-scale motion. Once again the overall transport coefficient is negative, indicating that this is not a gradient transport situation. Since this location is inside the shear layer it is seen that there are large numbers of both positive and negative concentration fluctuations. There appear to be two distinct flow situations here also, but the large-scale motion seems to influence all of the data. Given that $u'f' \approx (\Delta u) (\Delta f)$, notice in the conditional sampling results that when the concentration fluctuation (Δf) is negative and the relative mean velocity (Δu) is positive, $u'f' < 0$ and hence a negative mass transport coefficient. The same result is observed when the concentration fluctuation is positive. The data within the large-scale structure can be separated by observing the large jump in relative mean velocity and transport coefficient. One again, a small number of data samples appears to be responsible for the homogeneity of the axial mass transport. If the data with $f' < -0.2$ or $f' > .1$ is considered not part of the large scale, a weighted average of the large-scale data gives 36% of the samples accounting for 77% of the axial mass transport. The weighted average is calculated as the mean mass transport ratio for the large-scale data multiplied by the percent of the total number of samples that are included in the large-scale data.

Finally, Figure 11 is an example of data containing no large-scale structure. There are no large concentration fluctuations and the relative mean velocities are very small. This location is inside the recirculation zone in the outer region of the flow.

Precisely which concentration fluctuation ranges are included in the large-scale motion is an admittedly somewhat subjective decision. The conditional sampling program was run on axial and radial velocity concentration data at axial locations of 13, 51, 102, 152, 203, 254, and 305mm for the non-swirling case. It was run at 13, 25, 51, 102, and 152mm for the swirling flow case since Roback & Johnson (12) found that complete mixing occurred much more rapidly in this flow. In all cases, the data within the large-scale structure were separated out based on concentration fluctuation, as well as the clear jumps in relative mean velocity and mass transport coefficient. This technique, when applied to the Johnson & Bennett data set, resulted in a basically consistent set of results; it is thought that the scatter found in some of the results is due to the limited large-scale data available for the present investigation. Despite this, the hypothesis that large positive or negative concentration fluctuations can be used to identify large-scale motion appears to be valid. As stated earlier, the true test of a detector is the completeness of the pattern it yields. Once the concentration-velocity data for the large-scale structures were extracted, much information about the influence of these structures was available. The results, to be discussed, support this choice of detector and the resulting pattern is in fact well defined.

RESULTS

As mentioned previously, the data sets used for the present investigation were acquired by Johnson & Bennett (11) for non-swirling flow and Roback & Johnson (12) for swirling flow. The results reported here are those associated with the large-scale structures. As discussed in the Analysis section, these results were obtained using conditional sampling techniques; the large-scale samples were detected using the concentration fluctuations as the criterion.

Several parameters were examined using the output of the conditional sampling program. The complete set of results for the non-swirling flow at the axial station at 152mm is contained in Appendix B and consists of numerous sets of results for various r/R_0 : axial velocity or radial velocity, each taken simultaneously with concentration.

Using the procedures already described, several flow parameters were investigated as functions of r/R_0 for each axial location. The first parameter studied was the large-scale fraction defined as the ratio of samples with large concentration excursions compared to the total sample size. For the non-swirling flow, plots are included for the axial velocity (Figs. 12-19) and radial velocity (Figs. 20-25) data. In each case, the percentage appears to be maximized in the shear layer where the large scales are known to exist from flow visualization done previously (11). As already stated, the data acquisition rate was oriented toward repeatable overall statistics. Therefore the distribution between large-scale and non-large-scale data is believed to be representative of the actual flow.

It is seen that, with increasing downstream distance, the percentage of data in the large scale becomes a weaker function of radius, with the peak in the shear layer becoming less pronounced in the axial data. At 102mm (Fig. 14) there is a large peak in the shear layer at $r/R_0 \approx .2$ where over 40% of the data is in the large scale. This drops off rapidly and by $r/R_0 \approx .4$ is close to zero. At 152mm (Fig. 15) the curve is not as steep. From $r/R_0 = 0$ to $r/R_0 \approx .25$, 30-40% of the data is in the large scale. The percentage approached 0 at $r/R_0 \approx .5$; but overall, more of the data is in the large-scale structure at this axial location. By 203mm (Fig. 16) the curve is still flatter. From $r/R_0 = 0$ to $r/R_0 \approx .2$, 50-60% of the data is in the large scale, not approaching zero until $r/R_0 \approx .6$. Overall, a still larger percentage of the flow is part of the large-scale structure than in previous cases. Combining the axial velocity plots, a contour plot of percentage of data that is part of the large-scale structure was done (Fig. 19). It is seen that the largest percentage is located within the shear layer and spreads radially, moving downstream as the shear layer spreads also.

The radial velocity plots exhibit similar characteristics to the axial plots, with the peak spreading as the axial location increases. Figures 22 and 24 have curves that aren't quite so smooth as the others but the overall trend is similar. The percentage of data in the large scale must be the same for radial data as for axial; this is the case here for the most part. Any discrepancies can be attributed to the limited amount of large-scale data available.

Next, a calculation was made of the percentage of mass transport attributable to the large-scale portion of the flow. This was done for each radial location at a given axial station. This data, plotted as a function of r/R_0 for each axial station, is shown in Figures 26 through 38 for the non-swirling flow. The axial mass transport percentage plots (Figs. 26-32) are typified by Figure 27, at $z = 51\text{mm}$, which shows that the percentage attributable to the large scale is a maximum within the shear layer between the jets. It is well in excess of 50% throughout the shear layer.

Looking at the radial mass transport percentage plots at 13mm and 51mm (Figs. 33 and 34), they are similar to their axial counterparts (Figs. 26 and 27) although the percentage is higher for the radial data. Further downstream, these plots (Figs. 35-38) were considerably more involved, again with higher peak percentages than for the corresponding axial ones (Figs. 28-31).

Combining all of these results, it is possible to plot contours of percentage contribution to the mass transport due to the large-scale data. The axial mass transport plot (Fig. 39) shows that throughout the shear layer, 50-90% of the transport can be attributed to the large-scale motion. The increased complexity for radial mass transport became very evident when attempting to plot a similar contour plot for it. The limited locations with available data make it impossible to complete this figure. The existing data showed promise of a plot with similar features to the axial one, with somewhat higher percentages, but more data is needed to accurately complete this plot.

Looking at Figures 19 and 39, it is seen that there is qualitative agreement between the percentage of data that is part of the large-scale motion and the percentage contribution of the large scales to the mass transport. In the region where at least 50% of the mass transport is attributed to the large-scale motion, at least 10% of the data is part of these large scales. In the peak region of 80-90% contribution, at least 20% of the data is part of the large-scale motion. These plots certainly substantiate the importance of large-scale motion in the mass transport of the flow.

Figure 40 is a summary of the transport zones for axial mass transport. It is adapted from Figure 2 and includes the boundary of the region which Johnson & Bennett (10) found did not follow the traditional gradient transport model, as well as the boundary of the region for which the large-scale structure exerts a strong influence on the axial mass transport. The boundary of the large-scale region is based on a 50% contribution to the mass transport, although other values may be used by overlaying Figure 2 with Figure 40. The boundaries of these two regions are observed to follow each other very closely. This leads to the conclusion that consideration of the large-scale structures is essential in accounting for the axial mass transport in this region where the gradient transport model is inadequate. Of course, the presence of the large-scale structures means the flow includes multiple scales; gradient transport should not be expected to apply in such regions.

For the swirling flow, plots of large-scale fraction (Figs. 41-43) and mass transport percentage (Figs. 44-46) are included for axial velocity at axial stations of 13, 25, and 51mm. As Roback & Johnson (12) found, mixing for the swirling flow case occurs in approximately one third the downstream distance that it takes for the non-swirling flow. For this reason, large-scale structures were found to be influential in a much smaller region than for the non-swirling flow.

At 13mm (Fig. 41) the large-scale fraction peaks at approximately 30% of the data samples while at 25mm (Fig. 42) the peak is closer to 40%. In both cases the maximum occurs within the shear layer between the inner and annular jets as expected. By 51mm (Fig 43) the large-scale fraction is peaking at over 60% but the peak has shifted to the centerline. This is apparently due to the unsteadiness associated with the leading edge of the recirculation zone which occurs for the swirling flow and is consistent with the findings of Roback & Johnson (12). As expected, these percentages are somewhat higher at the same axial locations for the swirling flow than for the non-swirling flow.

The largest difference between swirling and non-swirling flow occurs at the 51mm location. The high values there are almost certainly associated with the unsteady motion of the recirculation zone noted earlier. Flow visualization (12) at this point clearly shows the very large structures present near the centerline. Also, as seen in the non-swirling flow, the overall percentage of data within the large-scale motion increases with downstream distance.

Swirling flow data were analyzed for large-scale structures at the 102 and 152mm locations. Though some indication of large structures was found, it represented, at most, 3% of the total samples at any one location. These results are not included as the statistics contain significant uncertainty due to the small sample size. We would agree with Roback & Johnson that large-scale structures exist at 102mm at least; but if the sample set is representative of the large-scale fraction, the large-scale structures are of no significance at this point.

The swirling flow mass transport percentage plots (Figs. 44-46) also exhibit some similarities to the non-swirling case. In each case the percentage is a maximum in the shear layer between the jets and the region of large-scale influence spreads radially with downstream distance. As already stated, the swirling flow mixes very rapidly and these plots reflect this. The percentages are high, like the non-swirl flow, but spread into the centerline much sooner axially than for the non-swirl flow.

A result of the rapid mixing for the swirling flow is that changes from station to station are much larger than for the non-swirl case. This makes it difficult to draw contours. As with the non-swirling flow, the influence of the large-scale motion is large and also consistent throughout the flow field.

An effort was undertaken to utilize the two-component velocity data to look at the large-scale contribution to the momentum transport. It was necessary to select a new detector to separate

the large-scale data since there is no concentration data available in this case. A modified conditional sampling program was written to try to find such a trigger. A flow chart is included in Figure 47 and a program listing is in Appendix A. This program was used on the concentration-velocity data previously sampled for the non-swirling flow using concentration fluctuation as a trigger. Calculations were made of a conditional mean velocity and rms velocity fluctuation based on the same concentration range already selected. These were then compared to the overall mean and rms for the data. A typical output from this program is shown (Fig. 48) together with a plot of the data (Fig. 49). This figure shows the velocity distribution, in this case, a radial velocity data set. The overall data exhibits the nearly normal distribution. The large-scale data is more skewed, with a significantly different mean velocity and somewhat different rms fluctuation velocity than the overall. It had been hoped that radial velocity or velocity fluctuation might be used as a detector for the large-scale structure in the two-component velocity data. However, based on the results typified by this figure, there is no way to use either to separate the large-scale data. Use of axial velocity as a trigger was ruled out also when plots of this type showed similar results.

Plots of mean velocity and rms velocity fluctuation as functions of r/R_0 were done for simultaneous non-swirling concentration-velocity (axial and radial) data at various axial stations. The overall and large-scale values were plotted

together for comparison purposes. Figure 50 is a typical plot for axial velocity. The mean velocity for the overall data and that for the large-scale data have very small differences, indicating that the coherent structures are moving at approximately the same axial velocity as the rest of the flow. This result for free shear layers is consistent with the results of Kovaszny et al (27) and several others (reviewed by Cantwell 18) who found large structure convection velocities in wall-bounded flows between 80 and 90 percent of the free stream mean velocity. Roshko (17) noted that for plane-mixing layers the large-scale vortices convect at approximately the average velocity of the two streams, with the velocity and density ratios having some influence.

Plots of mean radial velocity vs. r/R_0 are included for axial stations of 51, 102, 152, and 203mm. Figure 51 shows a negligible difference between the large-scale and overall data at 51mm. At 102mm, the differences are very significant (Fig. 52). For $0 \leq r/R_0 < .2$, the large-scale structures have a larger negative radial velocity than the mean flow. From $.2 \leq r/R_0 \leq .4$, the large-scale structures have a larger positive radial velocity than the mean flow, with the difference increasing with r/R_0 . In this region, the shear layer is spreading radially, assuming that the large-scale structures identify the shear region.

Further downstream, at 152mm (Fig. 53), there is a negligible difference between large-scale motion and overall data for $r/R_0 < .2$. This difference is significant, however, for $.275 \leq r/R_0 \leq .475$ and is approximately constant in this range. Again the coherent structures have a significantly larger radial velocity than indicated by the mean velocity of all the data.

At 203mm (Fig. 54), there are very small differences for $0 < r/R_0 < .3$. Large differences are found between the large-scale flow and overall for $.3 < r/R_0 < .6$. The radial mean velocity appears to be a linearly increasing function of r/R_0 for the large-scale and overall data, although the large-scale increase at a faster rate.

If the extent of the shear layer is assumed to correspond to the region where large-scale structures are found, the spreading rate of the shear layer for the non-swirling flow can be examined using Figures 12 through 17. Table 1 shows the radial extent of the large-scale structures for each axial station taken directly from the figures. Data were not taken at the same radial locations for all axial locations; therefore, comparisons of the exact same radial locations are not always possible. The data base is complete enough to observe that the spreading rate of the shear layer, or region where large-scale structures exist, increases approximately linearly with increasing axial location. This is consistent with other work on free shear layers (29) and consistent with the positive radial velocity found by Johnson & Bennett (11). These results emphasize the need for multiple scale modeling (15) since the large scales and overall flow have different radial convection velocities.

Figures 55, 56, and 57 are plots of the large-scale relative mean velocity as a function of concentration fluctuation, at axial locations of 51, 102, and 152mm respectively, for the non-swirling flow. The large-scale relative mean velocity is defined, at each axial and radial location, as the mean velocity for a given concentration fluctuation range minus the mean velocity for all of the large-scale data at the location. These plots provide

additional support for the selection of the large-scale structures in that the large-scale relative mean velocity is approximately zero, in each figure, for concentration fluctuation of zero.

At any location there is some fluctuation in the overall curve, attributed to eddy variations. Each curve has limited scatter though and the vortex like structures are quite well defined in that a given relative mean velocity suggests a preferred concentration fluctuation value. Since the structures are well defined, the lack of correlation reported by Johnson & Bennett (11) must be due to the random arrival times of the structures. This is also suggested by the 3-D calculations of Riley & Metcalfe (30) and leads to the conclusion that the present form of the structures is "3-D like" for the large-scales.

CONCLUSION

The initial or upstream development of shear flows is crucial to the performance of many aerodynamic components (i.e., combustors). Comparisons of experimental results with computer predictions show that present models are not sufficient for such flows. Historically, flow visualization has shown that large-scale structures are present within this upstream, non-equilibrium region. It has been generally hypothesized that any lack of agreement between prediction and experiment can be attributed to these structures. In general, no adequate model (including them) has been included in the numerical computer codes, primarily since little was known about them.

The present investigation set out to analyze the physical characteristics of large-scale structures in free shear layers and to evaluate their importance to turbulent transport (including the first ever results for mass transport). Utilizing previously acquired data, the conclusions are limited in that the data set was not optimized for this use. Regardless, several significant conclusions are possible; they include:

- (1) The large concentration fluctuations are indicative of the large structures. First, the sign of the transport is predictable with a model consistent with these structures. Secondly, the region with significant large concentration fluctuations is consistent with the large-scale region noted from flow visualization.

(2) The large structures, where present, account for most of the mass transport; the obvious implication of multiple scales is consistent with the lack of agreement with a gradient transport model.

(3) The large structures are found to be convected axially with the overall mean velocity but radially at a faster speed; this further strengthens the need for a multiple scale model.

(4) Any investigation of the influence of large-scale structures on momentum transport in three-dimensional free shear layers will most probably require concentration detection.

(5) The effects of large-scale motion for the swirling flow case or limited, at least for the data available, to the region just upstream of the recirculation zone and to the shear region between the jets.

The present investigation therefore has documented the importance of the large-scale structures and the need for them to be modelled if computer predictions are to be accurate. It is strongly suggested that the development of such a model is of the highest priority. Experimentally, this suggests several projects for further investigation. They include:

(1) A detailed analysis of the flow development with the large structures. What is the structure in physical space? What type of mixing occurs within them (is it a two-step process as suggested for two-dimensional shear layers)?

(2) A detailed analysis of momentum transport associated with the large structures. Does it significantly affect the results as would be predicted from the present mass transport results and from the results for other shear flows?

(3) An investigation of the influence of initial conditions on large-scale development. Certainly, such initial conditions are required for any computer simulation. What effects do changes in initial conditions have and what are the implications for accurate models?

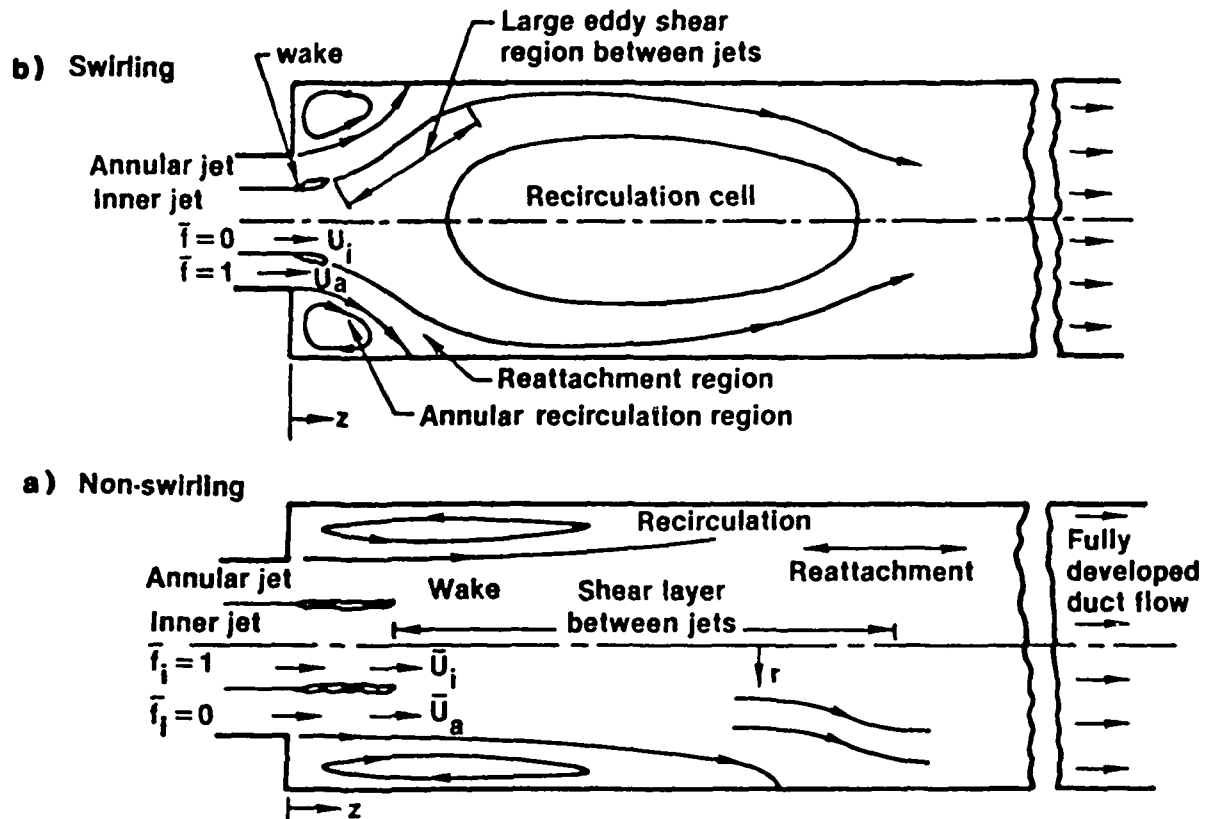
(4) An investigation of two-dimensional vs. Three-dimensional shear layers. Both the published experimental results and the recent computer simulations strongly suggest that such a delineation between two-dimensional and three-dimensional flows is not straightforward. What are the implications of such assumptions on the development of an accurate model?

TABLE 1 : SPREADING RATE OF SHEAR LAYER

STREAMWISE LOCATION	EXTENT OF SHEAR
z (mm)	LAYER , r/Ro
13	.250
51	.300
102	.400
152	.475
203	.600
254	.724

Fig. 1

SHEAR REGIONS OF COAXIAL JETS



reprinted from NASA CR-168252

AXIAL MASS TRANSPORT ZONES

- Constant concentration, no axial mass transfer
- ▨ Counter-gradient mass transport, $uf/(-\partial f/\partial z) < 0$
- Gradient mass transport, $uf/(-\partial f/\partial z) > 0$
- ▤ Low axial transport rate

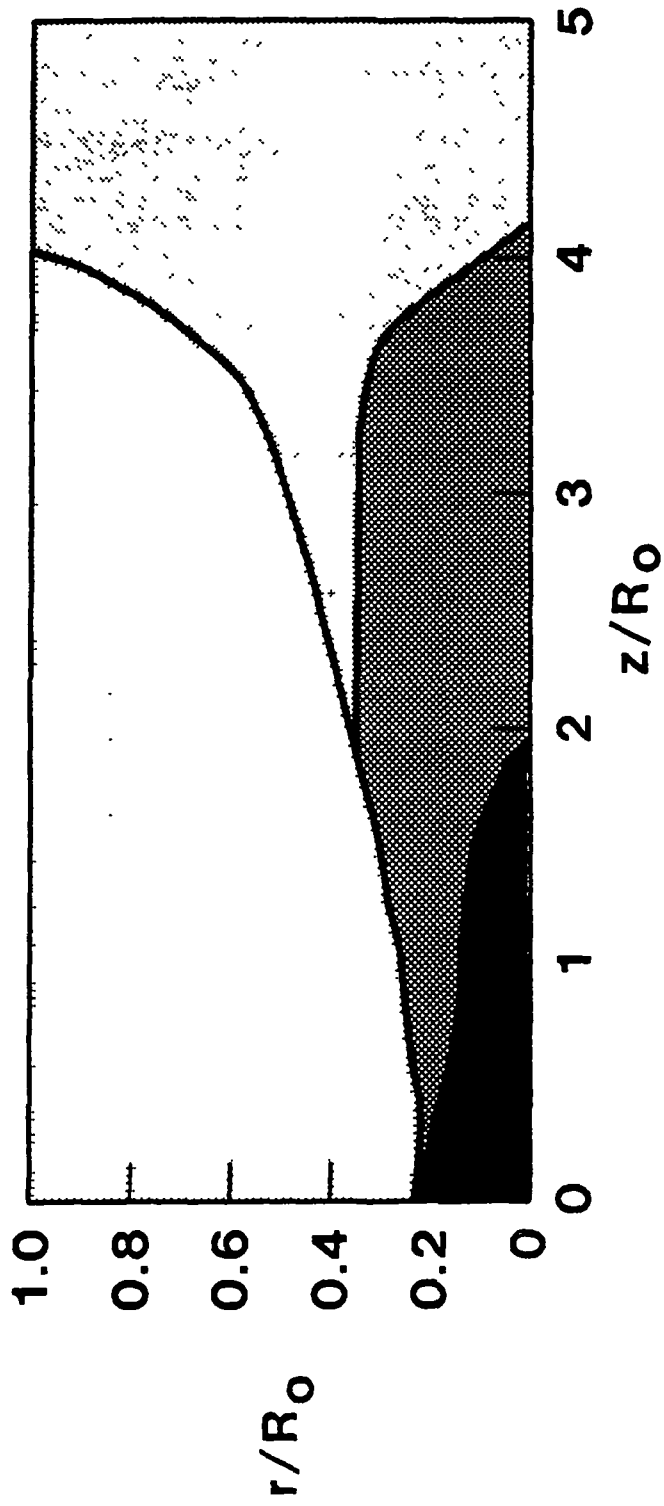


Fig. 2

Journal of Plant Anatomy, 1964, 14, pp. 1-4

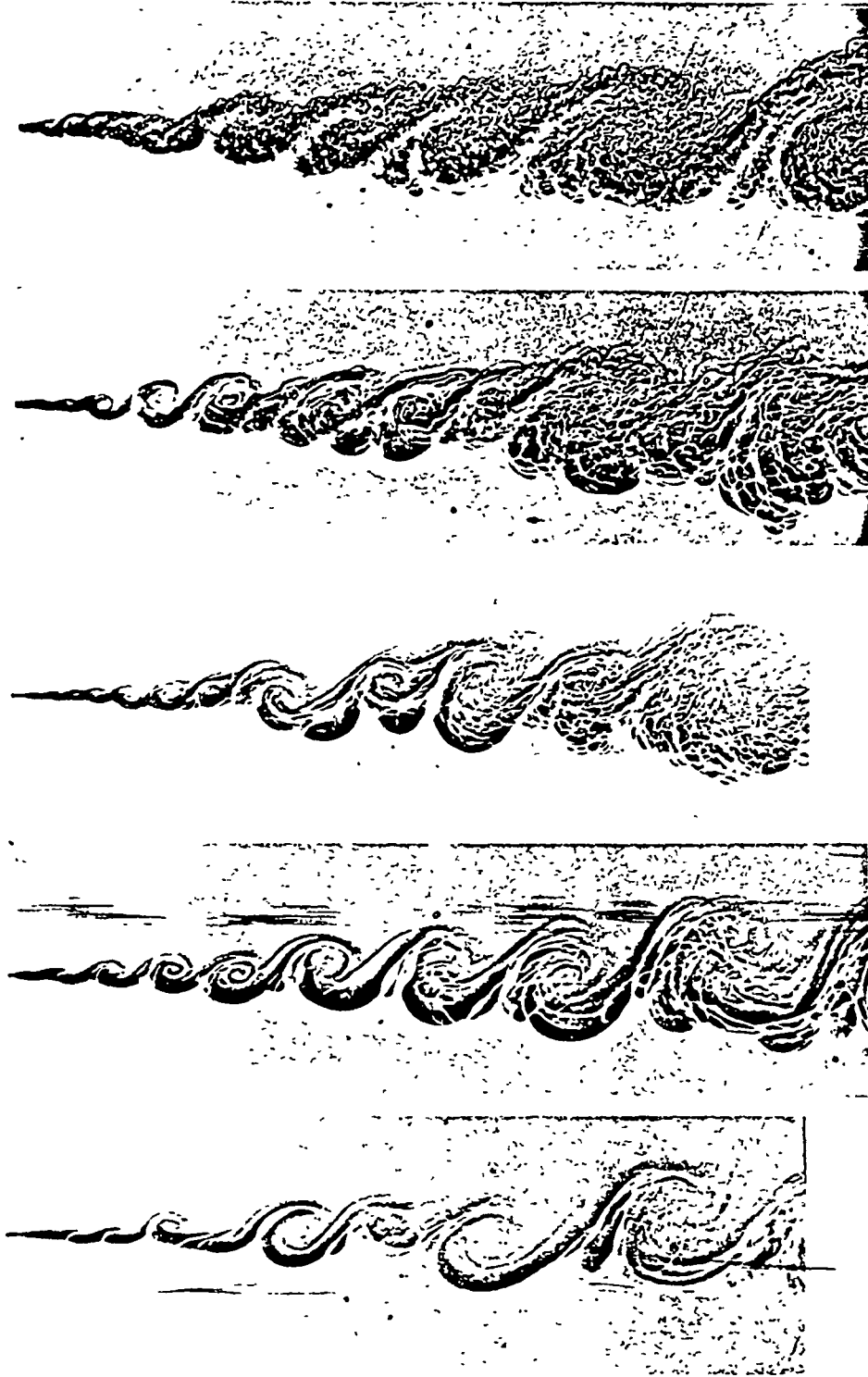


Fig. 3. (a) Root of *Phaseolus mungo* L. (10 days old) showing the cortex and the cortex-mesophyll boundary. (b) Root of *Phaseolus mungo* L. (10 days old) showing the cortex and the cortex-mesophyll boundary. (c) Root of *Phaseolus mungo* L. (10 days old) showing the cortex and the cortex-mesophyll boundary. (d) Root of *Phaseolus mungo* L. (10 days old) showing the cortex and the cortex-mesophyll boundary. (e) Root of *Phaseolus mungo* L. (10 days old) showing the cortex and the cortex-mesophyll boundary.

Fig. 4

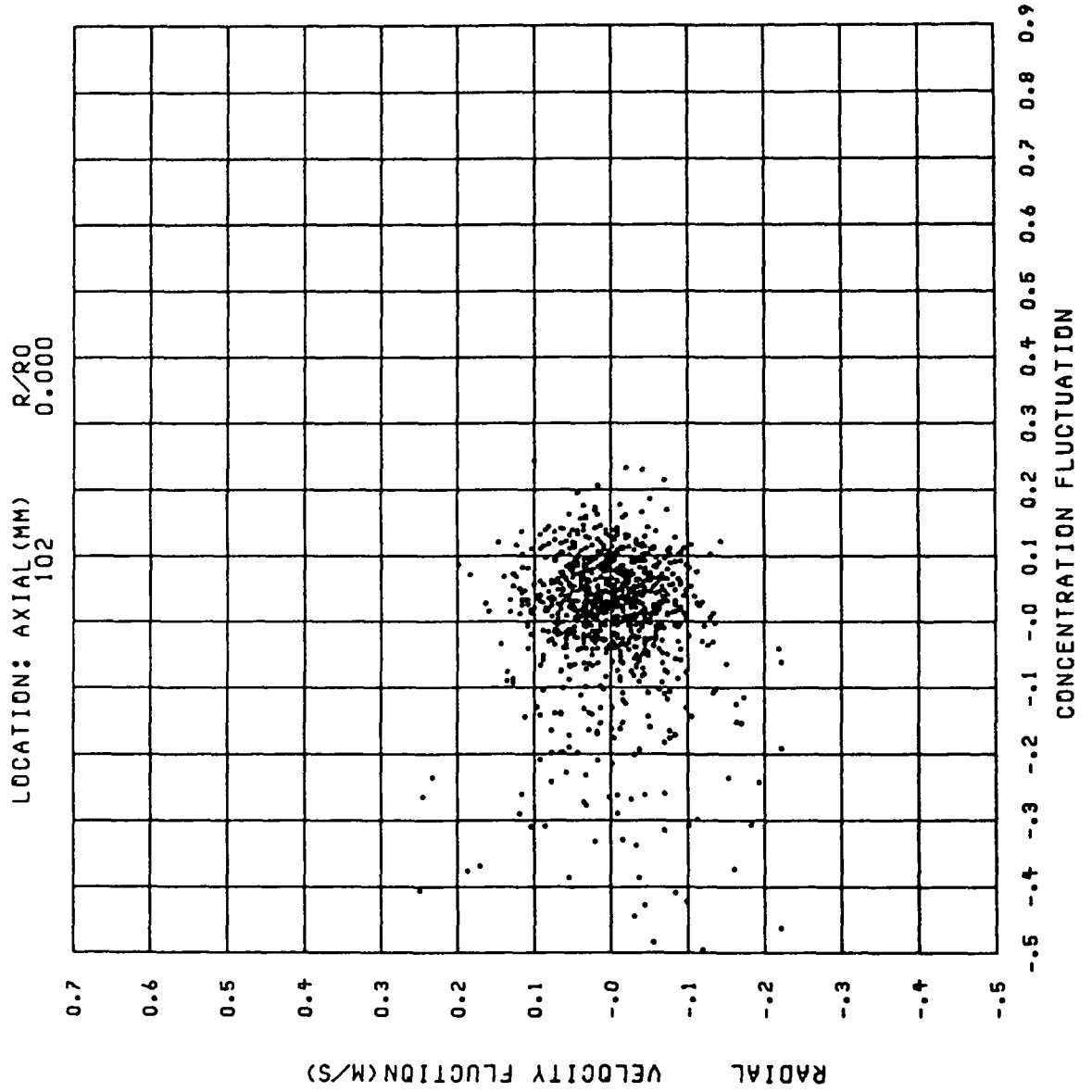


Fig. 5

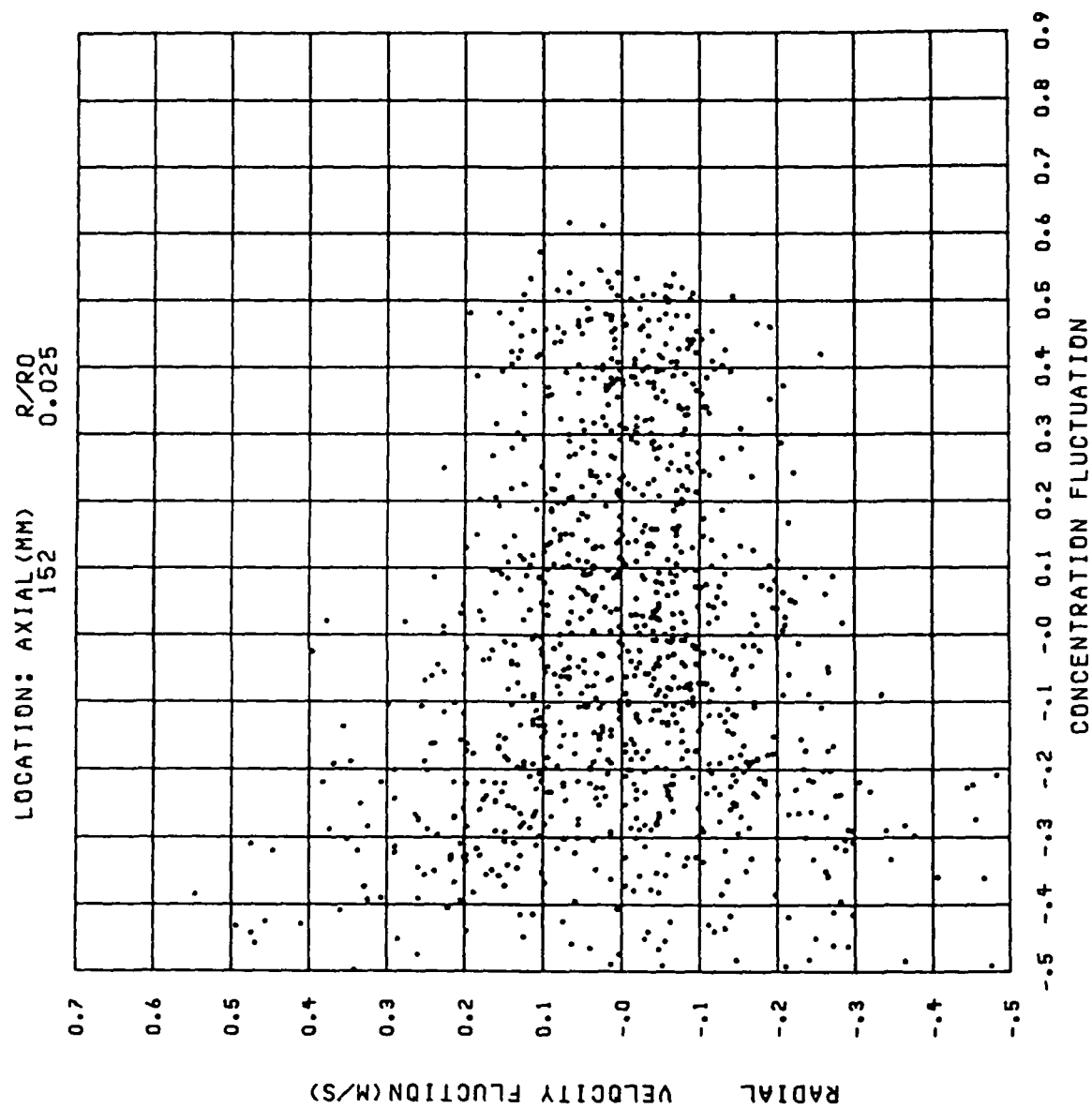


Fig. 6

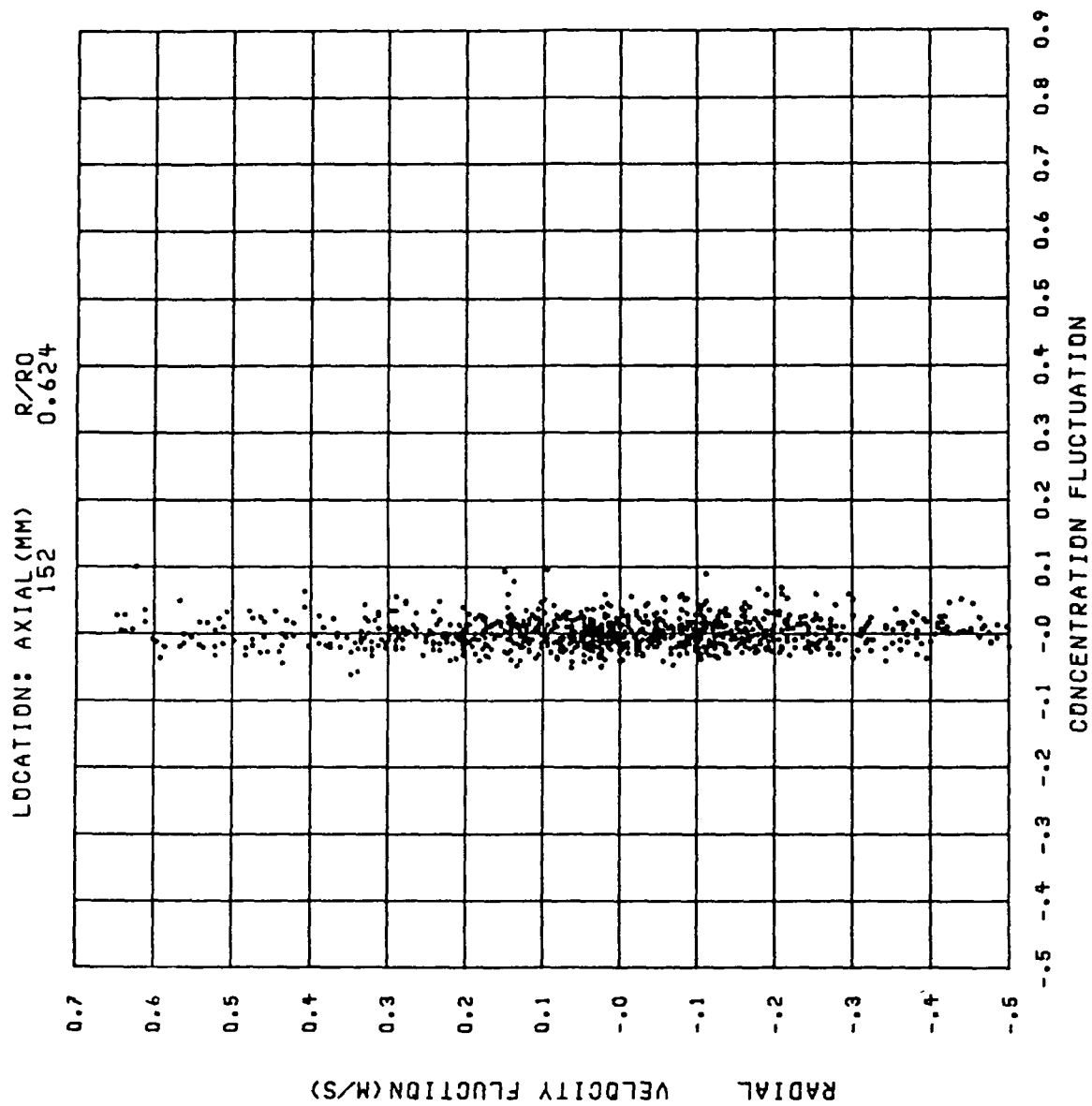


Fig. 7

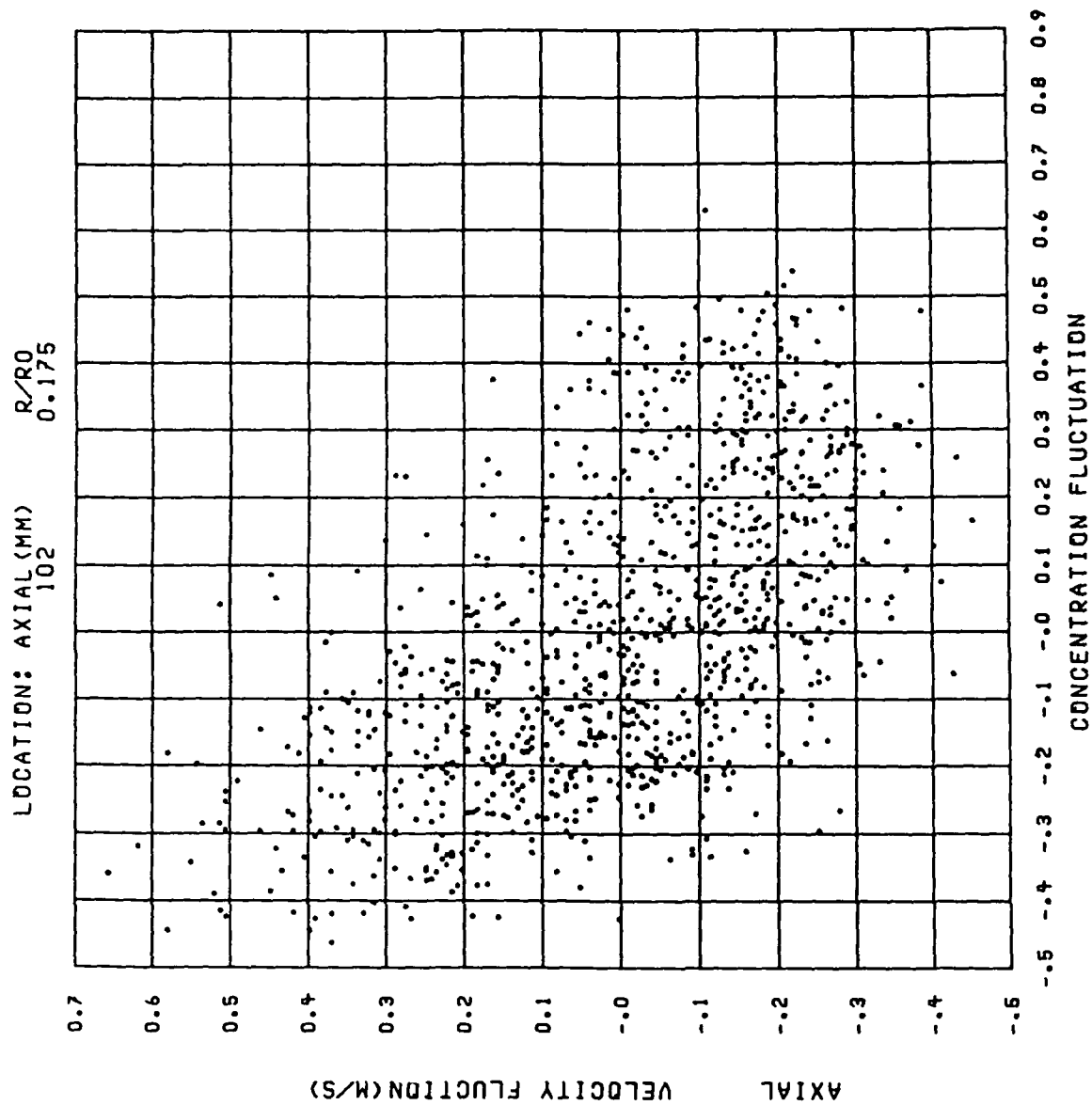
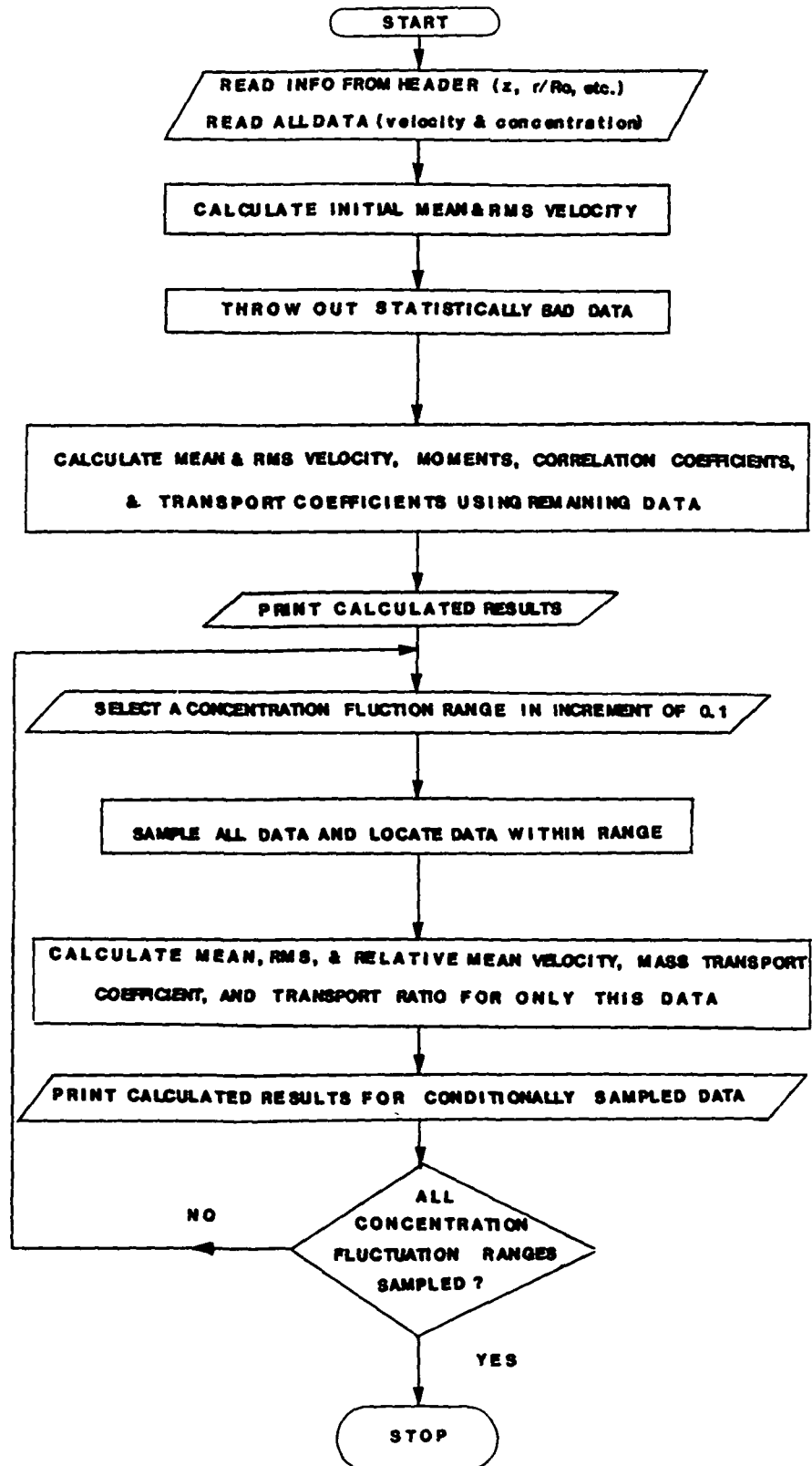


Fig. 8



SMILE 61.5
 SUCCESSFUL (TEMP) KESTOKE RUN61FS AS (TF5)
 CANCELLED: DNAME KMS UNKNOWN

DATA OUTPUT FOR RUN 61 POINT 5

AXIAL VELOCITY VS CONCENTRATION
 Z= 51 MM AND R/R0= 0.158
 NO= 999 AND N4=985
 VEAK= 0.7083 MFS
 UKMS= 0.0894 MFS
 THIRD MOMENT OF TURBULENCE= 0.15068E-03 MPS**3
 THIRD CORRELATION COEFFICIENT= 0.2112
 FOURTH MOMENT OF TURBULENCE= 0.20856E-03 MPS**4
 FOURTH CORRELATION COEFFICIENT= 3.2709
 CEAR= 0.775X
 CPMS= 0.154X
 CPPEAR= -0.000522
 OVERALL TRANSPORT COEFFICIENT= -0.038032

CONDITIONAL SAMPLING RESULTS

CONCENTRATION FLUCTUATION	NUMBER OF OCCURRENCES	MEAN	RELATIVE MEAN	RMS	TRANSPORT COEFFICIENT	TRANSPORT RATIO
-1.0 - -0.9001	0	0.8780	0.16968	0.00000	-7.72770	203.187
-0.9 - -0.8001	0	0.8580	0.14968	0.10100	-5.52904	145.377
-0.8 - -0.7001	0	0.7931	0.08480	0.10837	-2.70198	71.044
-0.7 - -0.6001	1	0.7270	0.01888	0.10087	-0.50036	13.156
-0.6 - -0.5001	2	0.7163	0.00798	0.10603	-0.18062	4.749
-0.5 - -0.4001	17	0.7004	-0.00775	0.10964	0.06358	-1.672
-0.4 - -0.3001	31	0.6894	-0.01873	0.08799	0.05972	-1.570
-0.3 - -0.2001	76	0.7002	-0.00813	0.07993	-0.00778	0.204
-0.2 - -0.1001	101	0.7167	0.00834	0.07600	0.08703	-2.288
-0.1 - -0.0001	140	0.7417	0.03338	0.07767	0.53998	-14.198
0.0 - 0.0999	304					
0.1 - 0.1999	262					
0.2 - 0.2999	31					
0.3 - 0.3999	0					
0.4 - 0.4999	0					
0.5 - 0.5999	0					
0.6 - 0.6999	0					
0.7 - 0.7999	0					
0.8 - 0.8999	0					
0.9 - 0.9999	0					

END OF RUN 61 -POINT 5
 TERMINATED: STOP

Fig. 9

Fig. 10

SAMPLE 61.6
 SUCCESSFUL (TEMP) RESTORE RUN61F6 MS (TF6)
 CANCELLED: DDNAME RMD5 UNKNOWN

DATA OUTPUT FOR RUN 61 POINT 6

AXIAL VELOCITY VS CONCENTRATION
 Z= 51 MM AND R/R0= 0.208
 NO= 999 AND N4=999
 UEAR= 1.0037 MPS
 VRMS= 0.2193 MPS
 THIRD MOMENT OF TURBULENCE= 0.32597E-02 MPS**3
 THIRD CORRELATION COEFFICIENT= 0.3090
 FOURTH MOMENT OF TURBULENCE= 0.56079E-02 MFS**4
 FOURTH CORRELATION COEFFICIENT= 2.5103
 CRAR= 0.3672
 CRMS= 0.1712
 CPVPRAR= -0.018305
 OVERALL TRANSPORT COEFFICIENT= -0.488753

CONDITIONAL SAMPLING RESULTS

CONCENTRATION FLUCTUATION	NUMBER OF OCCURANCES	MEAN	RELATIVE MEAN	RMS	TRANSPORT COEFFICIENT	TRANSPORT RATIO
-1.0 - -0.9001	0					
-0.9 - -0.8001	0					
-0.8 - -0.7001	0					
-0.7 - -0.6001	0					
-0.6 - -0.5001	0					
-0.5 - -0.4001	0					
-0.4 - -0.3001	11	1.2878	0.28411	0.12489	-2.43854	4.989
-0.3 - -0.2001	82	1.1762	0.17253	0.18350	-1.09923	2.249
-0.2 - -0.1001	217	1.0975	0.09381	0.20346	-0.39192	0.802
-0.1 - -0.0001	226	1.0394	0.03572	0.20658	-0.06921	0.142
0.0 - 0.0999	199	0.9664	-0.03726	0.20343	-0.05765	0.118
0.1 - 0.1999	117	0.8656	-0.13807	0.17301	-0.52990	1.084
0.2 - 0.2999	73	0.8365	-0.16718	0.14165	-1.07212	2.194
0.3 - 0.3999	46	0.8497	-0.15402	0.12301	-1.38951	2.843
0.4 - 0.4999	19	0.8247	-0.17897	0.08073	-2.11066	4.318
0.5 - 0.5999	2	0.7225	-0.28121	0.03950	-4.07154	8.330
0.6 - 0.6999	0					
0.7 - 0.7999	0					
0.8 - 0.8999	0					
0.9 - 0.9999	0					

END OF RUN 61 -POINT 6
 TERMINATED: STOP

Fig. 11

SAMPLE 52,14
 SUCCESSFUL (TEMP) RESTORE RUN52F14 AS (TF11)
 CANCELLED: DNAME RND5 UNKNOWN

DATA OUTPUT FOR RUN 52 POINT 14

RADIAL VELOCITY VS CONCENTRATION
 Z=102 MM AND R/R0= 0.550
 NOS. 999 AND N4=992
 VBAR= 0.0422 MFS
 VRMS= 0.2375 MFS
 THIRD MOMENT OF TURBULENCE= 0.13084E-02 MFS**3
 THIRD CORRELATION COEFFICIENT= 0.1111
 FOURTH MOMENT OF TURBULENCE= 0.89393E-02 MFS**4
 FOURTH CORRELATION COEFFICIENT= 3.3354
 CRMS= 0.0082
 CFMS= 0.0162
 CFVBAR= -0.000505
 OVERALL TRANSPORT COEFFICIENT= -0.139573

CONDITIONAL SAMPLING RESULTS

CONCENTRATION FLUCTUATION	NUMBER OF OCCURRENCES	MEAN	RELATIVE MEAN	RMS	TRANSPORT COEFFICIENT	TRANSPORT RATIO
-1.0 - -0.9001	0					
-0.9 - -0.8001	0					
-0.8 - -0.7001	0					
-0.7 - -0.6001	0					
-0.6 - -0.5001	0					
-0.5 - -0.4001	0					
-0.4 - -0.3001	0					
-0.3 - -0.2001	0					
-0.2 - -0.1001	0					
-0.1 - -0.0001	521	0.0665	0.02432	0.22888	-0.13017	0.933
0.0 - 0.0999	471	0.0153	-0.02690	0.22297	-0.15001	1.075
0.1 - 0.1999	0					
0.2 - 0.2999	0					
0.3 - 0.3999	0					
0.4 - 0.4999	0					
0.5 - 0.5999	0					
0.6 - 0.6999	0					
0.7 - 0.7999	0					
0.8 - 0.8999	0					
0.9 - 0.9999	0					

END OF RUN 52 -POINT 14
 TERMINATED: STOP

ORIGINAL PAGE IS
OF POOR QUALITY

Fig. 12

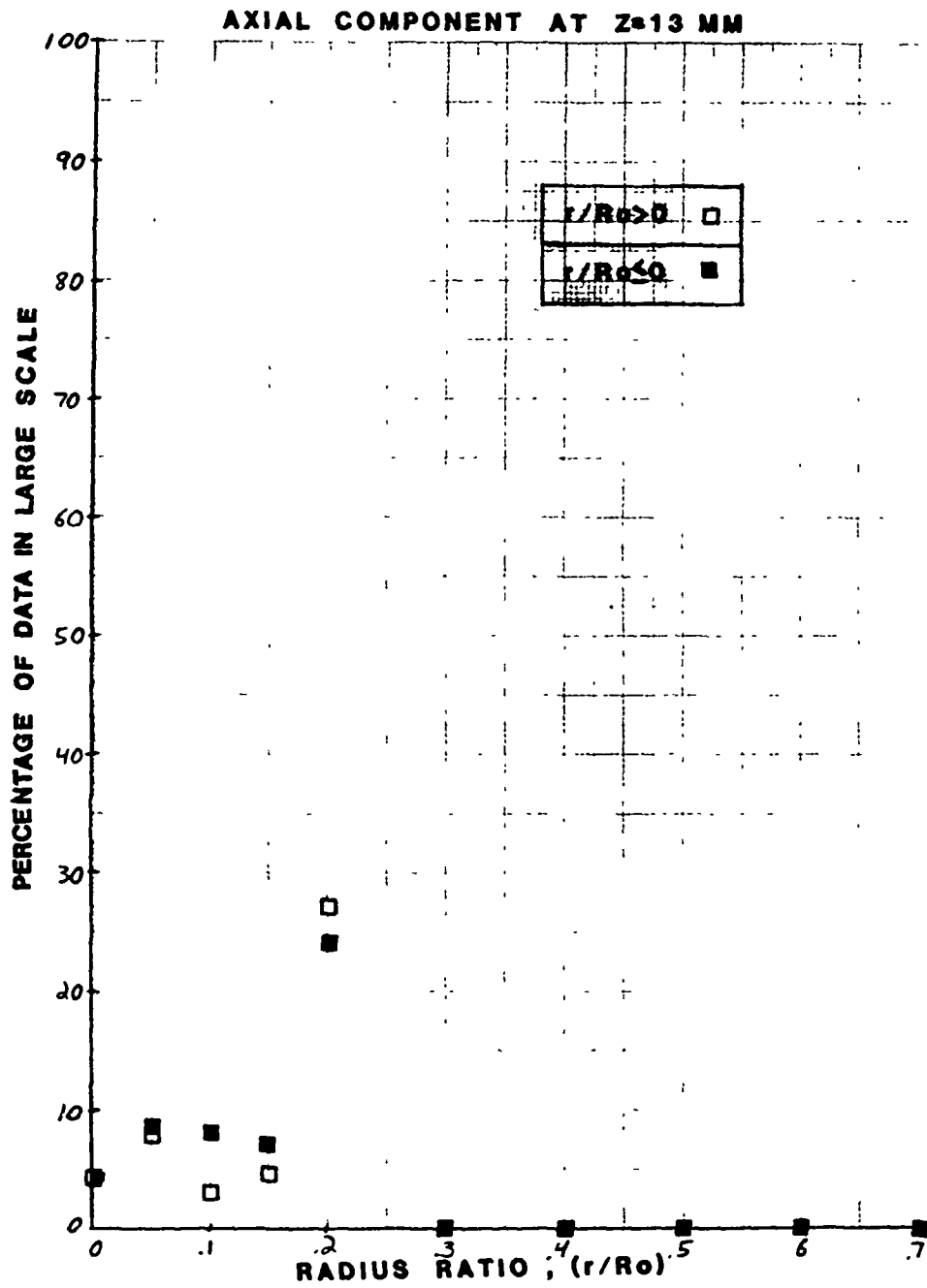


Fig. 13

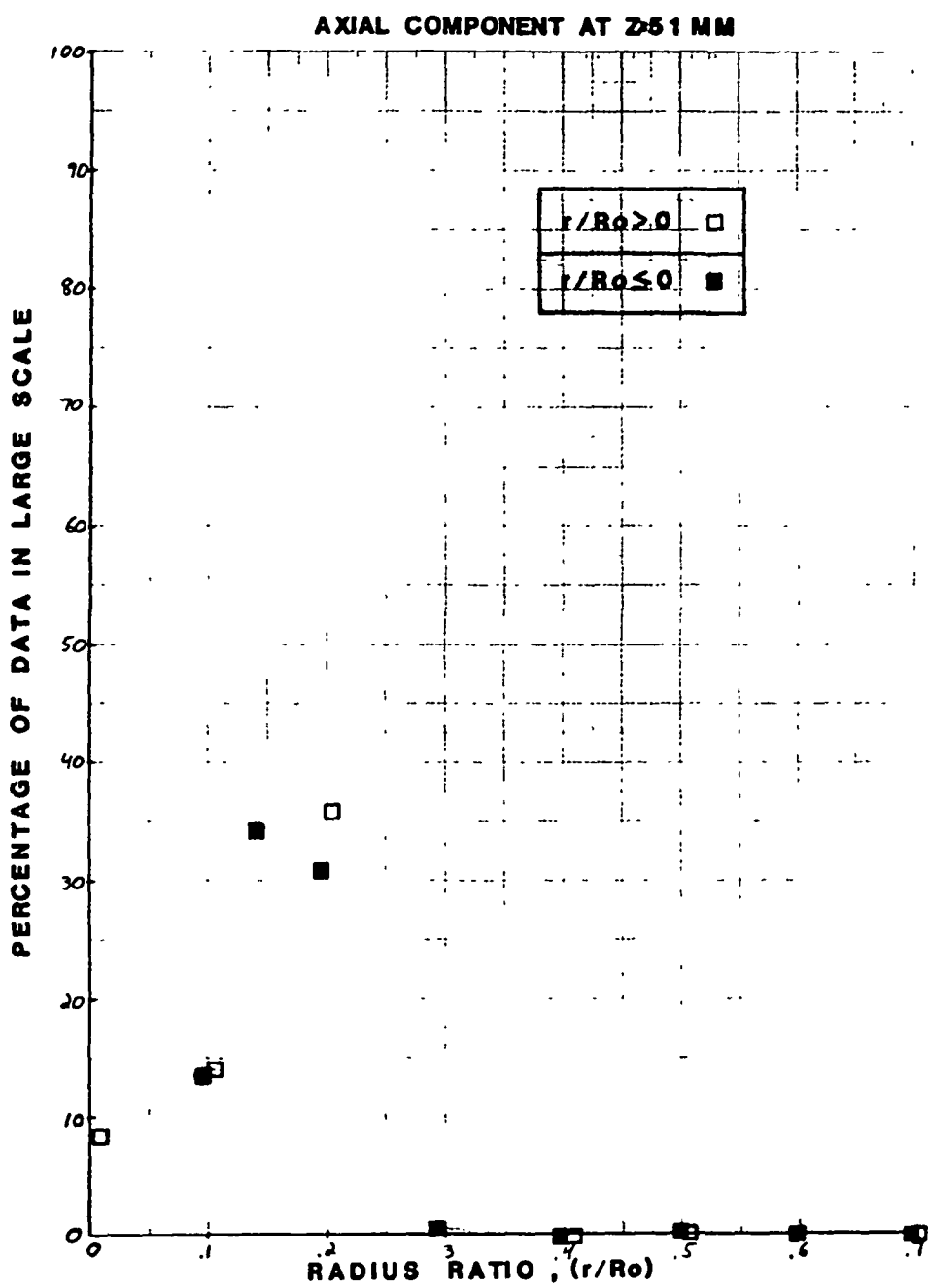


Fig. 14

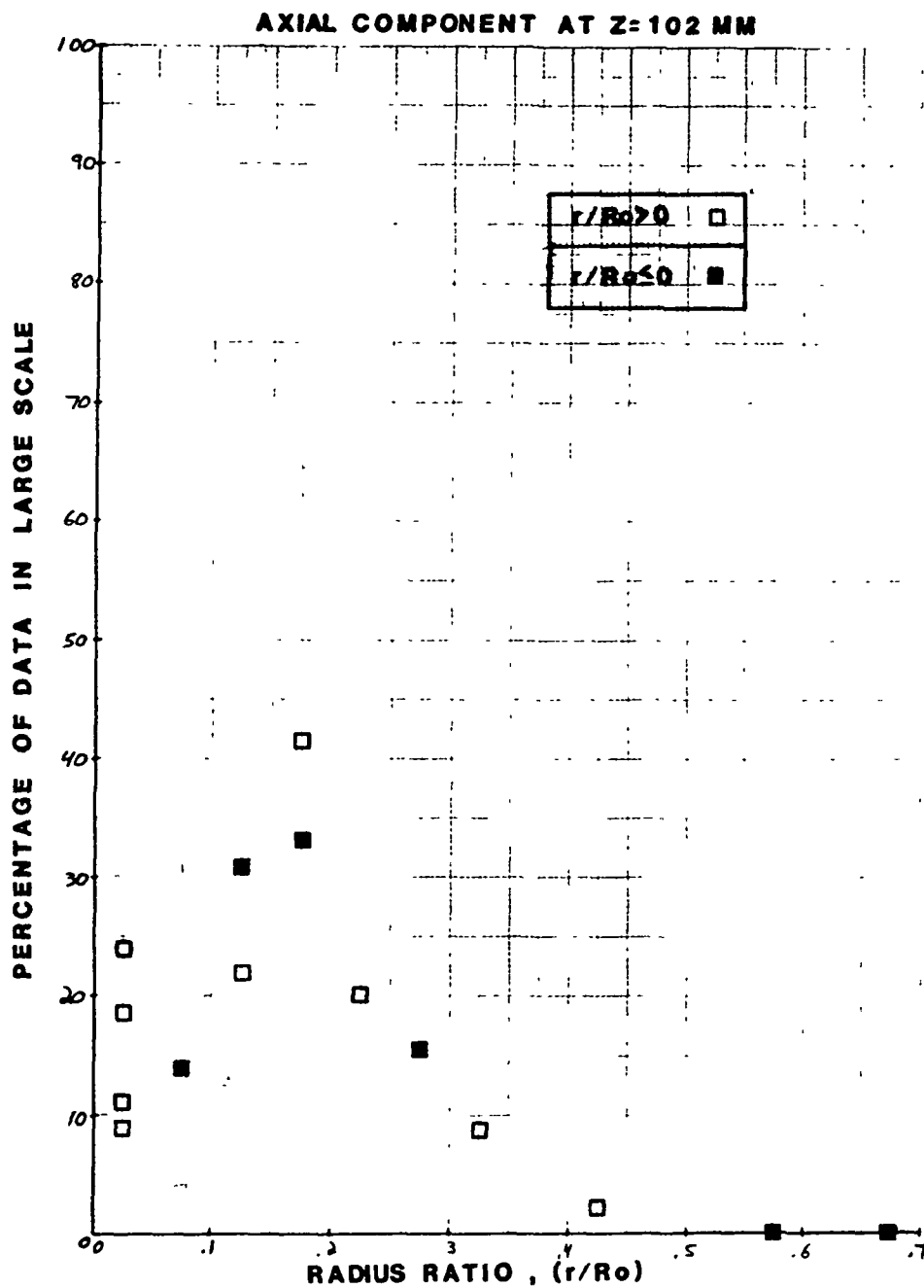


Fig. 15

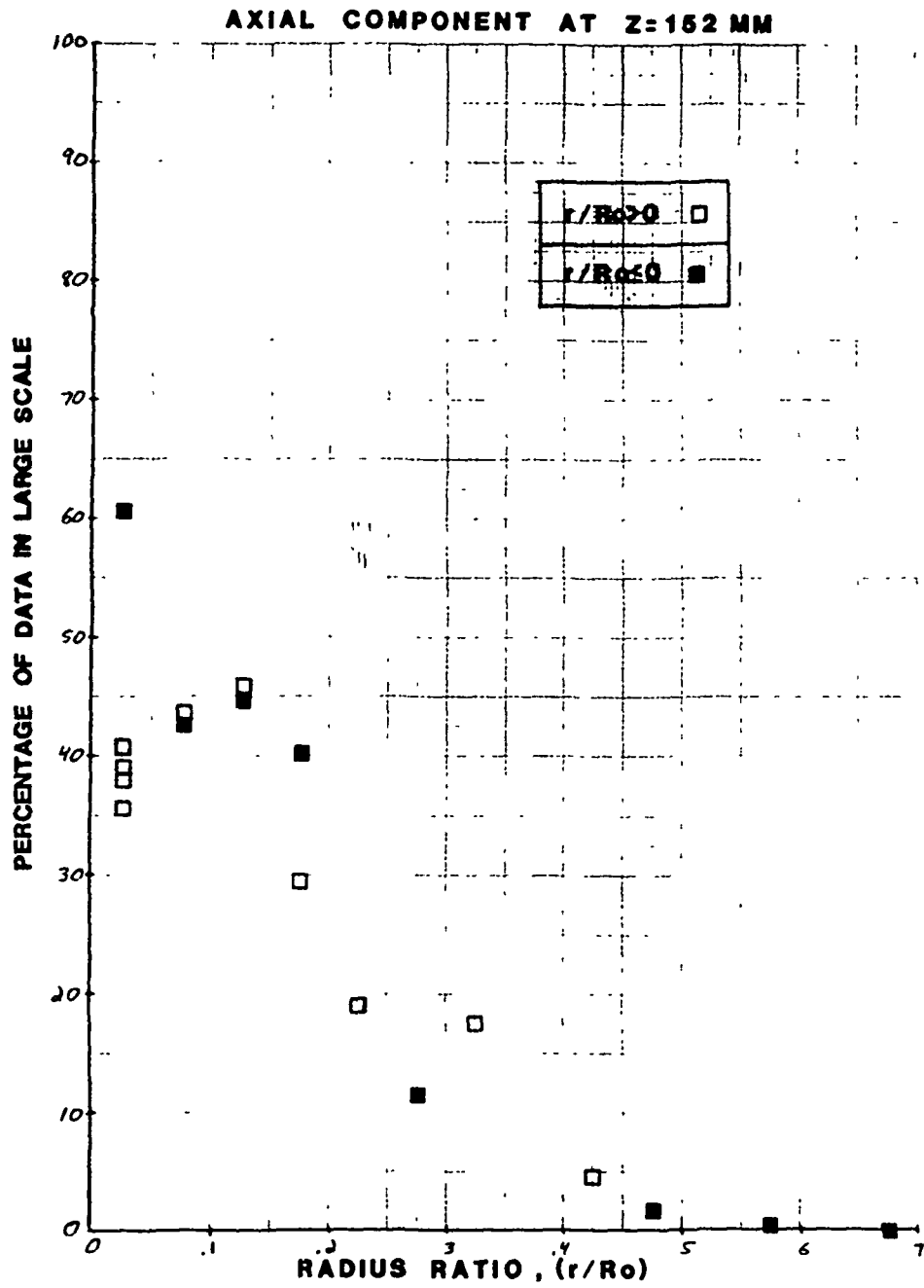


Fig. 16

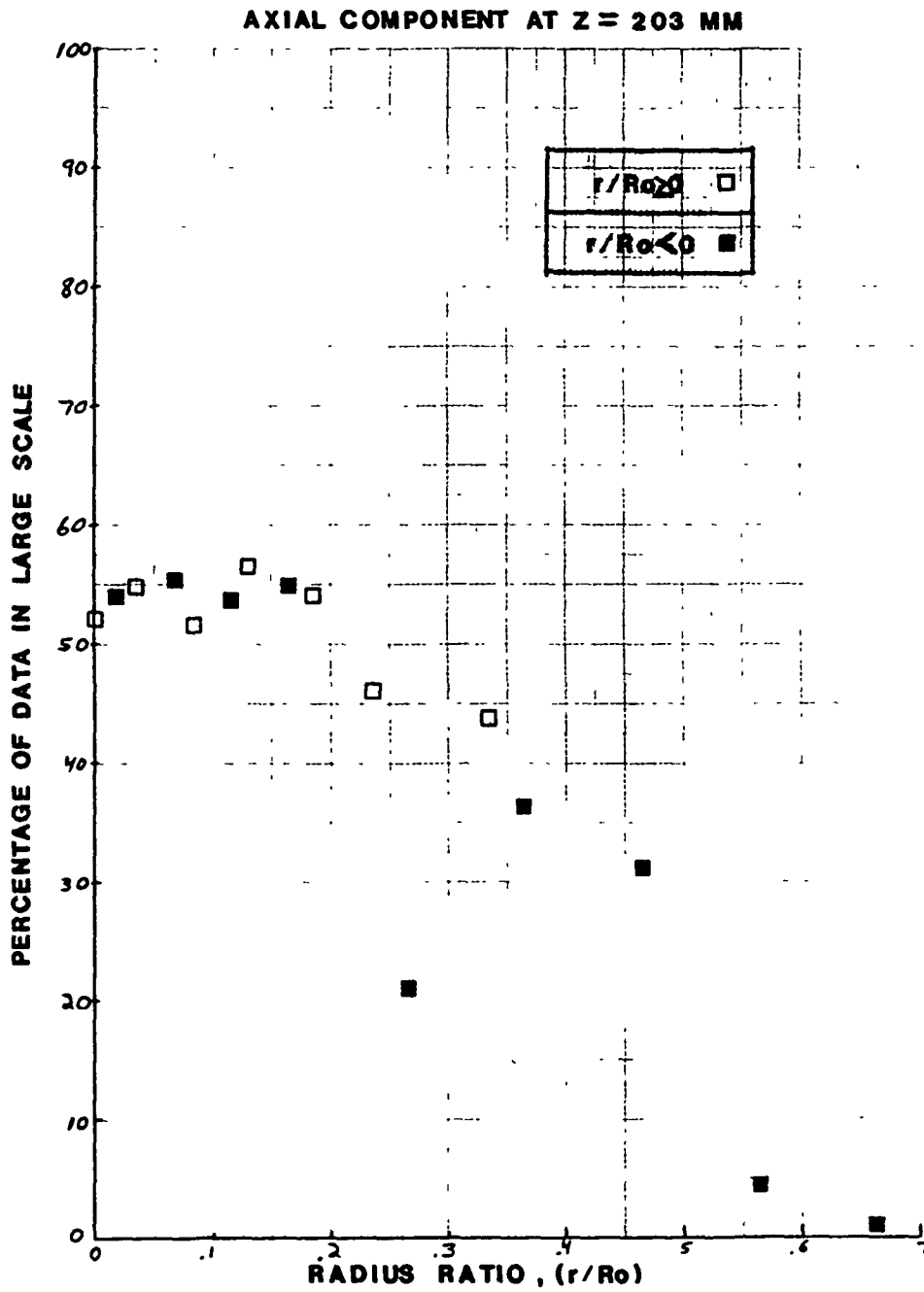


Fig. 17

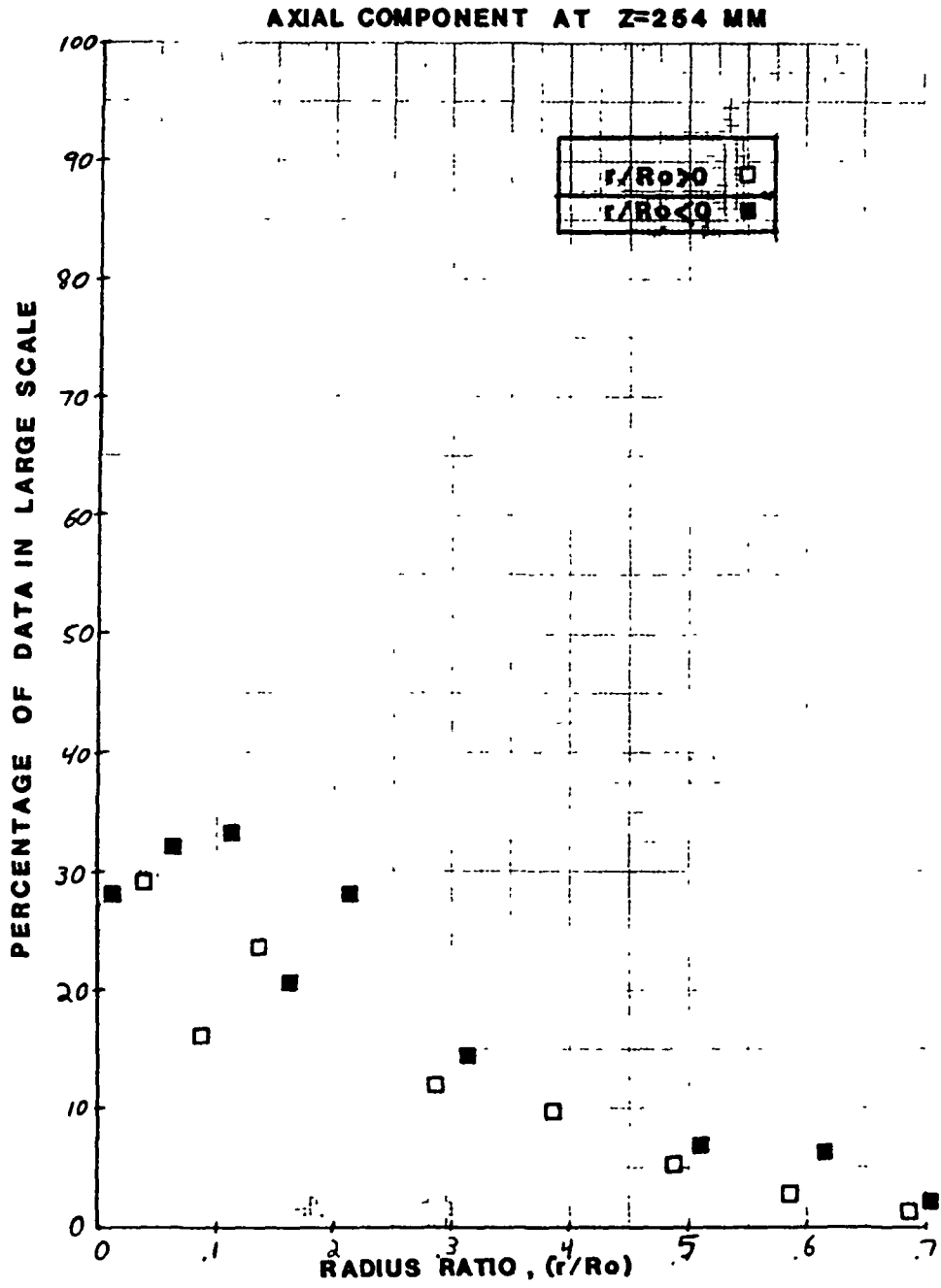


Fig. 18

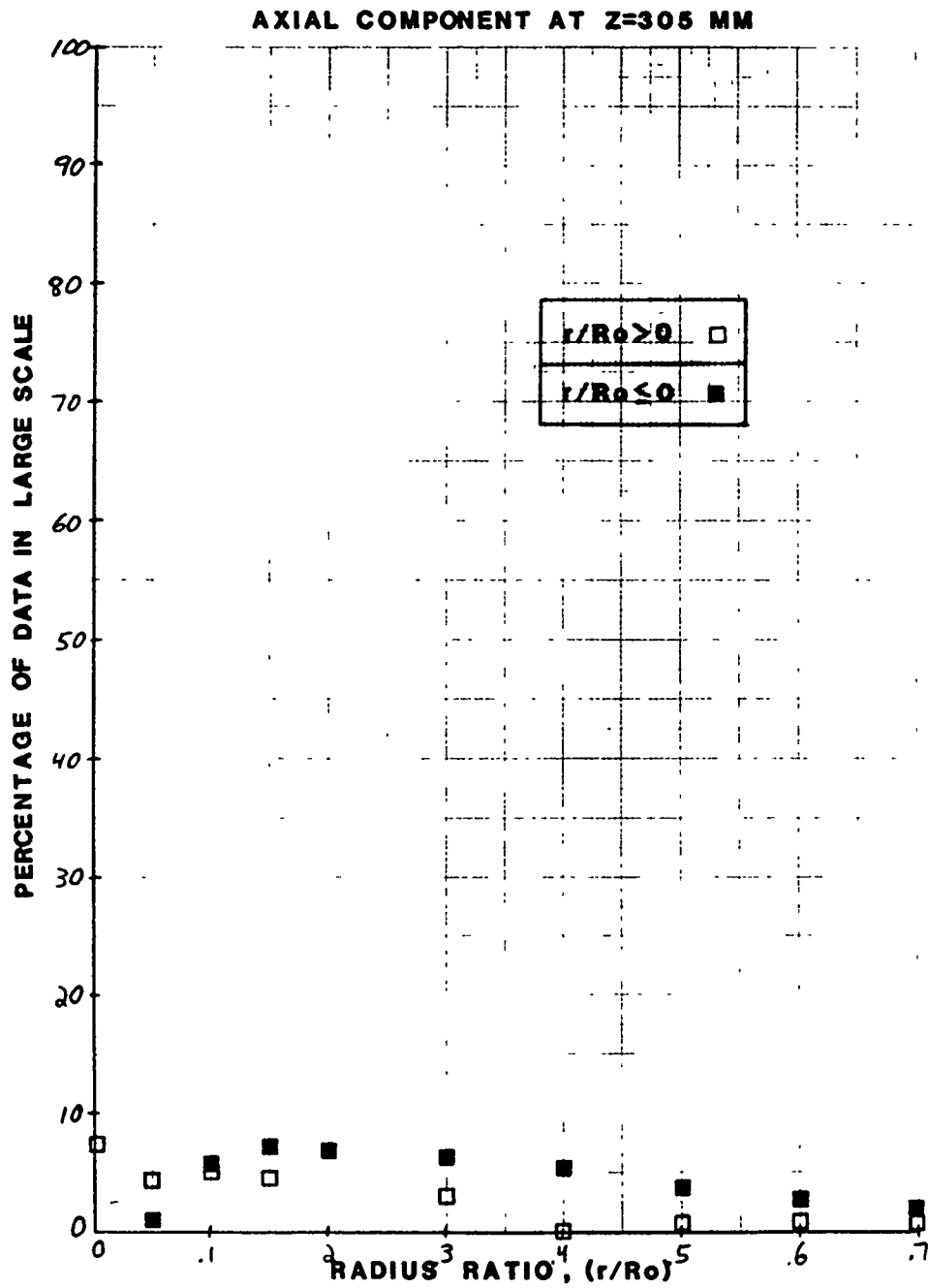


Fig. 19

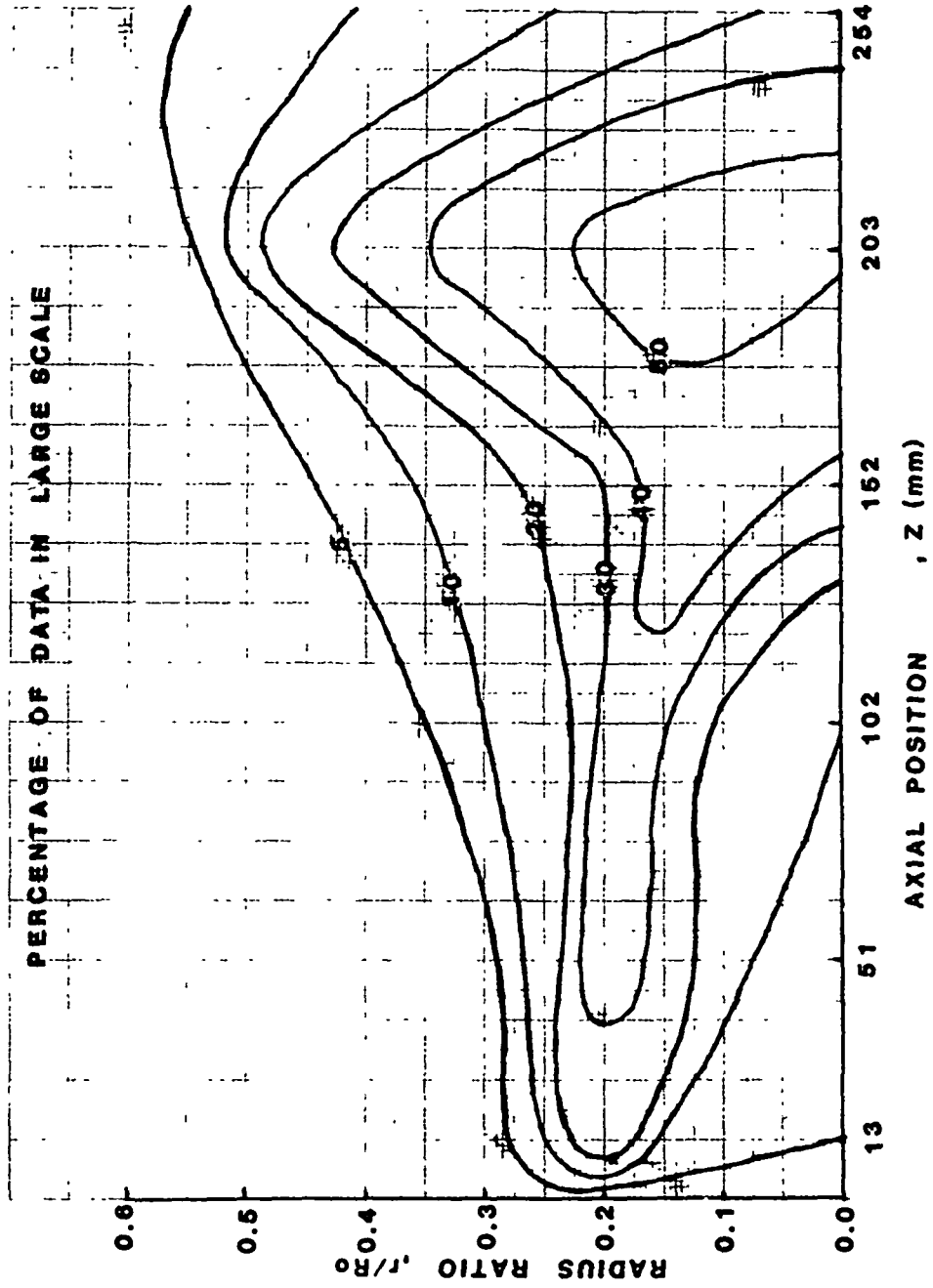
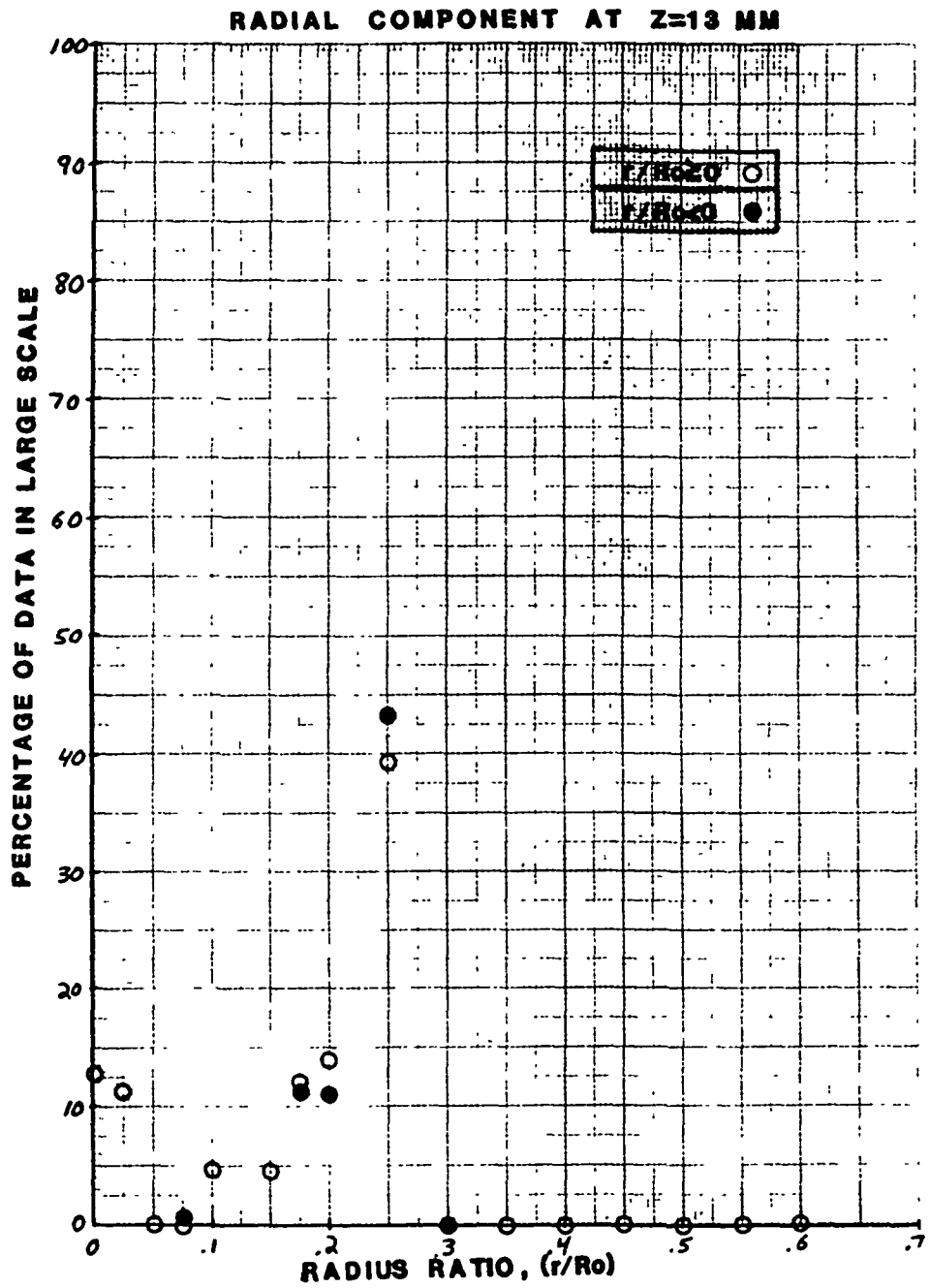


Fig. 20



ORIGINAL PAGE IS
OF POOR QUALITY

Fig. 21

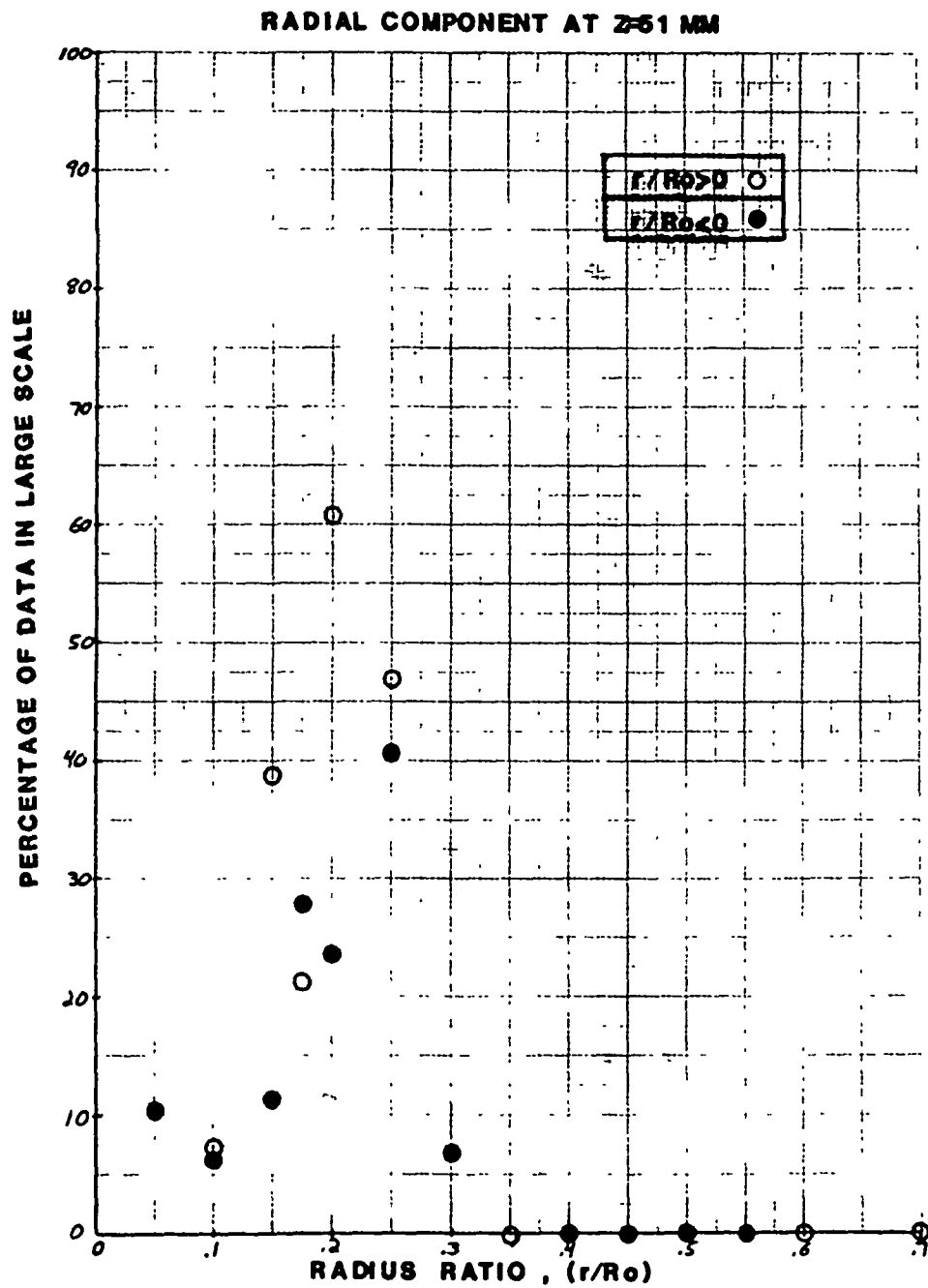
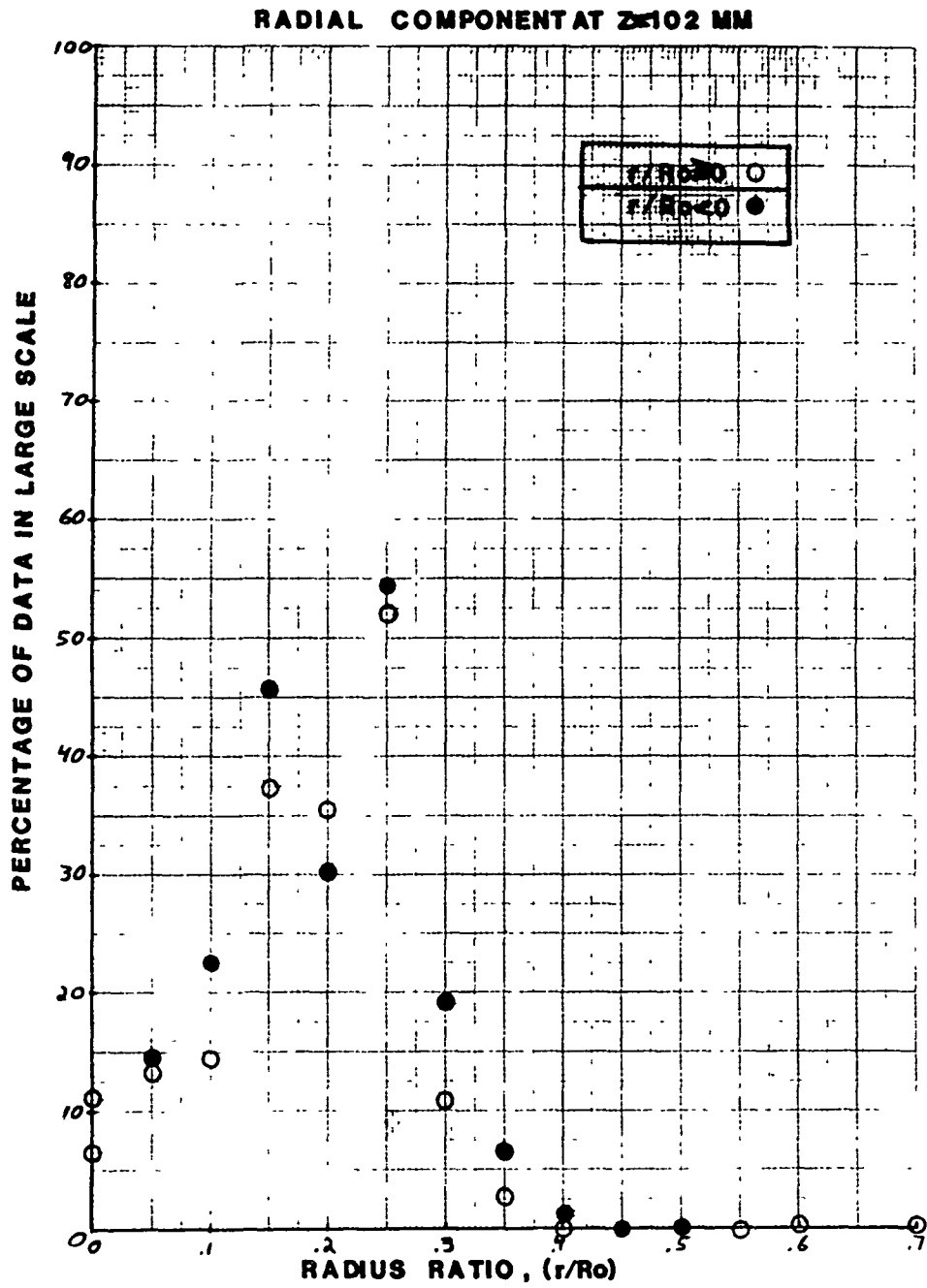


Fig. 22



ORIGINAL PAGE IS
OF POOR QUALITY

Fig. 23

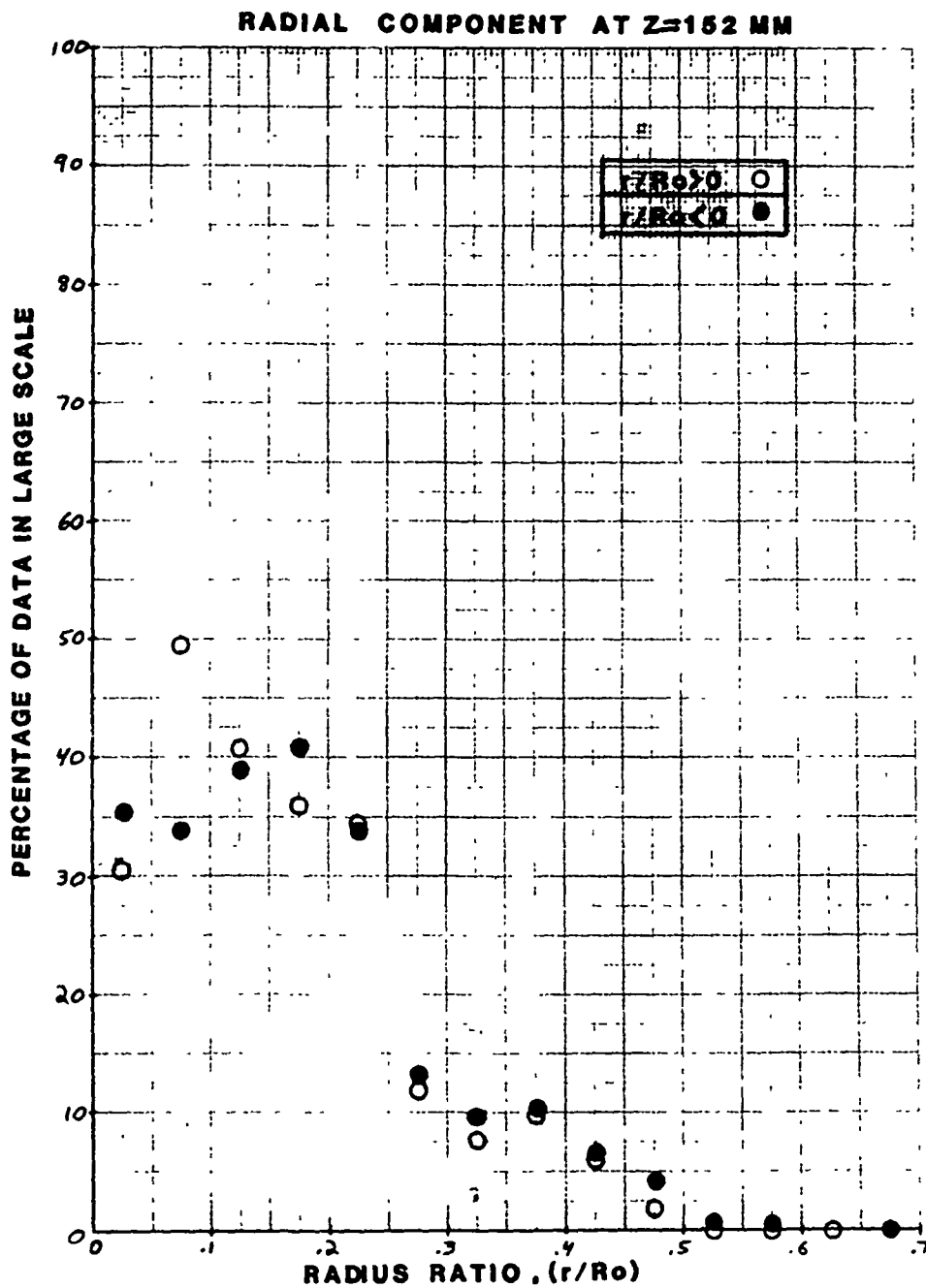


Fig. 24

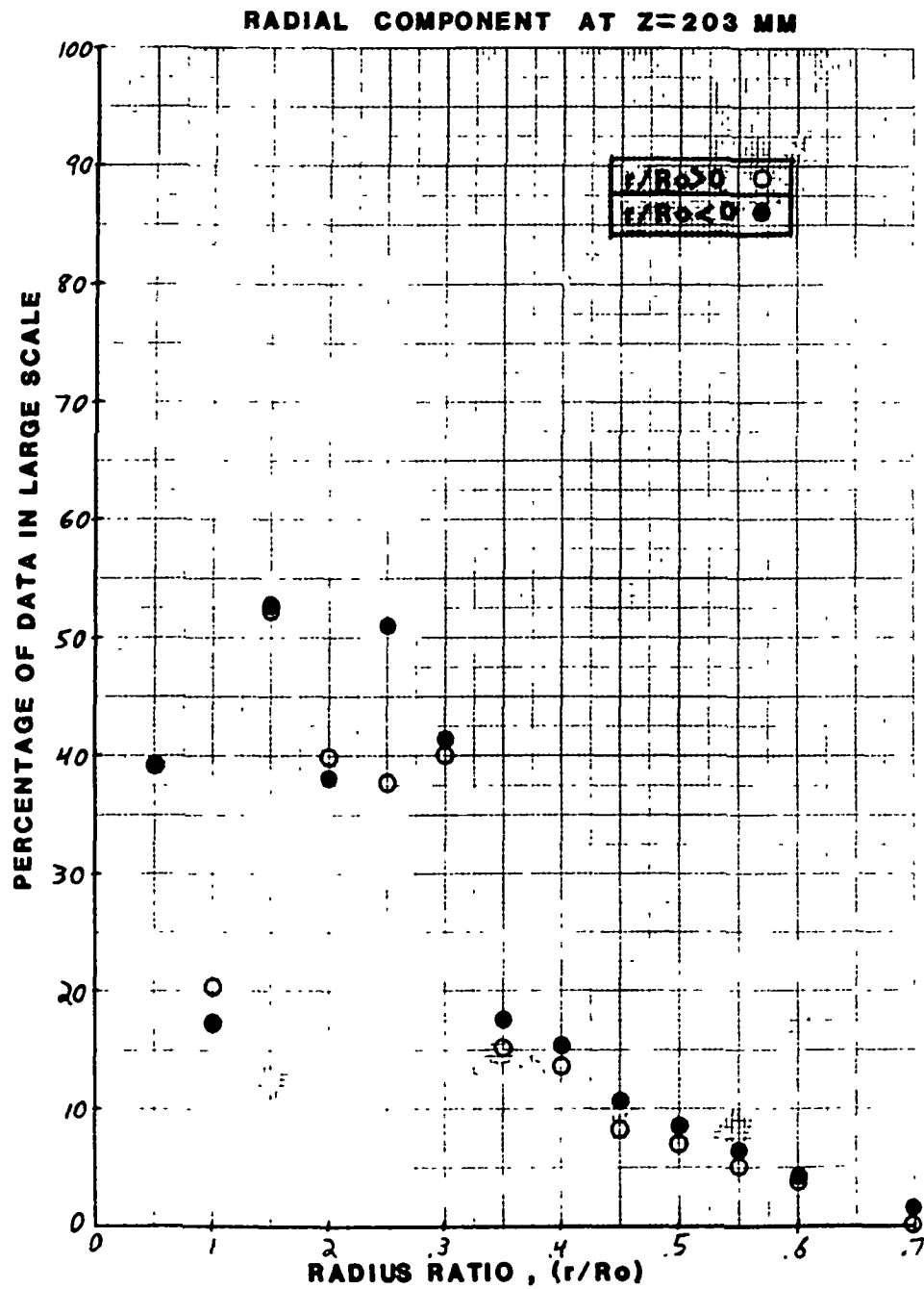


Fig 25

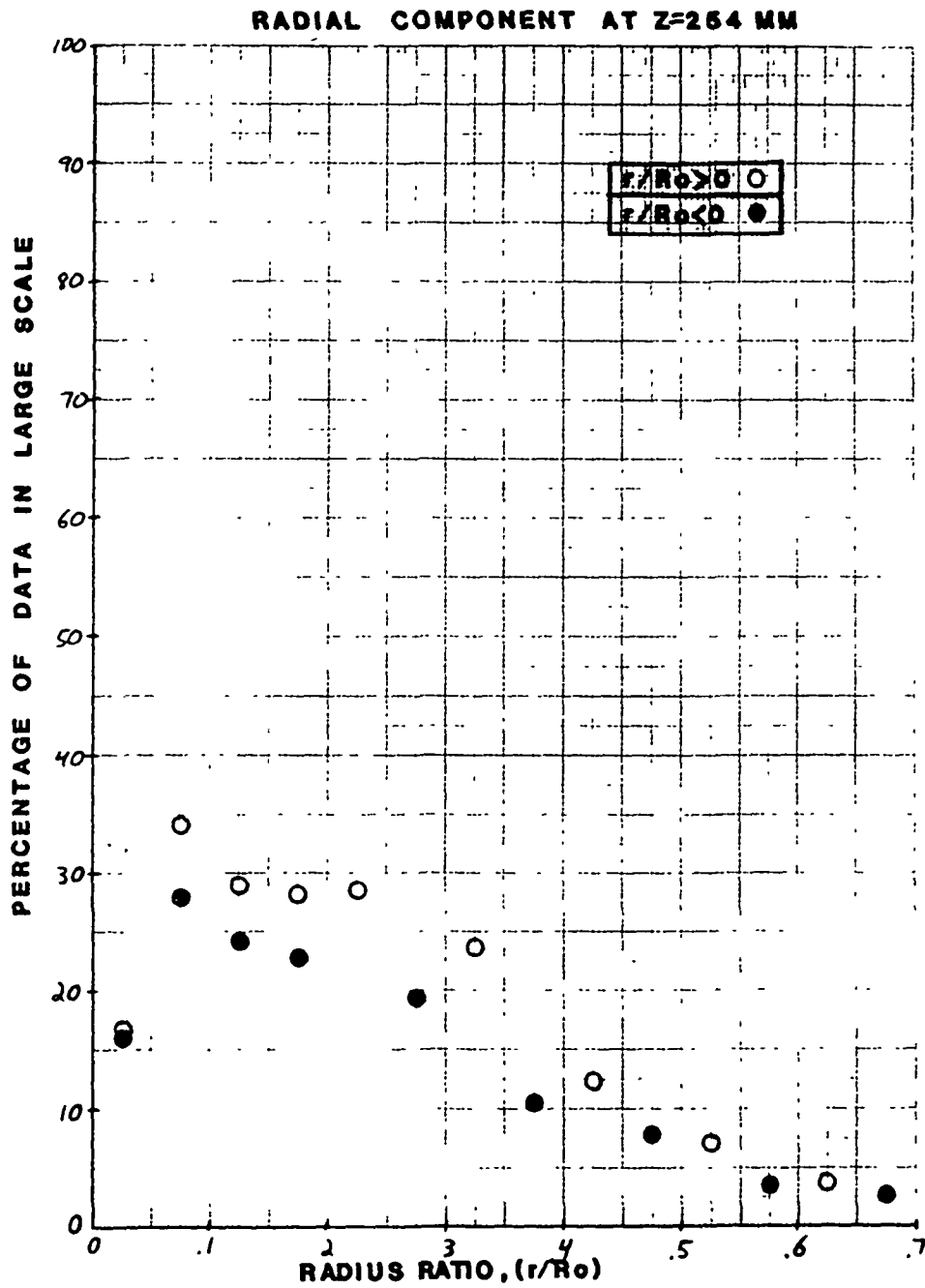


Fig. 26

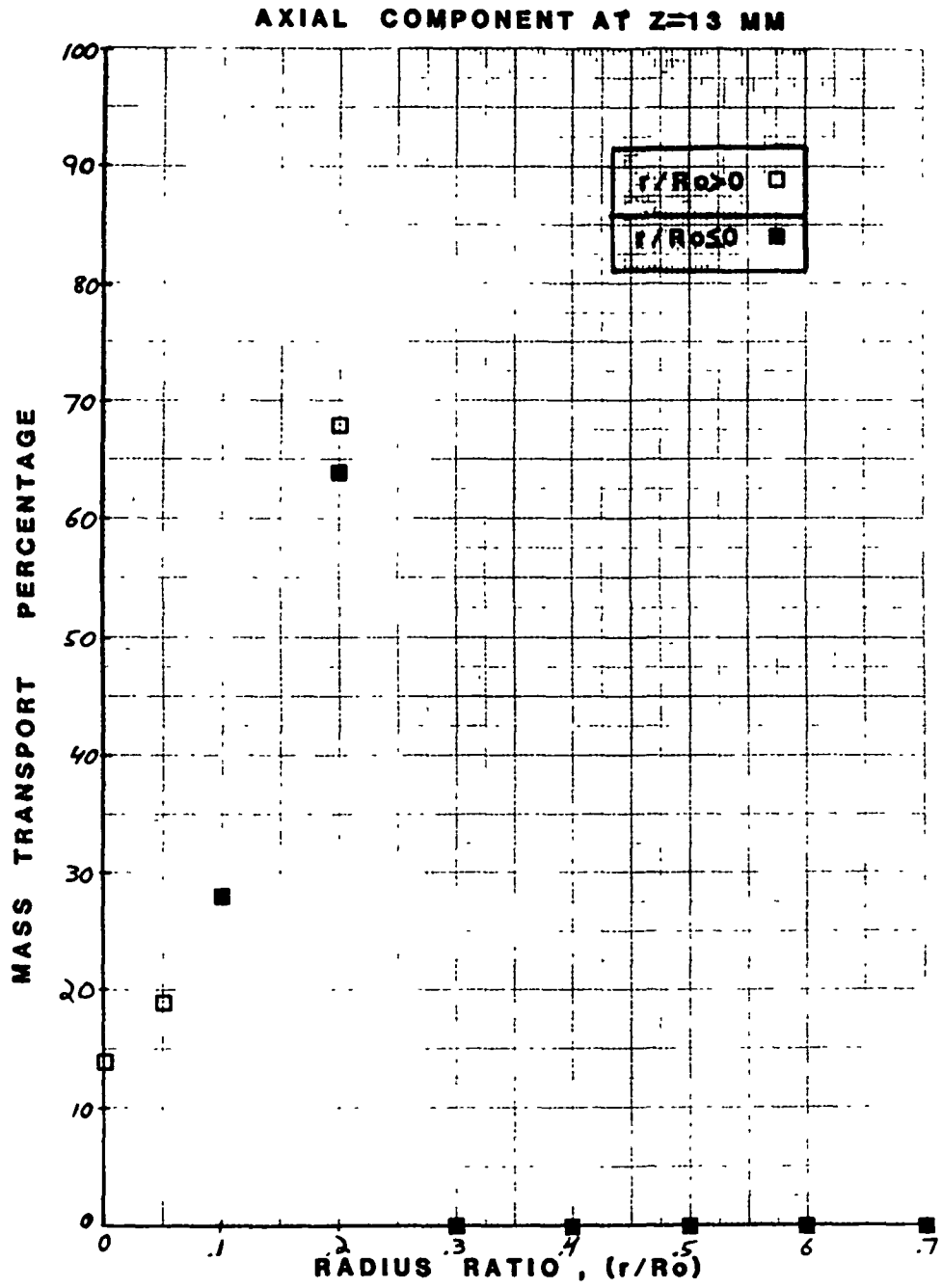


Fig. 27

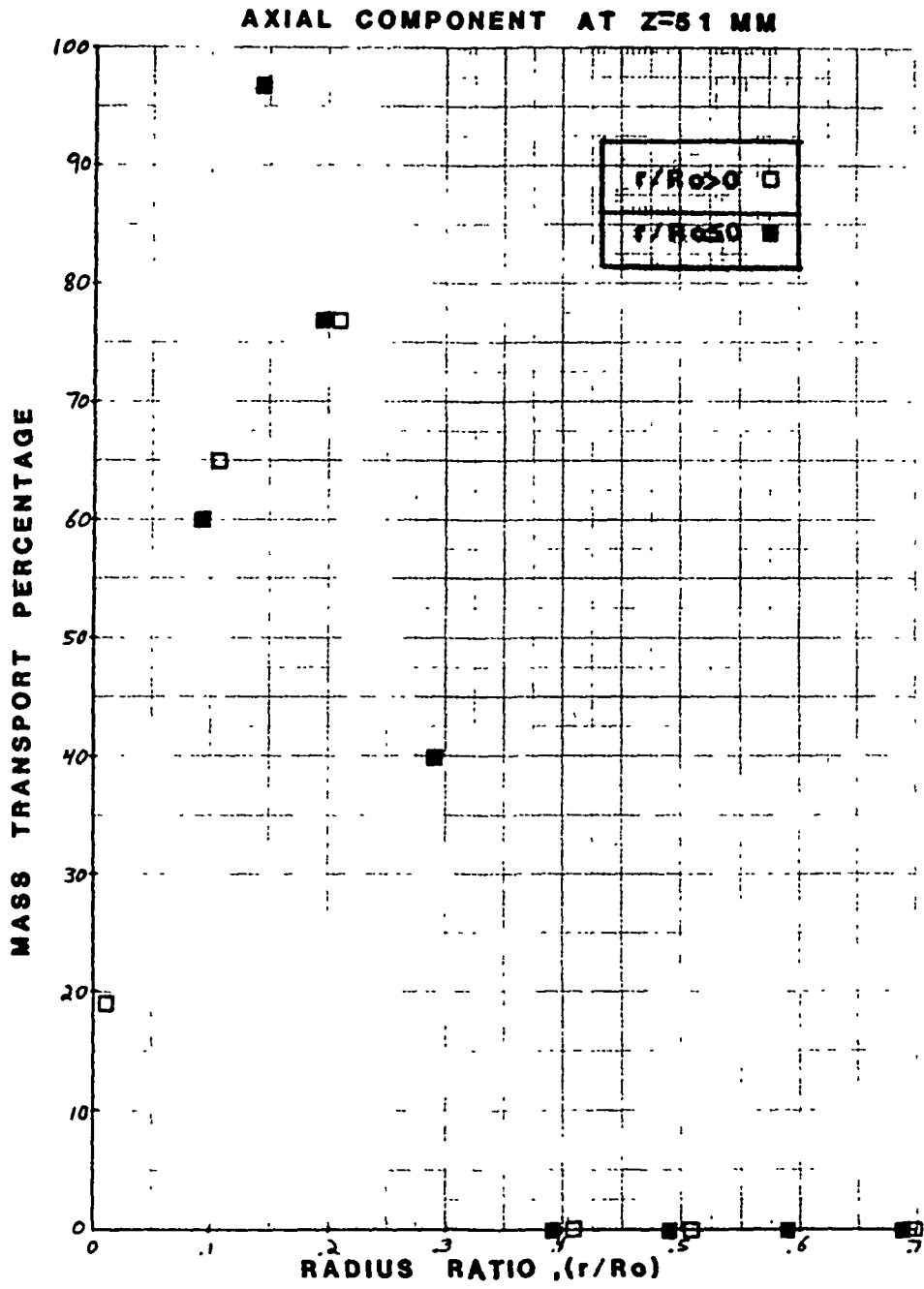
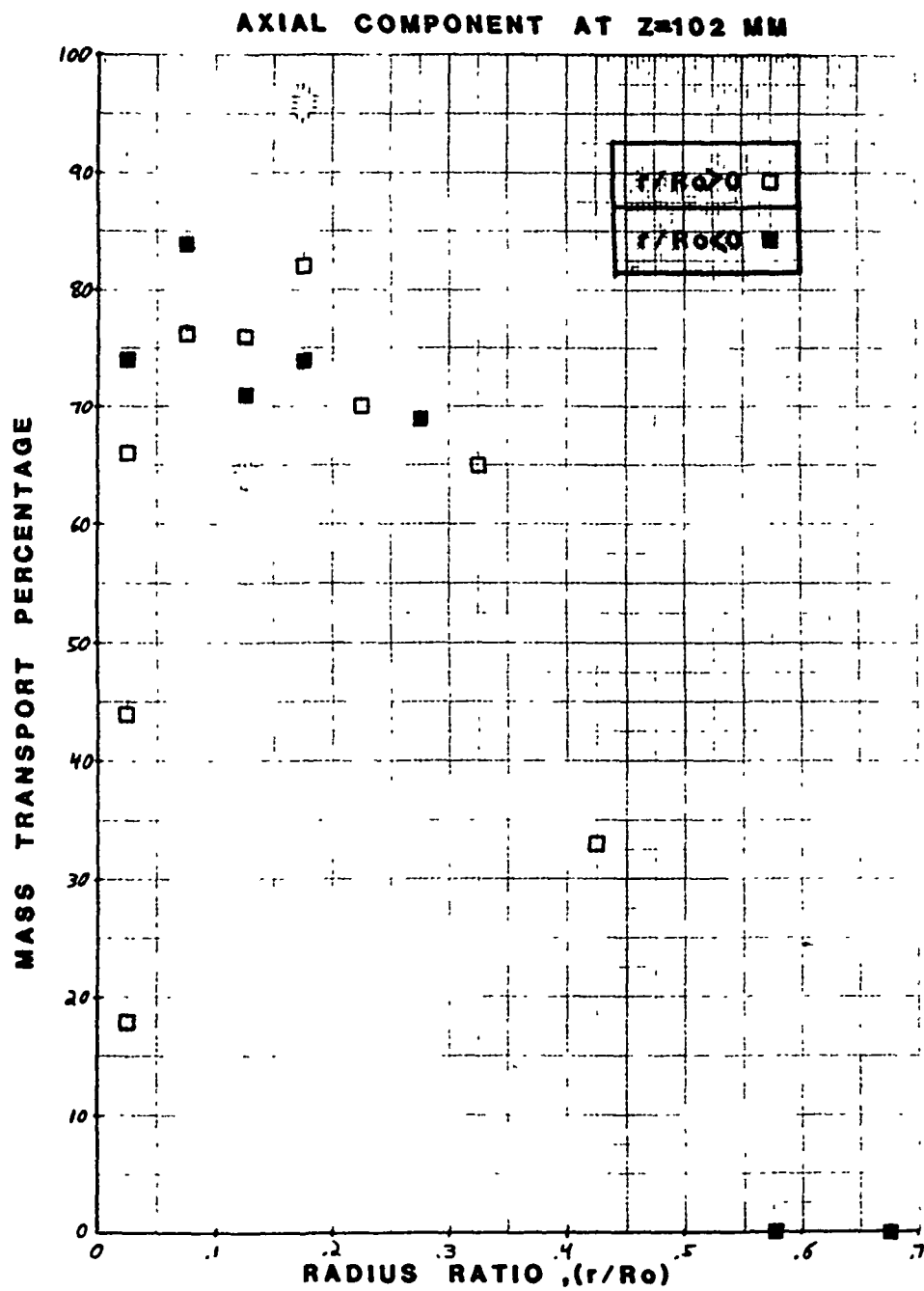


Fig. 28



ORIGINAL PAGE IS
OF POOR QUALITY

Fig 29

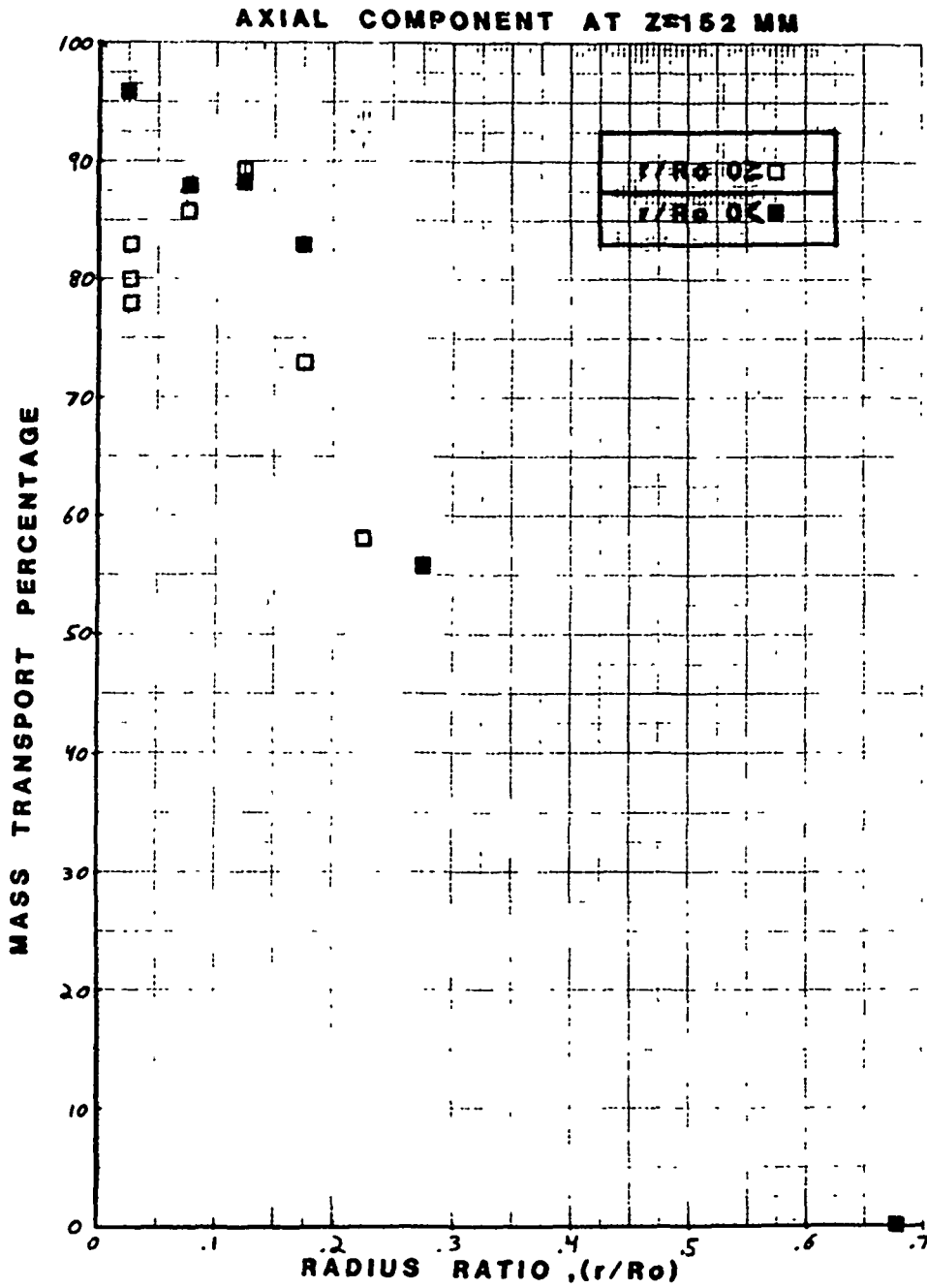
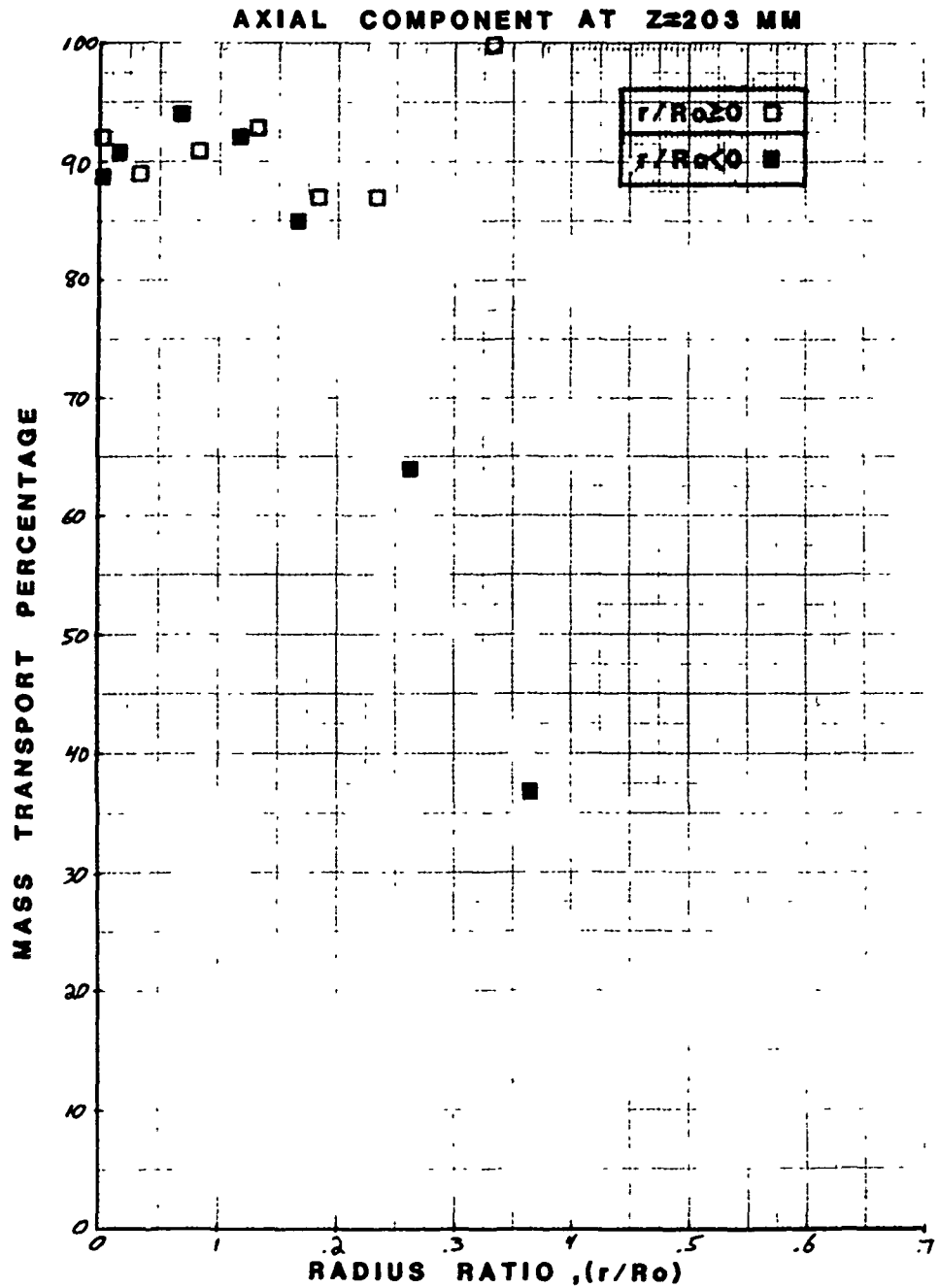


Fig. 30



ORIGINAL PAGE IS
OF POOR QUALITY

Fig. 31

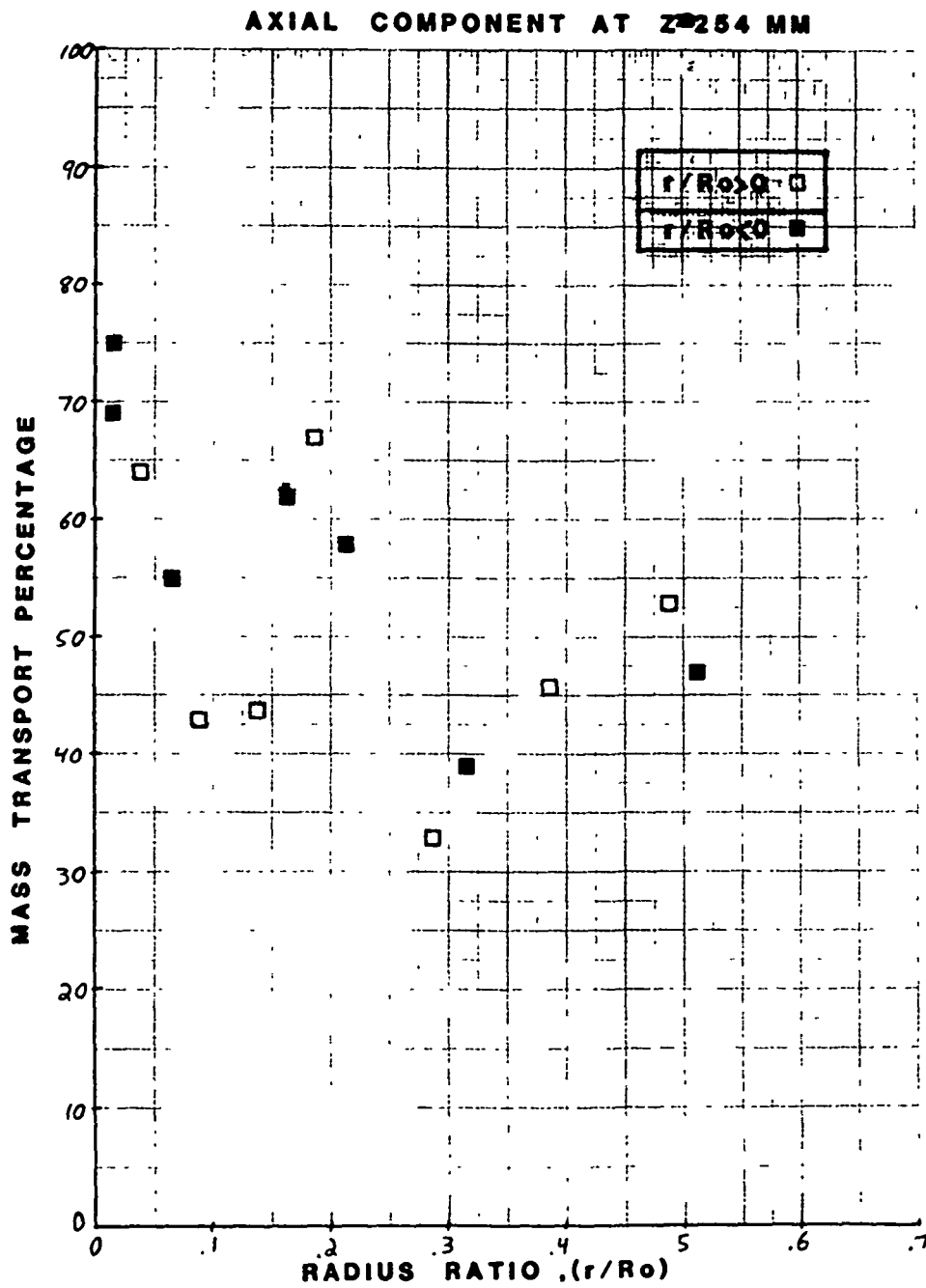


Fig. 32

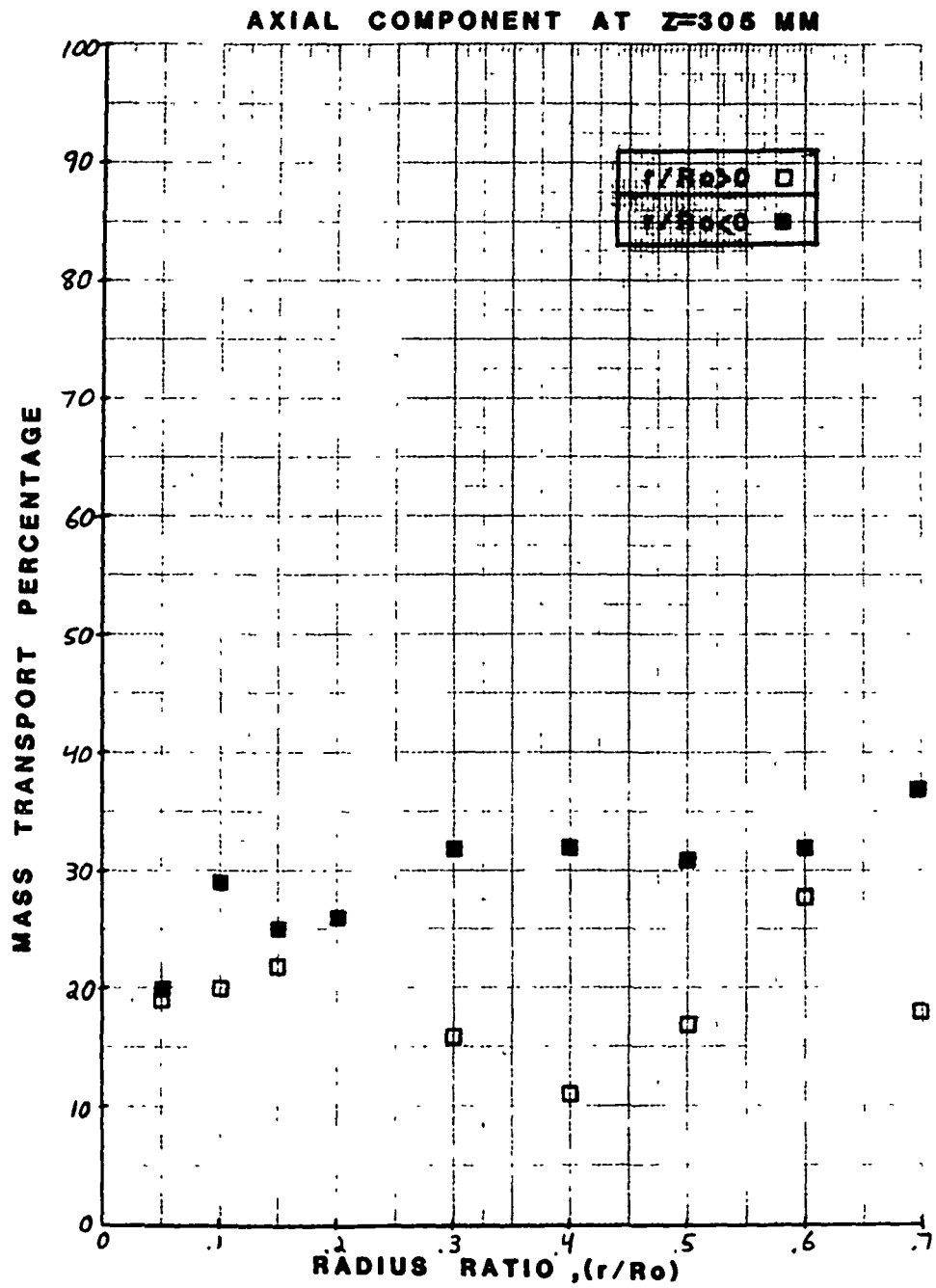


Fig. 33

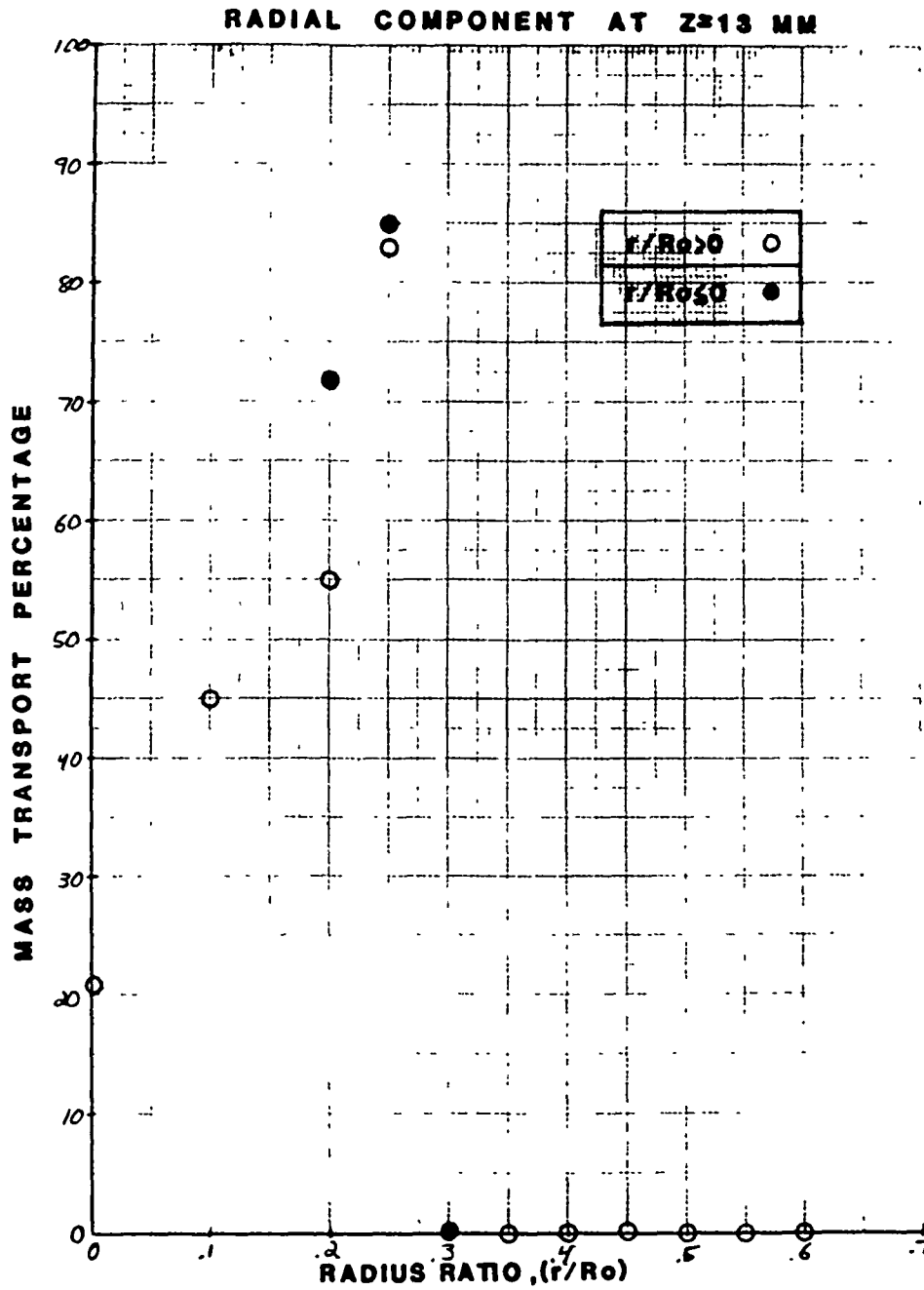
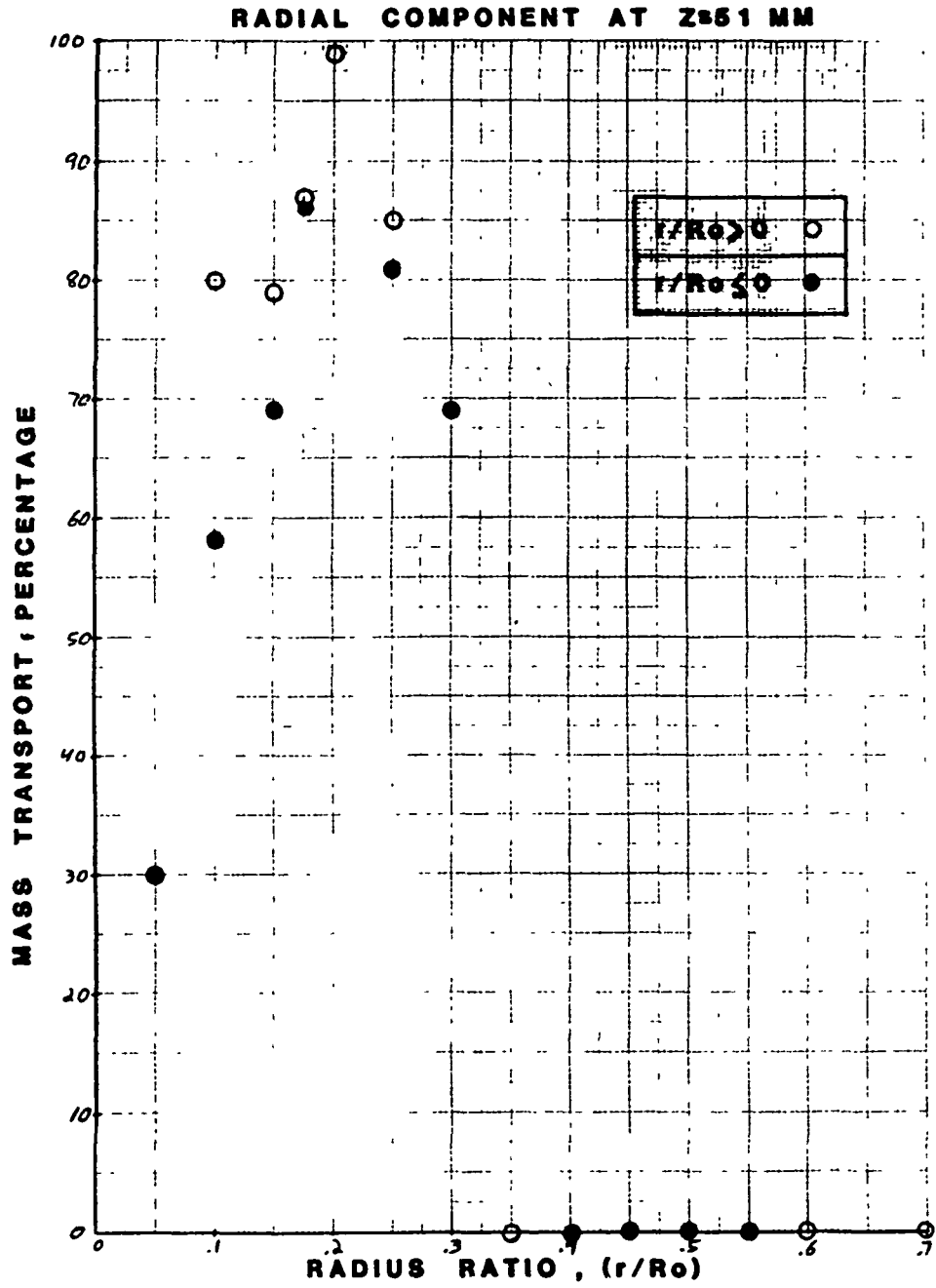


Fig. 34



ORIGINAL PAGE IS
OF POOR QUALITY

Fig. 35

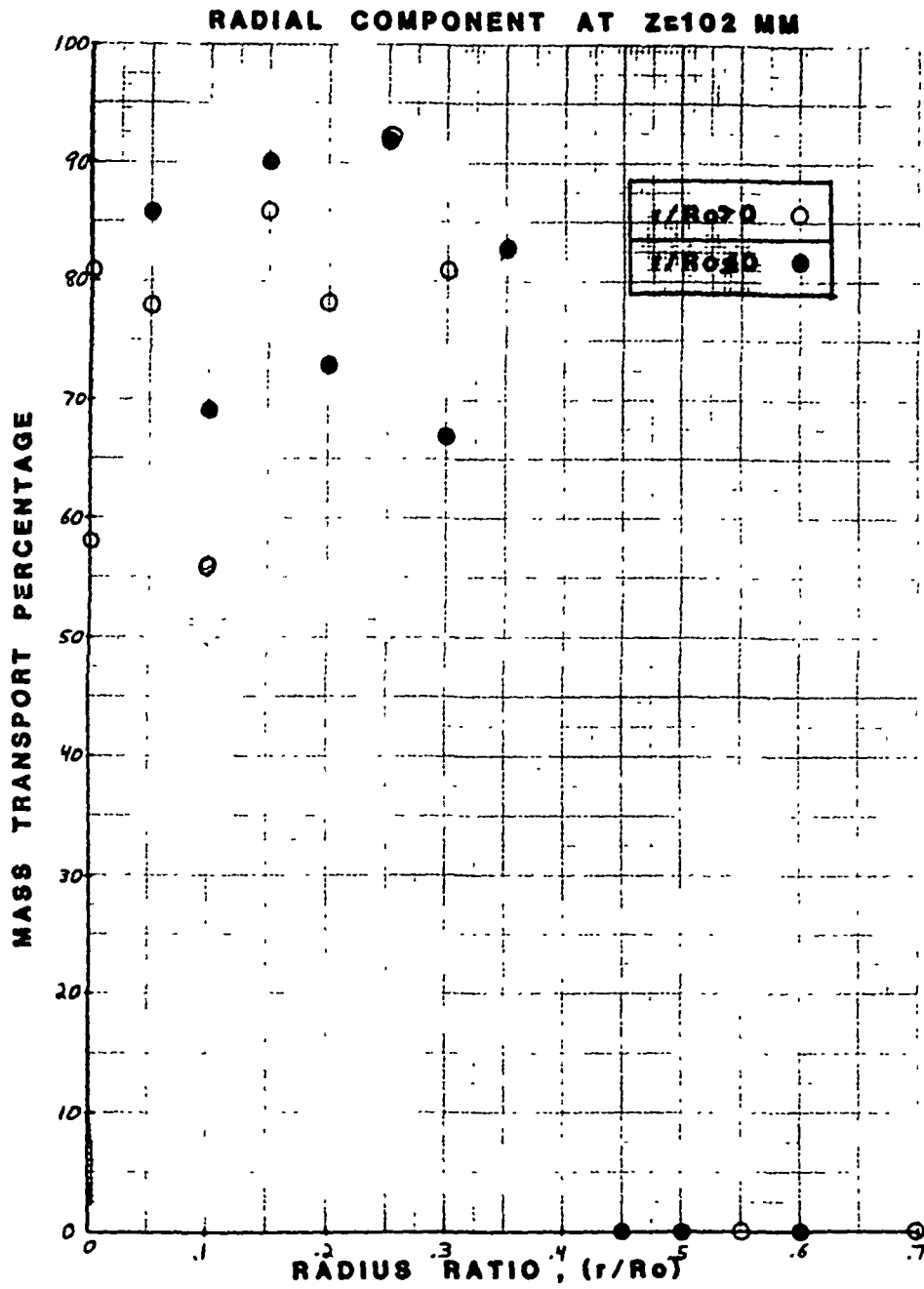


Fig. 36

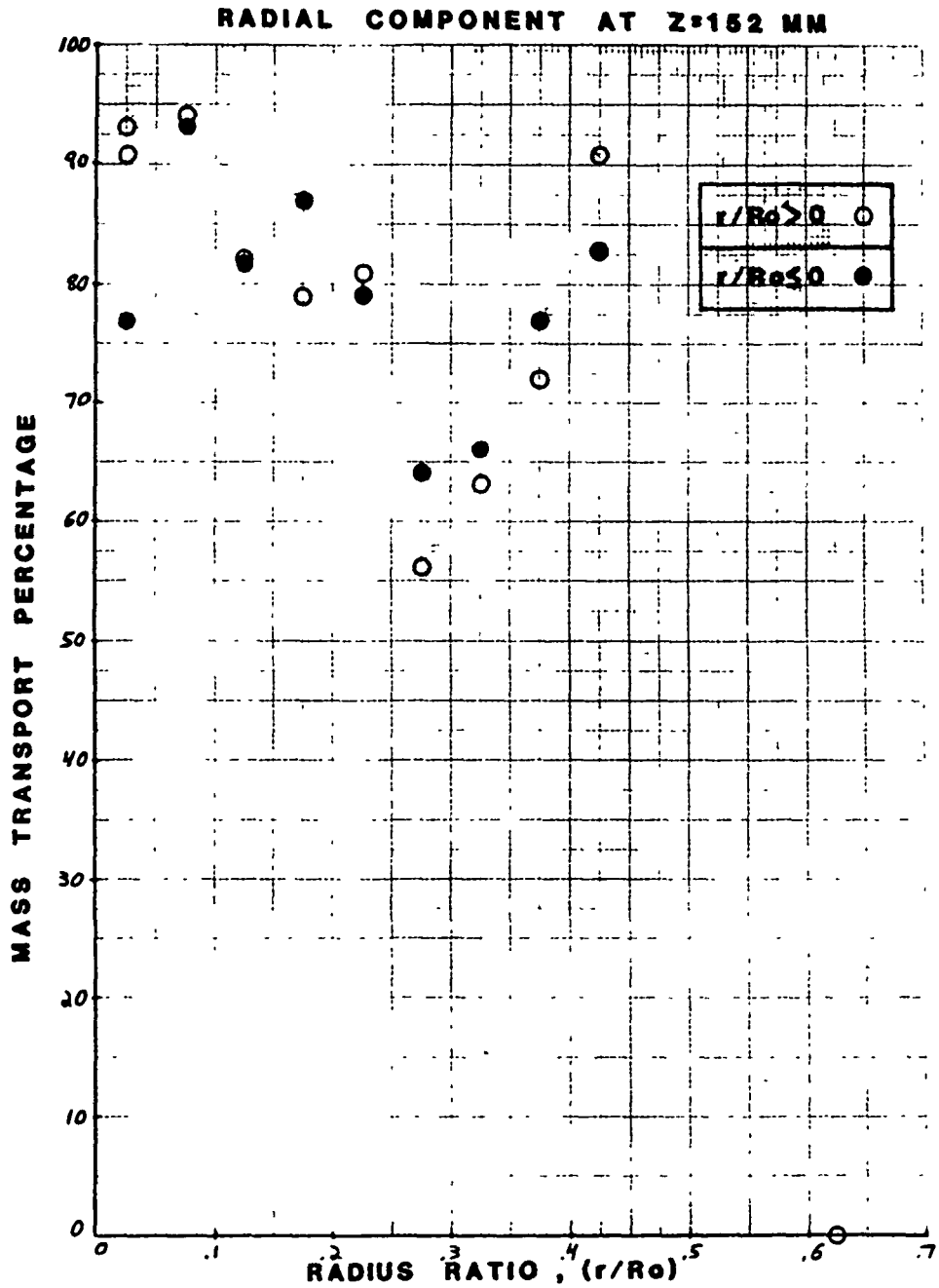


Fig. 37

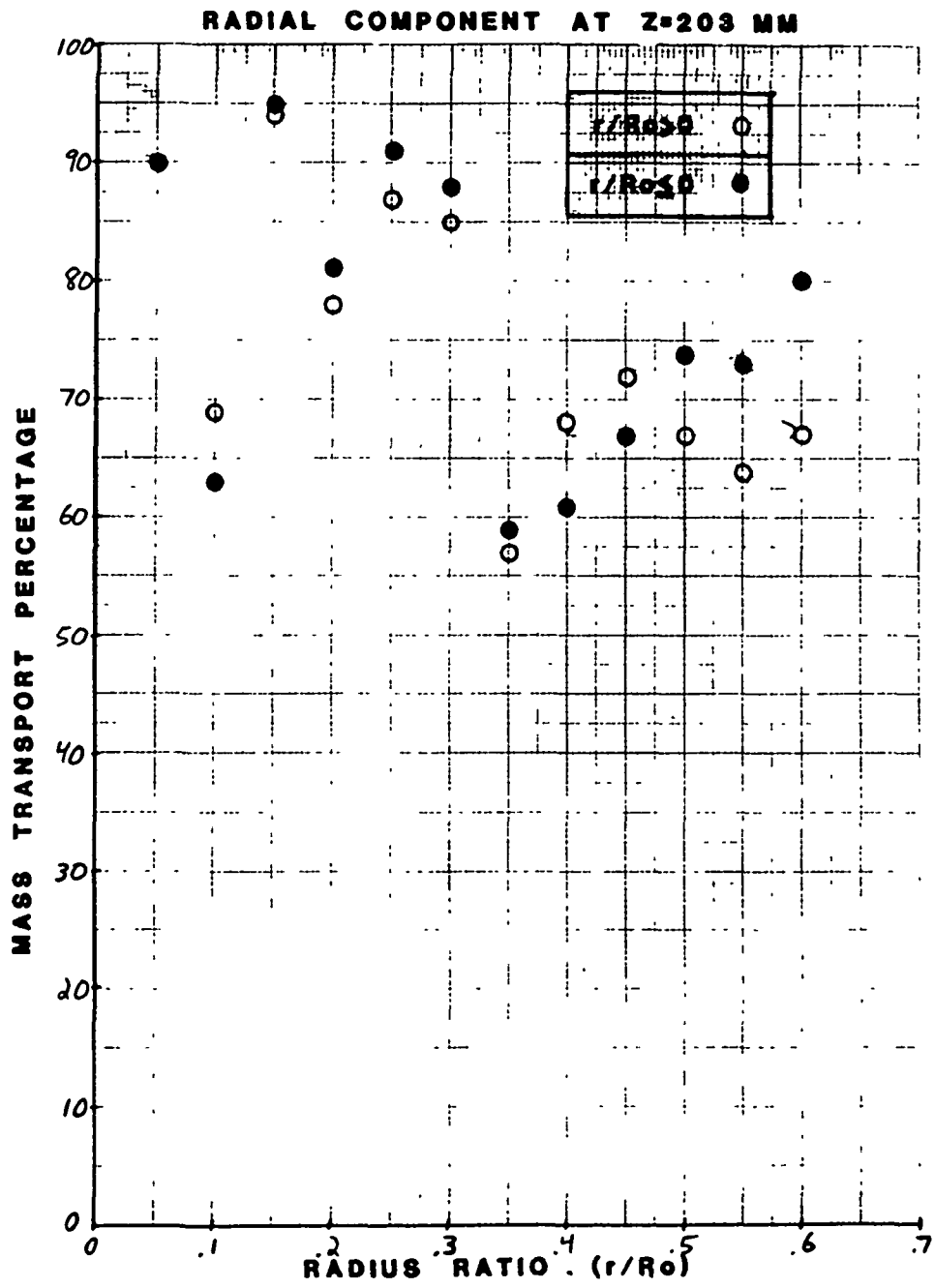
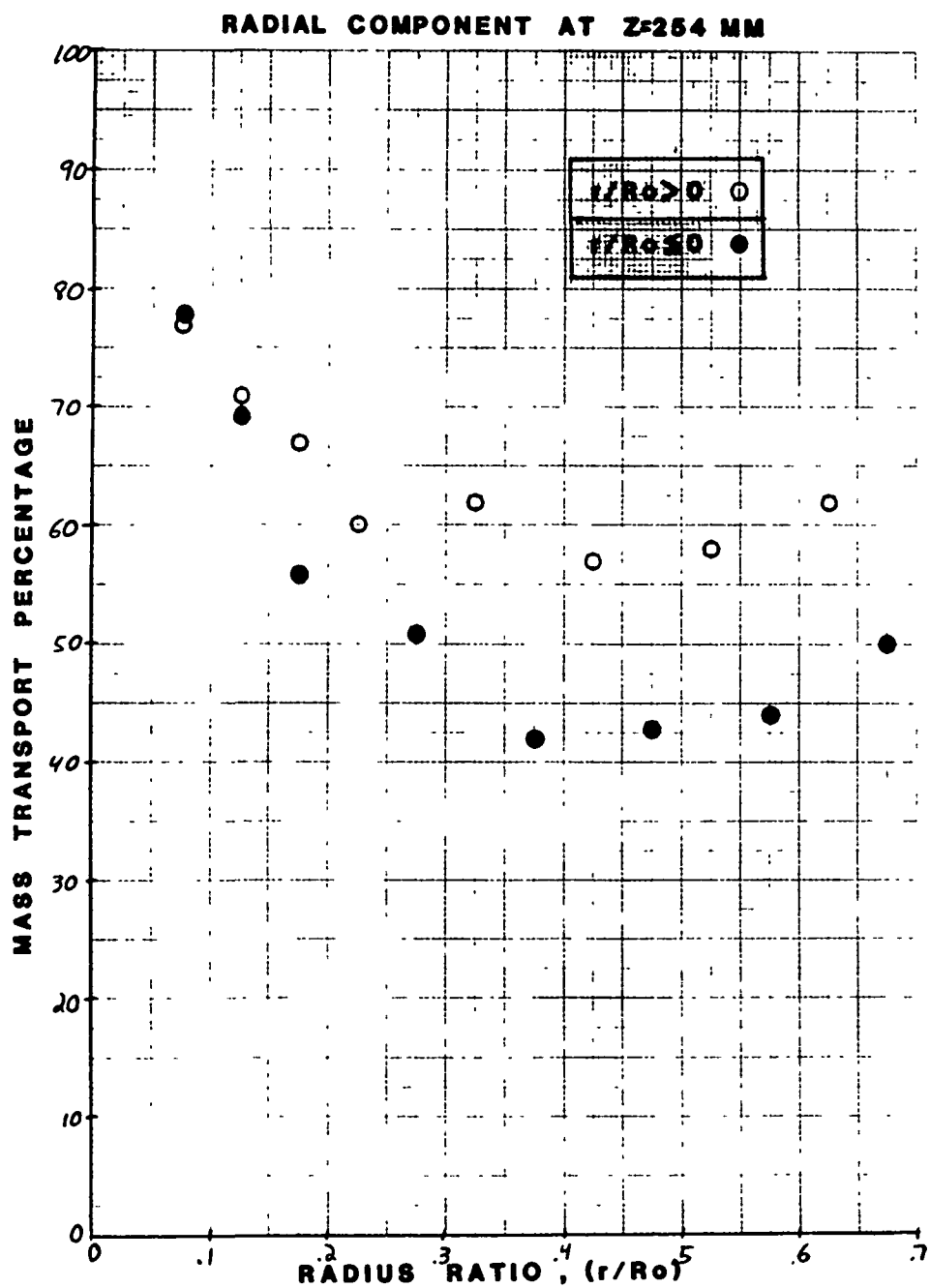
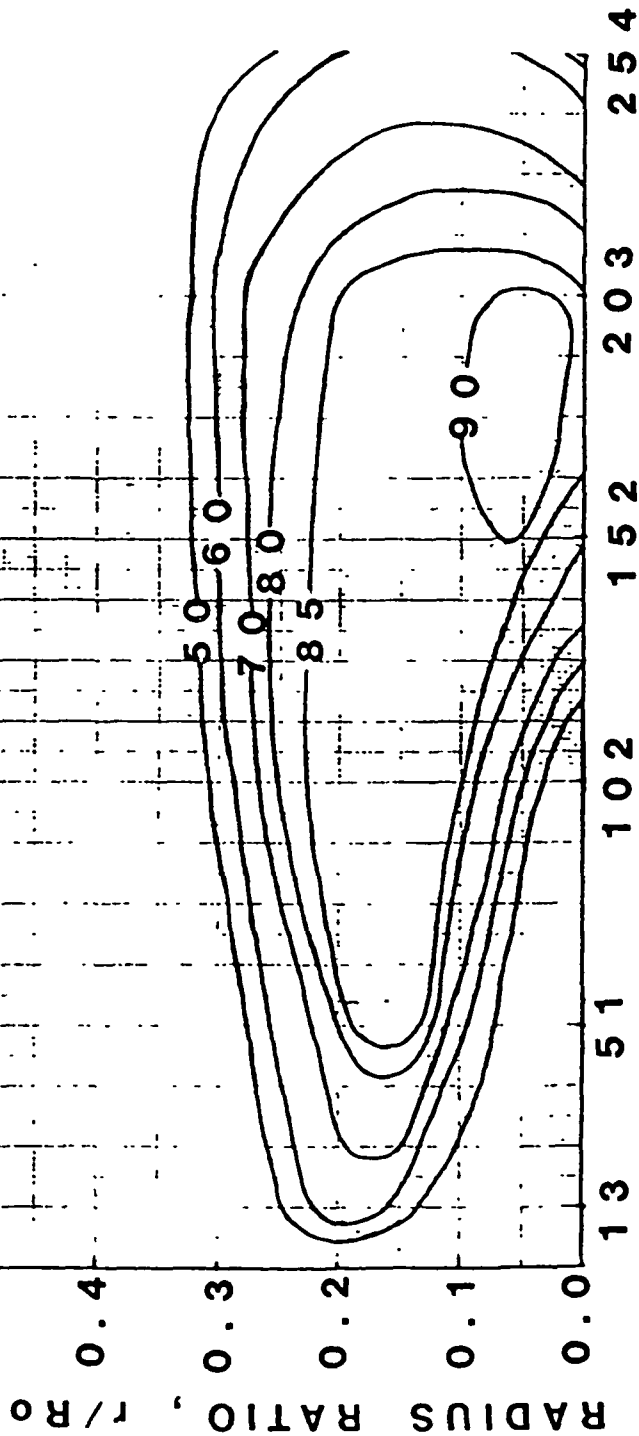


Fig. 38



AXIAL MASS TRANSPORT LARGE SCALE CONTRIBUTION



AXIAL POSITION, Z (mm)

ORIGINAL PAGE IS
OF POOR QUALITY

Fig. 39

TRANSPORT ZONES SUMMARY

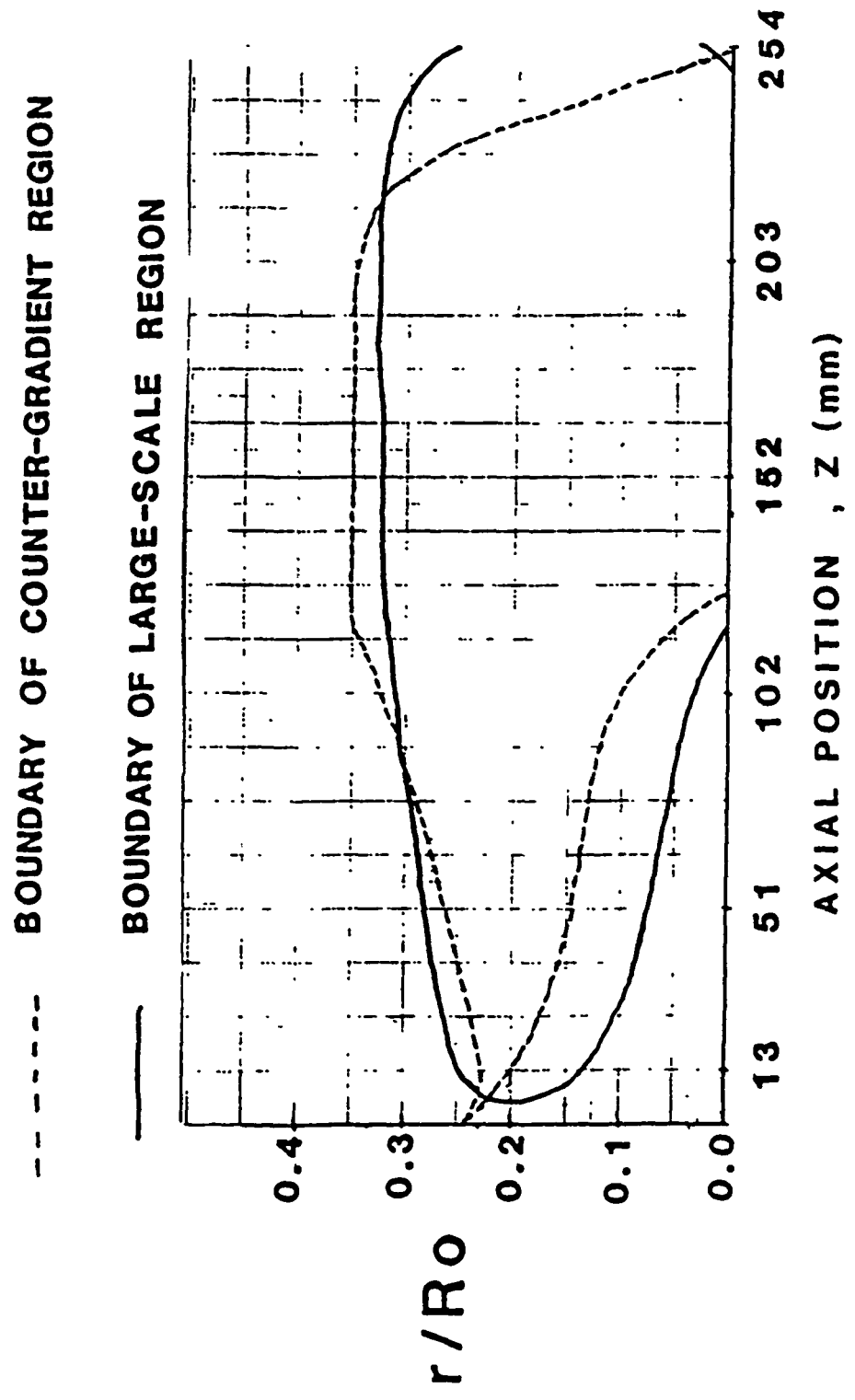


Fig 40

Fig. 41

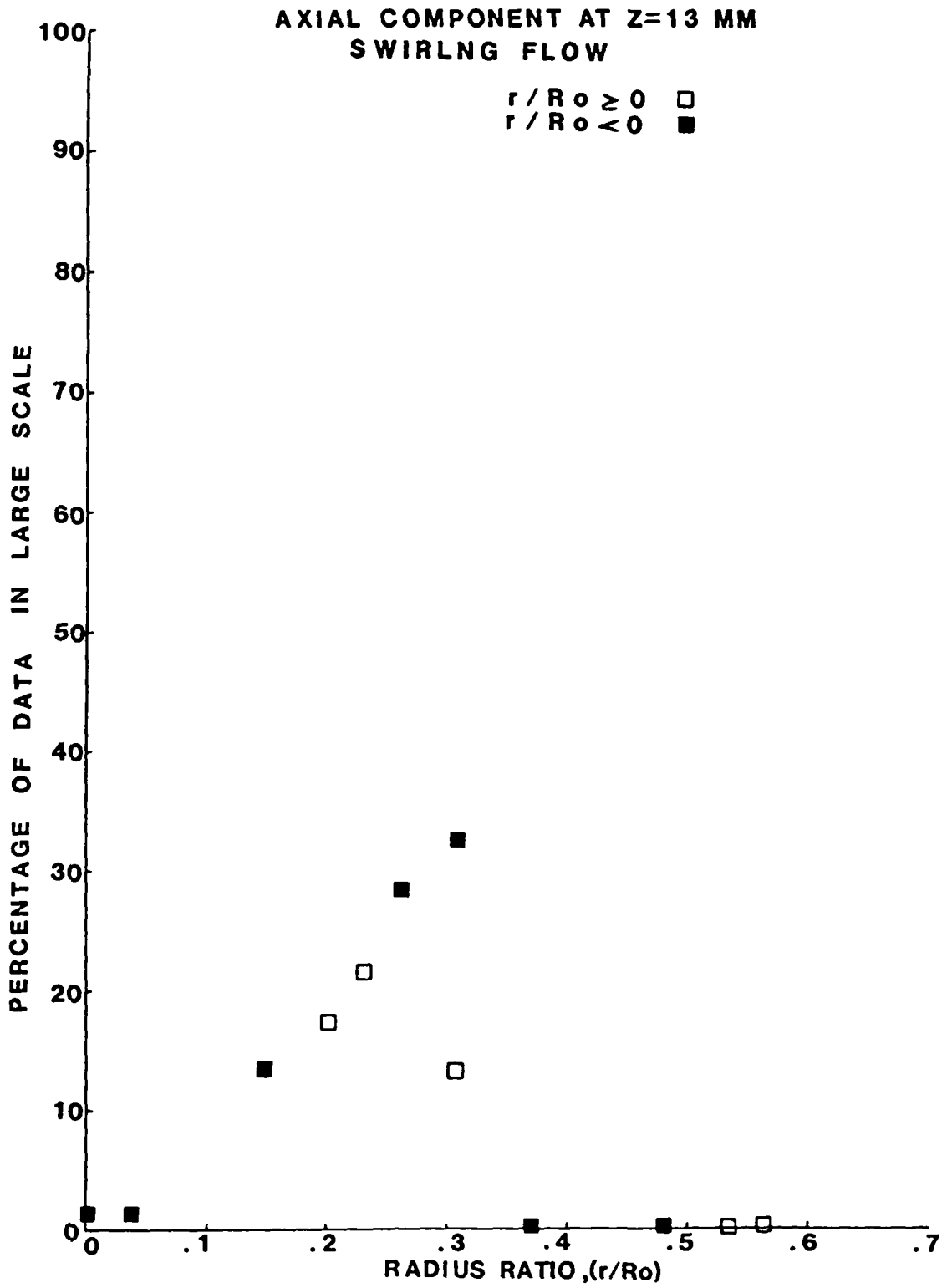


Fig. 42

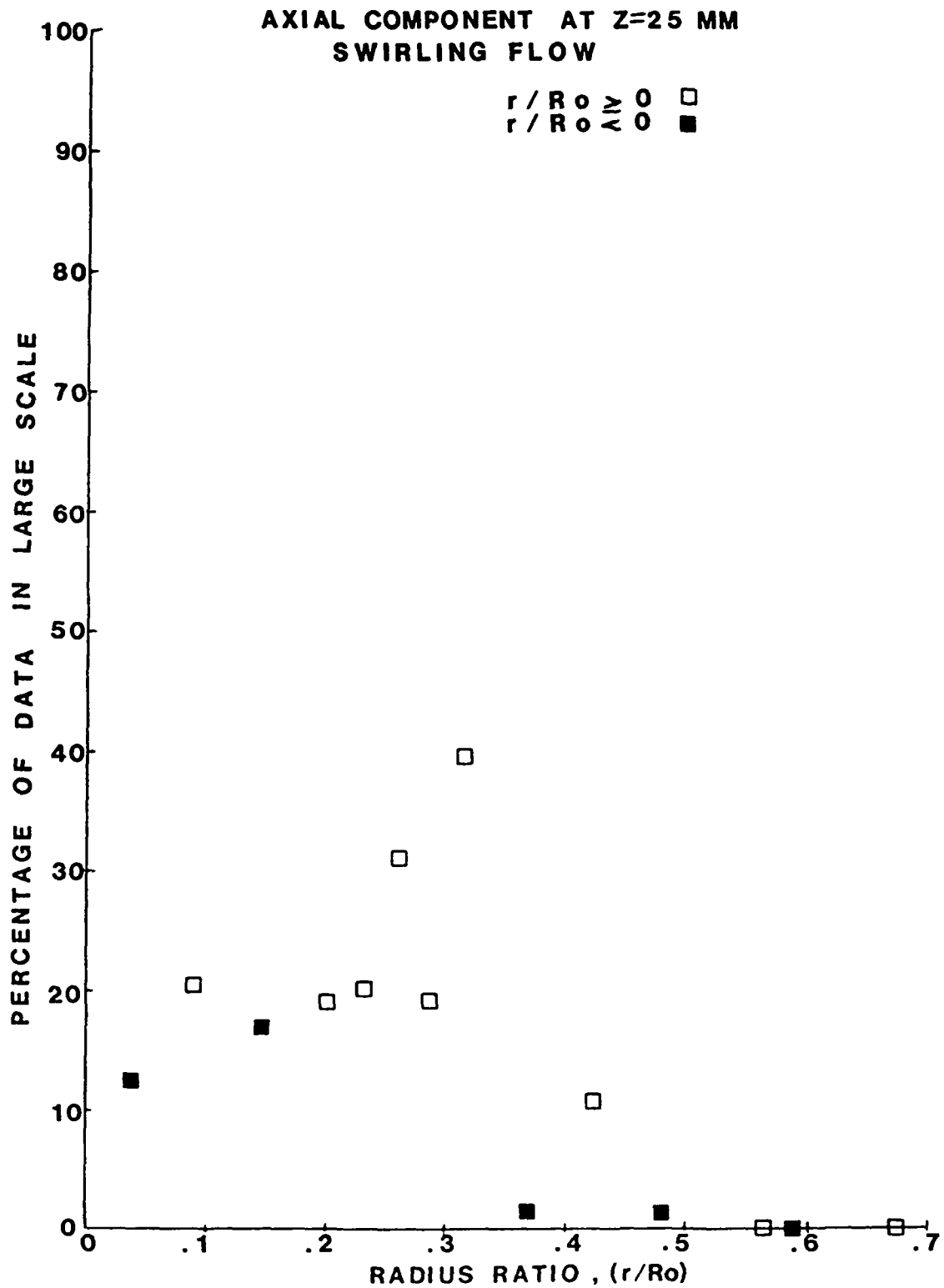


Fig. 43

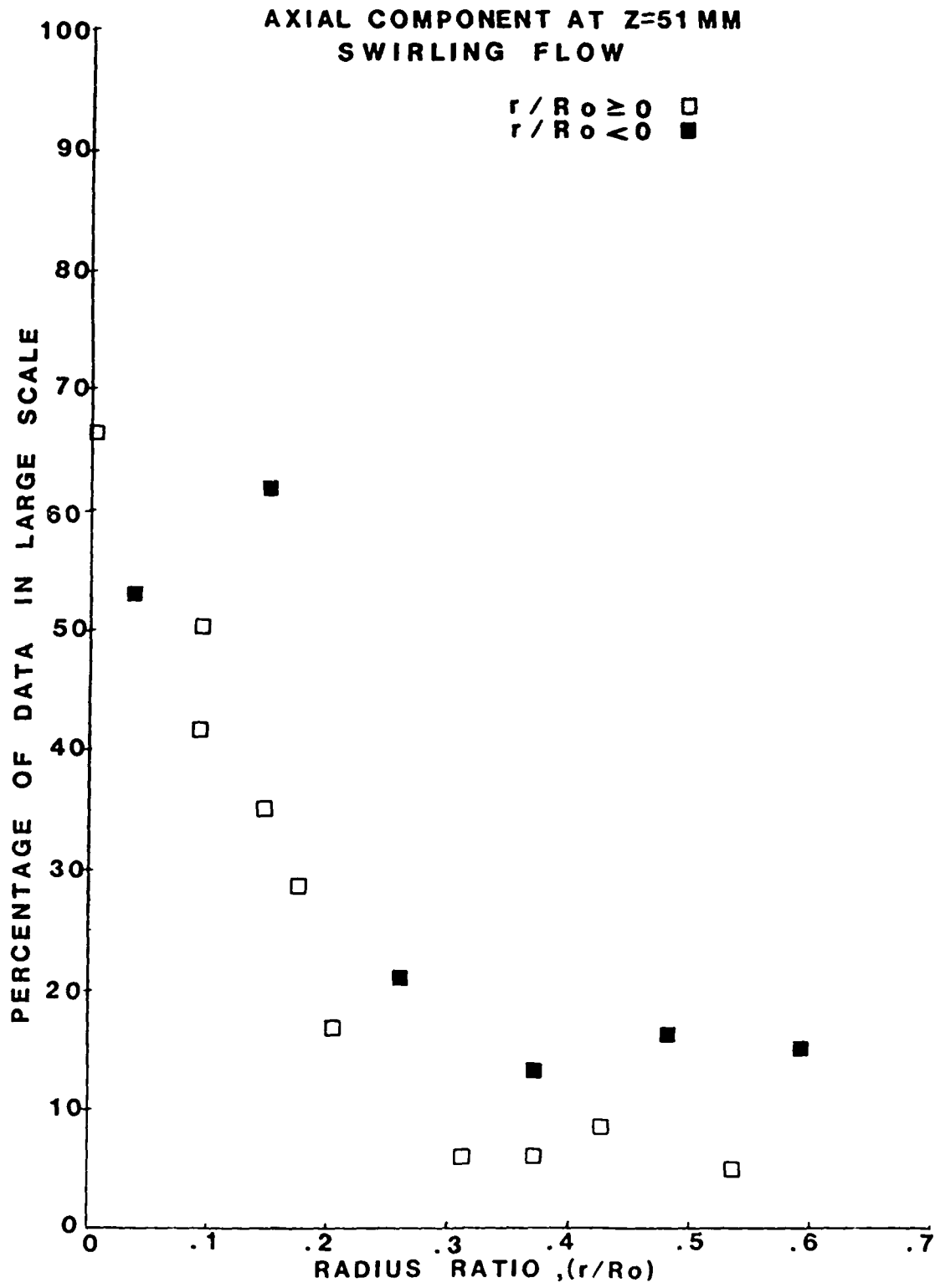


Fig. 44

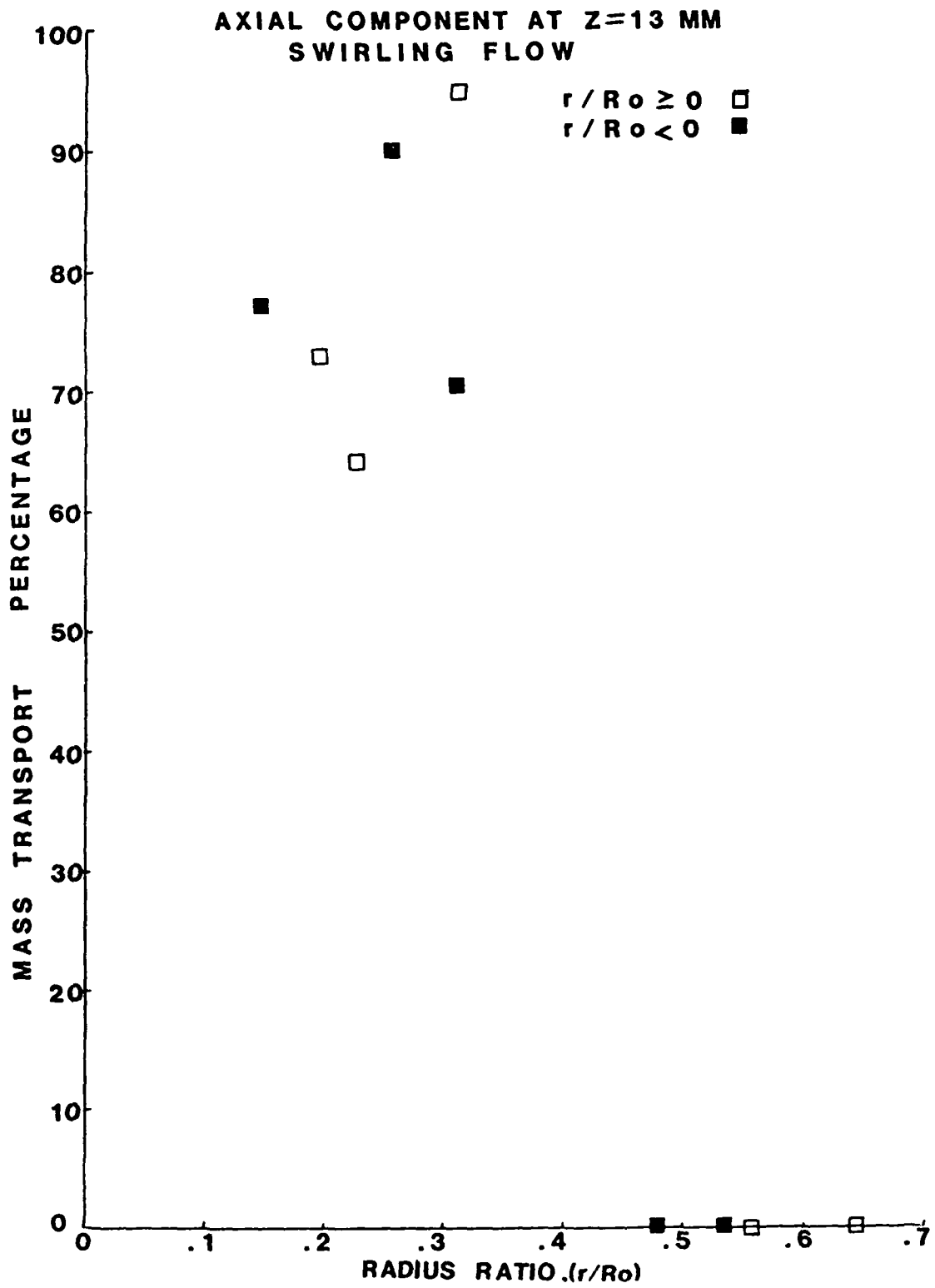


Fig. 45

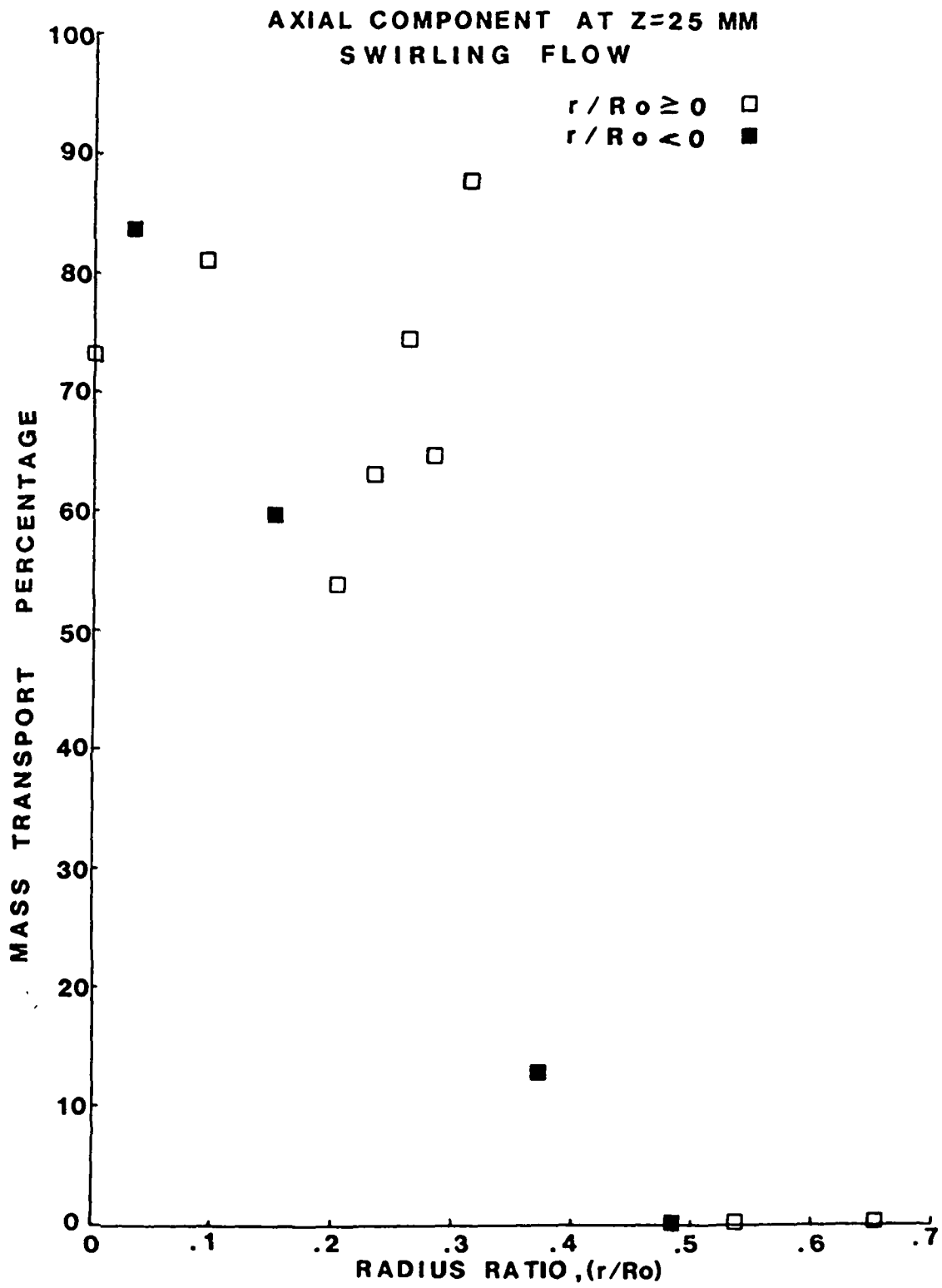


Fig. 46

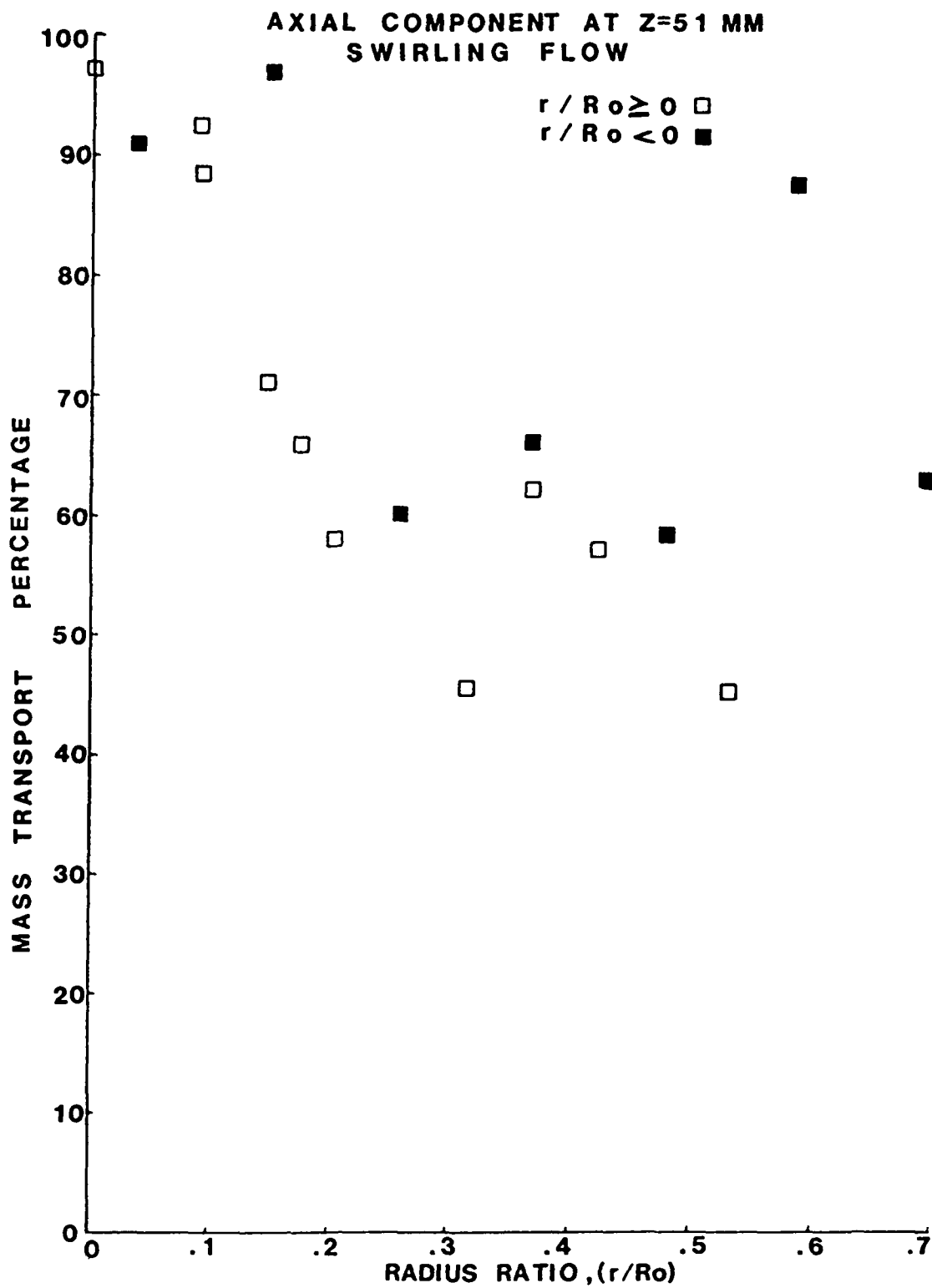


Fig 47

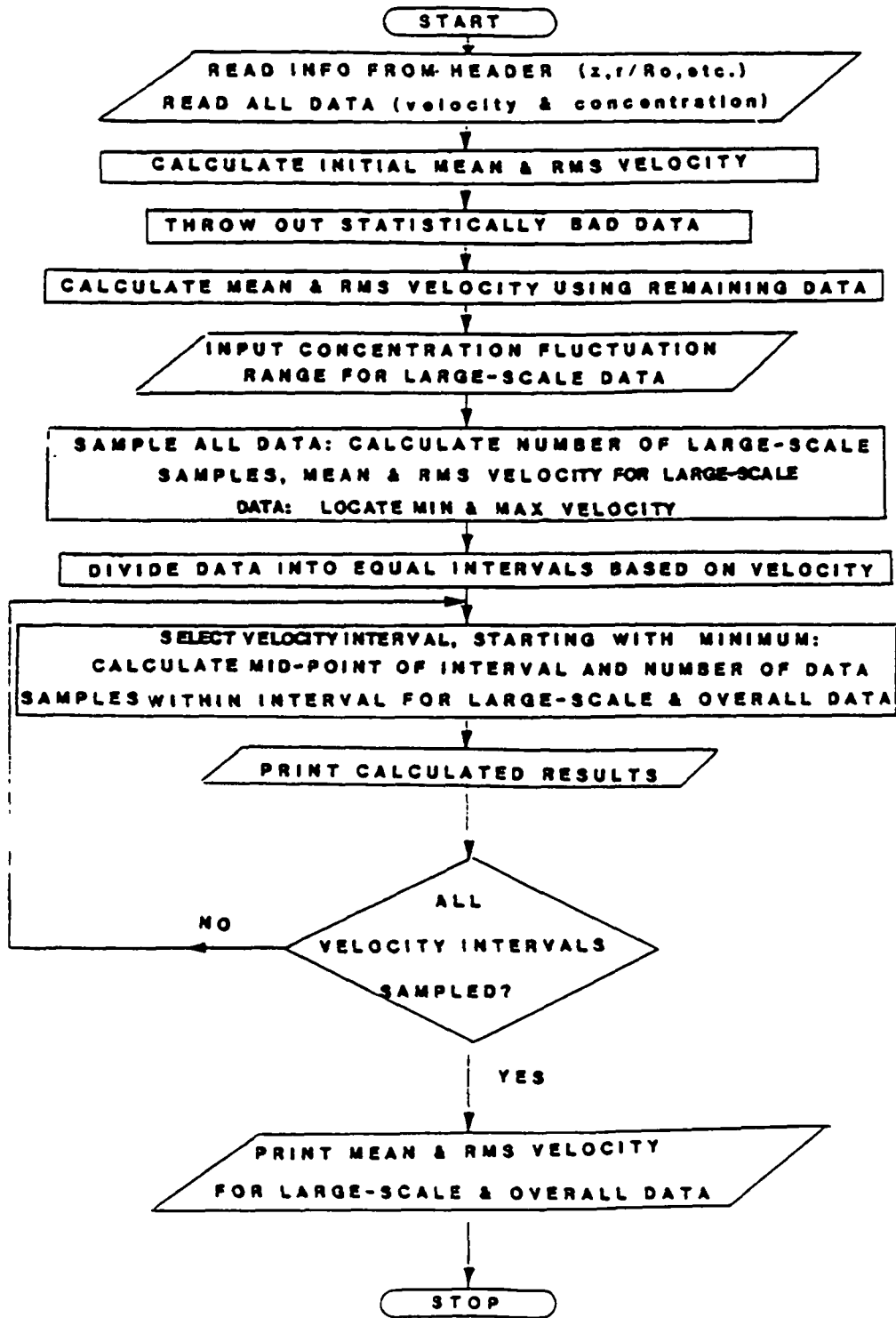


Fig. 48

PROB 51.15
 SUCCESSFUL TEMP RESTORE RUNSIP15 AS (TF15)
 CANCELLED: 3DNAME RMDS UNKNOWN

DATA OUTPUT FOR RUN 51 POINT 15

RADIAL VELOCITY VS CONCENTRATION
 Z=152 MM AND R/RO= 0.324

SELECT MINIMUM POSITIVE AND NEGATIVE CONCENTRATION FLUCTUATION
 TO BE INCLUDED IN LARGE SCALE STRUCTURE USING F4.1 FORMAT:

CPPOS=
 0.2
 CPNEG=
 -1.0

NUMBER OF SAMPLES: ORIGINAL=999 GOOD DATA=984 LARGE SCALE= 76

I	VMID(M/S)	NUMBER OF SAMPLES	
		L.S.	OVERALL
1	-0.522	0	2
2	-0.500	0	2
3	-0.478	0	2
4	-0.456	0	3
5	-0.434	0	2
6	-0.412	0	9
7	-0.390	0	1
8	-0.368	0	8
9	-0.346	0	9
10	-0.324	0	6
11	-0.302	0	8
12	-0.280	0	12
13	-0.258	0	15
14	-0.236	0	24
15	-0.214	0	17
16	-0.192	2	22
17	-0.170	0	31
18	-0.148	0	24
19	-0.126	2	36
20	-0.104	0	27
21	-0.082	0	35
22	-0.059	1	27
23	-0.037	2	47
24	-0.015	3	46
25	0.007	3	53
26	0.029	2	48
27	0.051	1	55
28	0.073	5	53
29	0.095	2	46
30	0.117	4	57
31	0.139	0	25
32	0.161	7	45
33	0.183	1	16
34	0.205	5	38
35	0.227	5	31
36	0.249	1	12
37	0.271	5	24
38	0.293	5	18
39	0.315	4	10
40	0.337	4	10
41	0.359	5	9
42	0.381	0	1
43	0.403	0	3
44	0.425	1	2
45	0.447	1	4
46	0.470	2	4
47	0.492	0	2
48	0.514	1	2
49	0.536	0	0
50	0.558	0	1

MEAN VELOCITY(M/S): OVERALL= 0.018 & LARGE SCALE= 0.188
 RMS VELOCITY(M/S): OVERALL= 0.184 & LARGE SCALE= 0.155
 CBAR= 0.087 CPPOS= 0.200 CPNEG=-1.000
 TERMINATED: STOP

Fig. 49

RADIAL VELOCITY DISTRIBUTION

Z = 152 mm r/Ro = .324

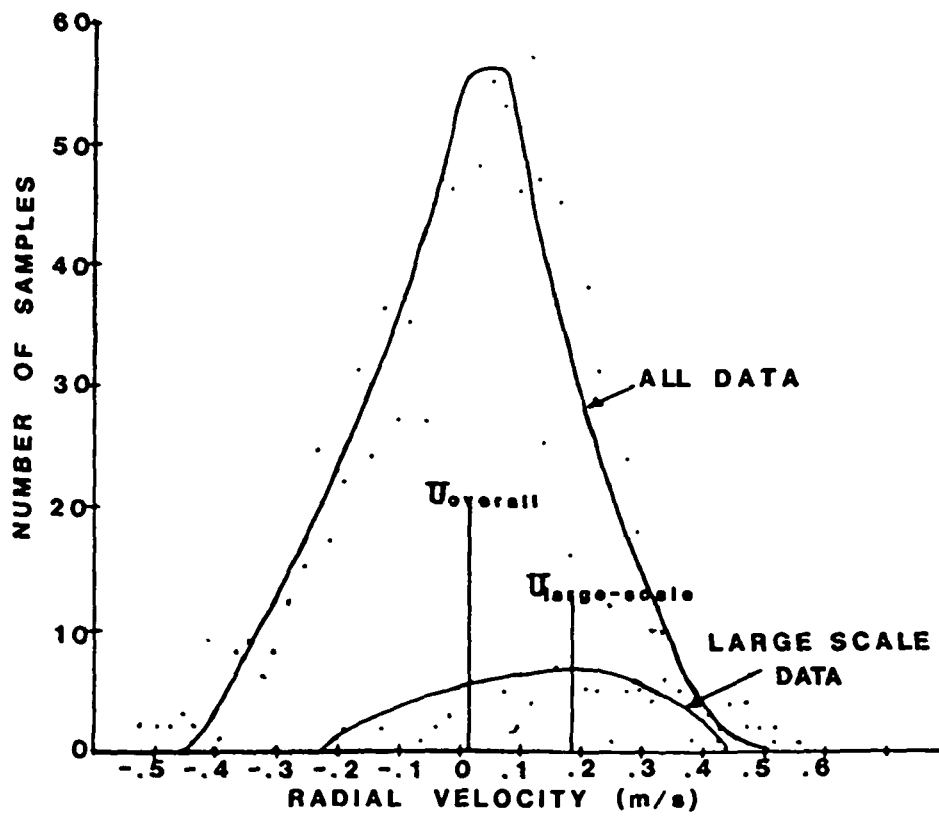


Fig. 50

AXIAL MEAN VELOCITY

Z = 152 MM

LARGE SCALE	OVERALL
$r/R_o > 0$ □	$r/R_o > 0$ ○
$r/R_o < 0$ ■	$r/R_o < 0$ ●

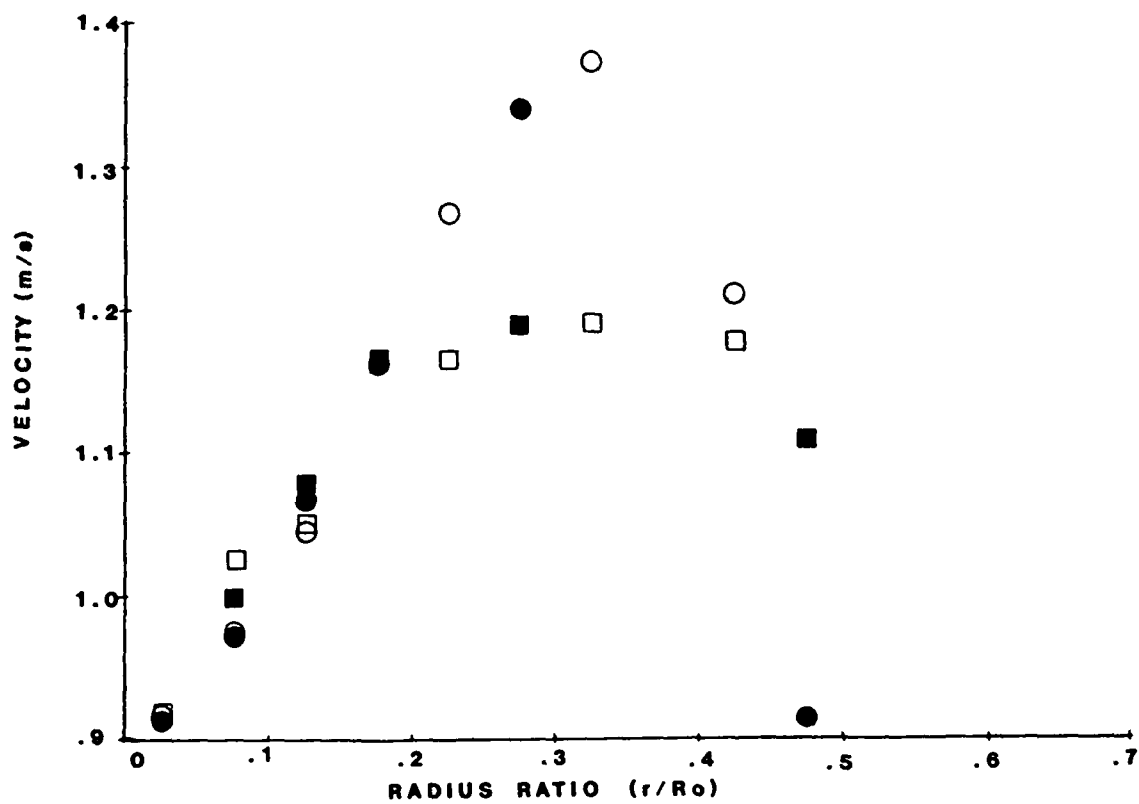


Fig. 51

RADIAL MEAN VELOCITY

Z = 51 mm

LARGE SCALE	OVERALL
$r/R_0 \geq 0$ □	$r/R_0 \geq 0$ ○
$r/R_0 < 0$ ■	$r/R_0 < 0$ ●

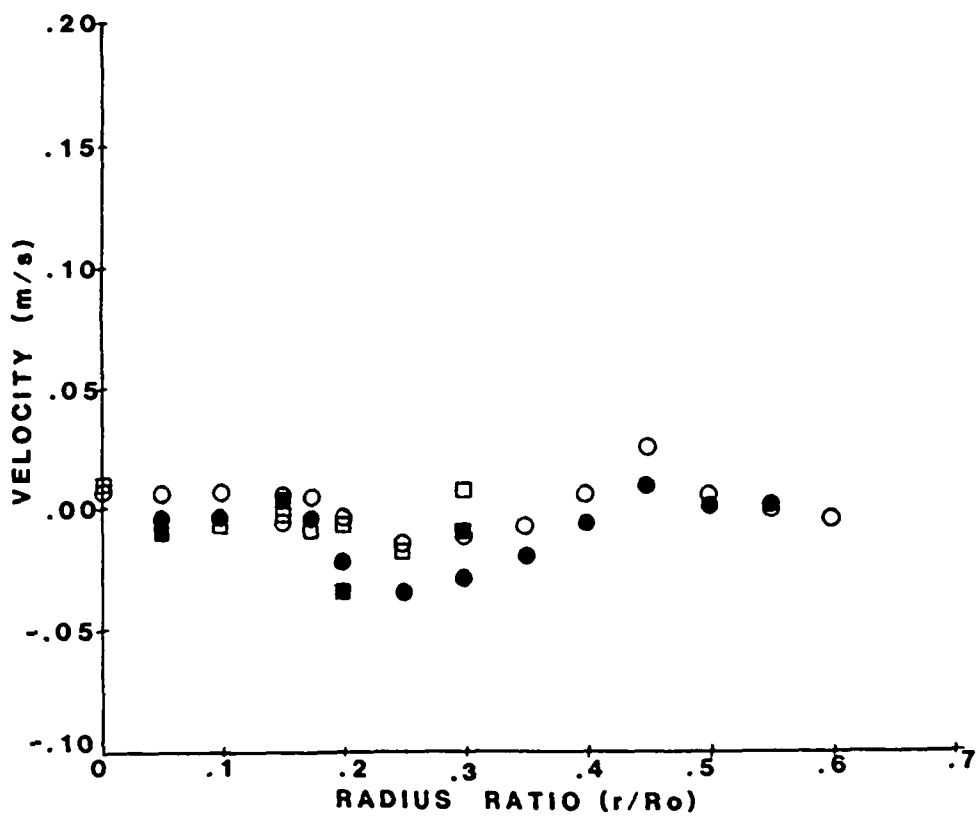


Fig. 52

RADIAL MEAN VELOCITY

Z = 102 mm

LARGE SCALE	OVERALL
$r/R_0 \geq 0$ □	$r/R_0 \geq 0$ ○
$r/R_0 < 0$ ■	$r/R_0 < 0$ ●

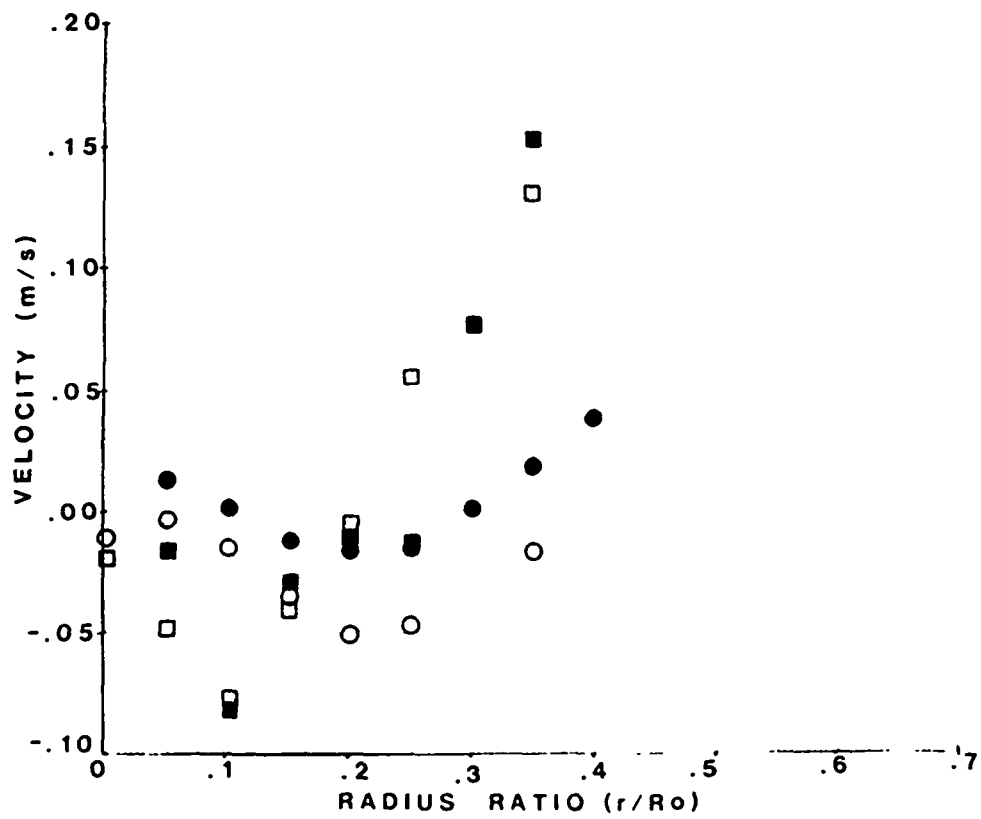


Fig. 53

RADIAL MEAN VELOCITY $Z=152$ mm

LARGE SCALE	OVERALL
$r/R_0 \geq 0$ □	$r/R_0 \geq 0$ ○
$r/R_0 < 0$ ■	$r/R_0 < 0$ ●

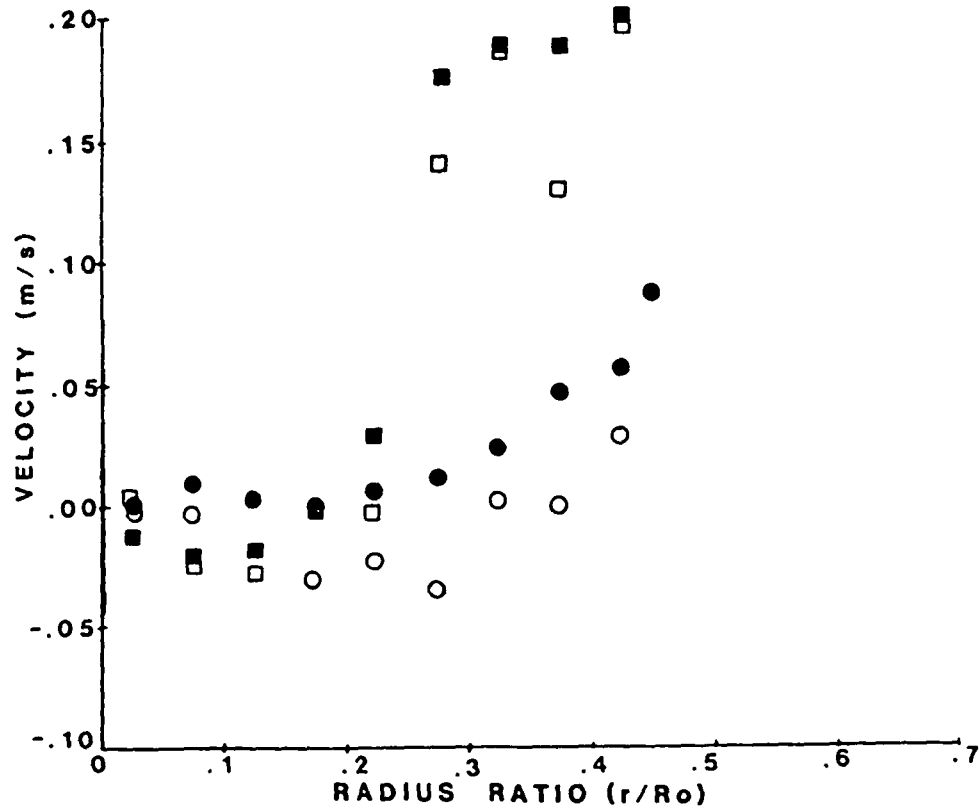
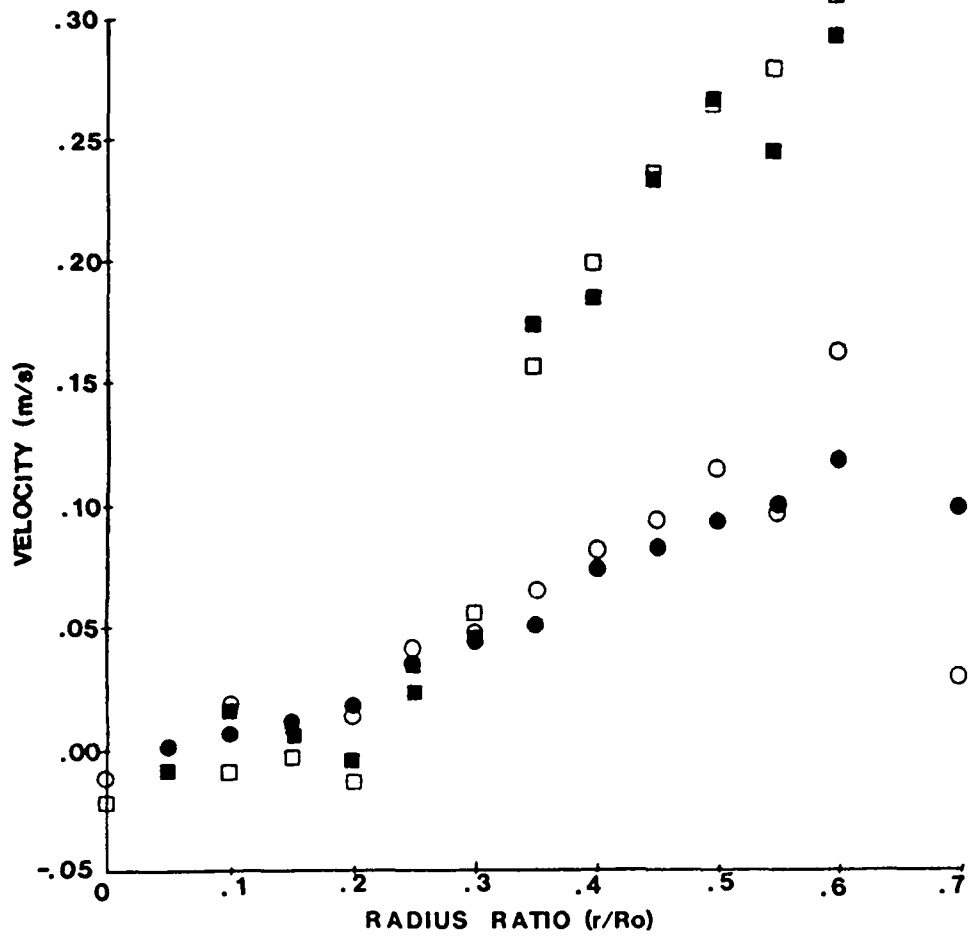


Fig. 54

RADIAL MEAN VELOCITY

Z=203 mm

LARGE SCALE	OVERALL
$r/R_o \geq 0$	$r/R_o \geq 0$
$r/R_o < 0$	$r/R_o < 0$



ORIGINAL PAGE IS
OF POOR QUALITY

Fig. 55

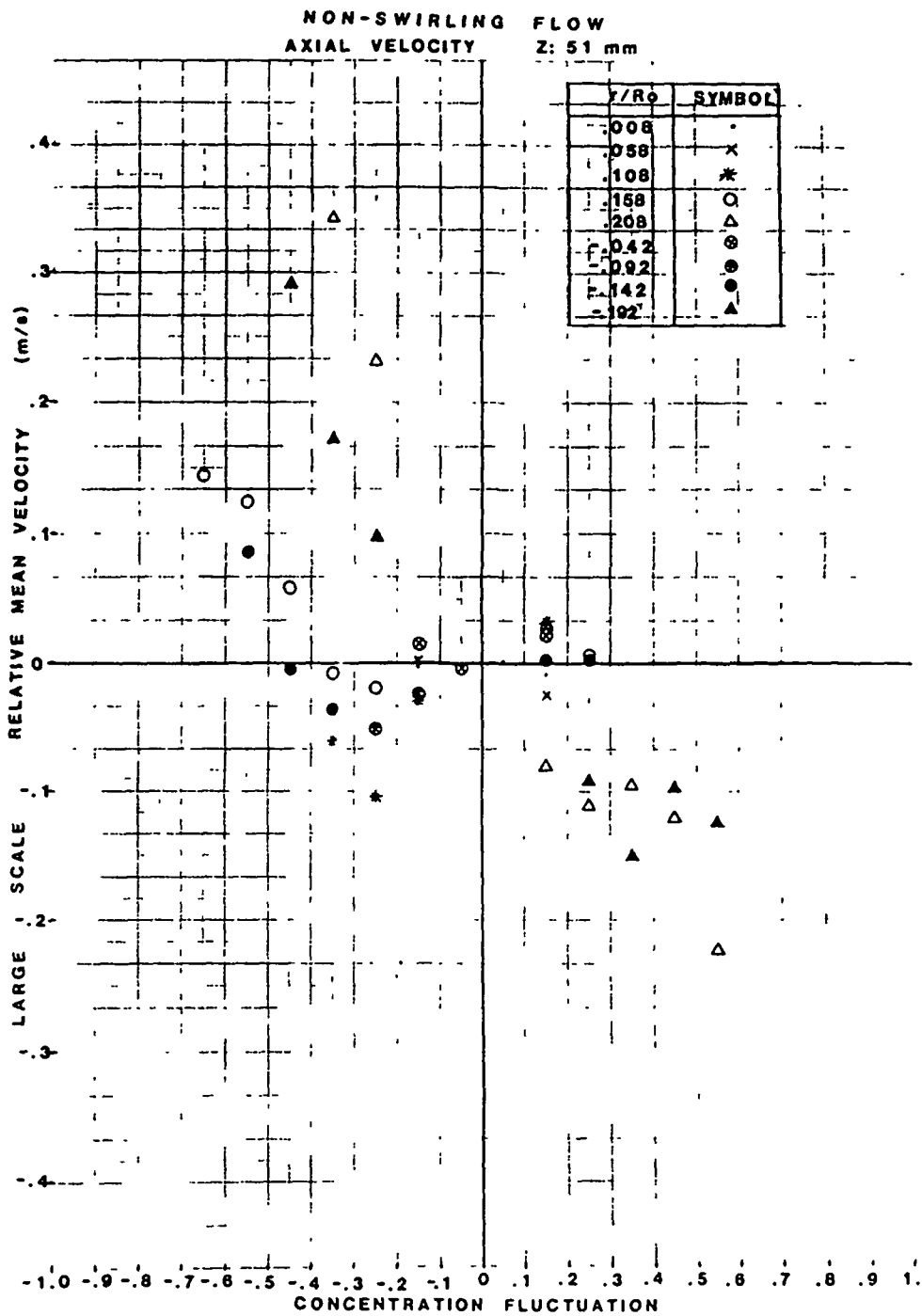
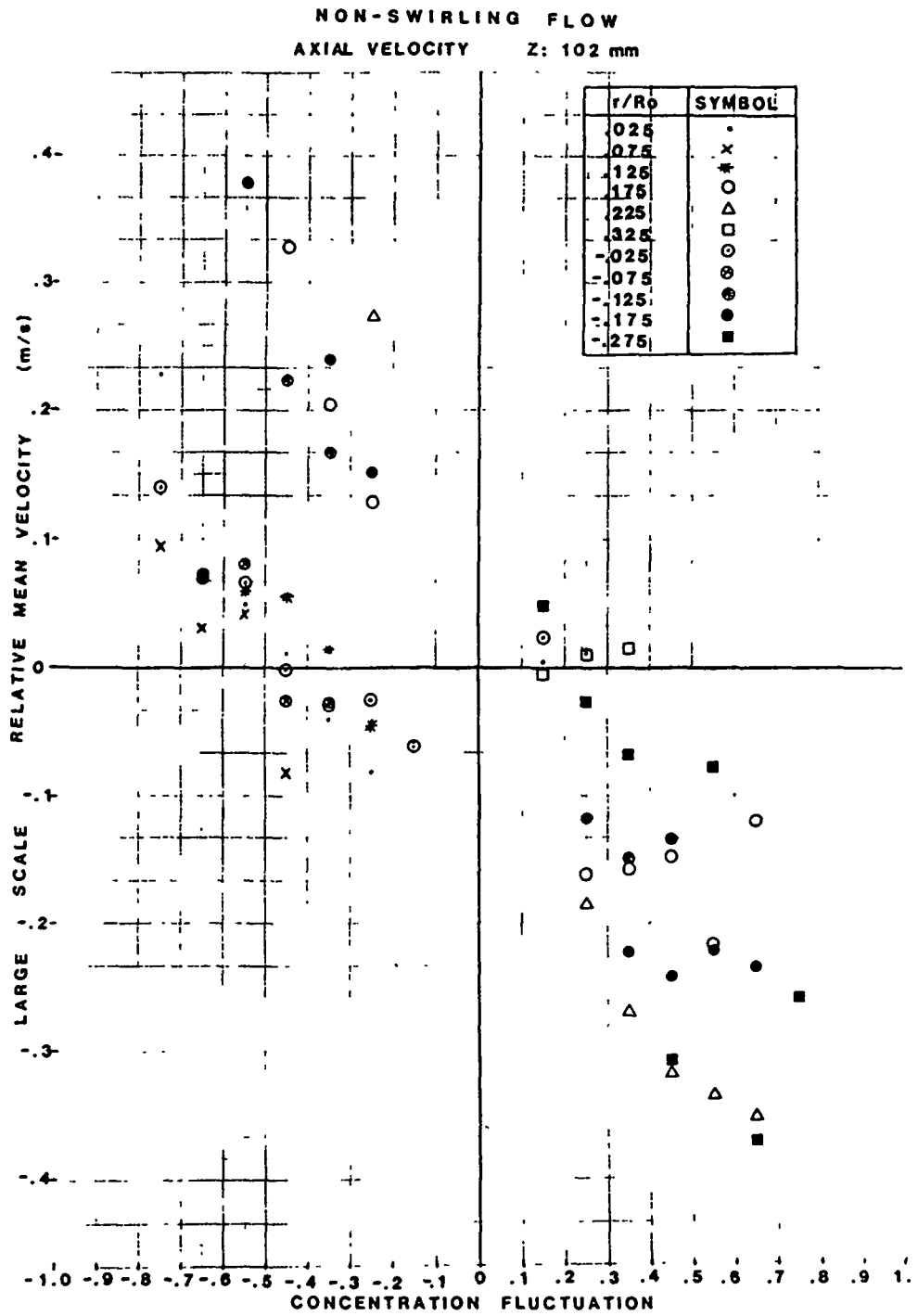
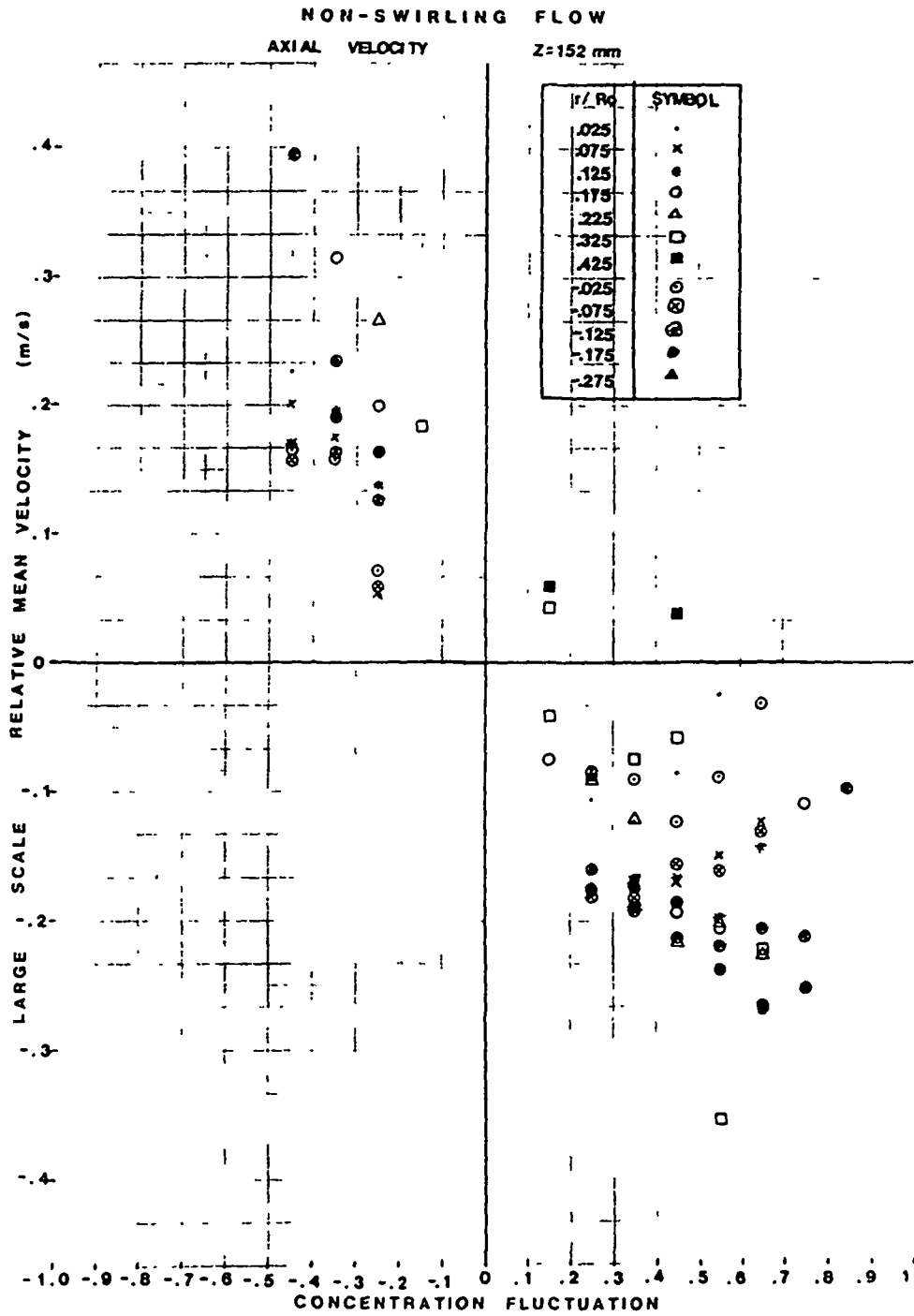


Fig. 56



ORIGINAL PAGE IS
OF POOR QUALITY

Fig. 57



REFERENCES

1. Gerstein, M. (Ed.), "Fundamentals of Gas turbine Combustion". NASA Conference Publication 2087, 1979.
2. Hudson, D.W., "Combustion Modelling Needs for the 80's". AIAA Preprint, 80-1288.
3. Mellor, A.M., "Turbulent Combustion Interaction Models for PrActical High Intensity Combustors". Seventeenth Symposium on Combustion, pg. 377, Combustion Institute, 1979.
4. Johnson, B.V., and Bennett, J.C., "Mass and Momentum Turbulent Transport Experiments with Confined Coaxial Jet". Fourth Symposium on Turbulent Shear Flows, Karlsruhe, Germany, September, 1983.
5. Morganthaler, J.H., "Turbulent Mixing and Reacting flow Characterization". Fluid Mechanics of Combustion, pp. 21-34, ASME, N.Y., 1974.
6. Johnson, B.V., and Bennett, J.C., "Velocity and Concentration Characteristics and Their Cross Correlations for Coaxial Jets in a Confined Sudden Expansion, Part I: Experiments". Proceedings of ASME Symposium on the Fluid Mechanics of Combustions Systems, Boulder, CO, June, 1981.
7. Syed, S.A., and Sturgess, G.J., "Velocity and Concentration Characteristics and Their Correlations for Coaxial Jets in a Confined Sudden Expansion, Part II: Predictions". Proceedings of ASME Symposium on the Fluid Mechanics of Combustion Systems, Boulder, CO, June, 1981.
8. Habib, M.A., and Whitelaw, J.H., "Velocity Characteristics of a Confined Coaxial Jet". ASME Journal of Fluids Engineering, Vol. 101 (December 1979), pg. 521-529.
9. Habib, M.A., and Whitelaw, J.H., "Velocity Characteristics of Confined Coaxial Jets With and Without Swirl". ASME Journal of Fluids Engineering, Vol. 102 (March 1980), pg. 47-53.
10. Johnson, B.V., and Bennett, J.C., "Statistical Characteristics of Velocity, Concentration, Mass Transport, and Momentum Transport for Coaxial Jet Mixing in a Confined Duct". Journal of Engineering for Gas Turbines and Power, Vol. 106 (January 1984), pg. 121-127.
11. Johnson, B.V., and Bennett, J.C., "Mass and Momentum Turbulent Transport Experiments with Confined Coaxial Jets", NASA Contractor Report NASA CR-165574, UTRC Report R81-915540-9, November, 1981.

12. Roback, R. and Johnson, B.V., "Mass and Momentum Turbulent Transport Experiments with Confined Coaxial Swirling Jets", NASA Contractor Report CR-168252, UTRC Report R83-915540-26, August, 1983.
13. Schetz, J.A., "Injection and Mixing in Turbulent Flow", Progress in Astronautics and Aeronautics (Vol. 68), Edited by M. Summerfield. New York: AIAA, 1980.
14. Mathieu, J., and Jeandel, D., "Pathological Cases in Turbulent Field and Spectral Approach", Prediction Methods for Turbulent Flows, Edited by W. Kollmann. Washington: Hemisphere Publishing, 1980.
15. Launder, B.E., and Schiestel, R., On the Use of Multiple Time Scales in Modelling Turbulent Flow. C.R.A.S., A, 1978.
16. Borghi, R., "Models of Turbulent Combustion for Numerical Predictions", Prediction Methods for Turbulent Flows, Edited by W. Kollmann. Washington: Hemisphere Publishing, 1980.
17. Roshko, A., "Structures of Turbulent Shear Flows: A New Look". A.I.A.A. Journal, Vol. 14 (October 1976), pg. 1349-1357.
18. Cantwell, B.J., "Organized Motion in Turbulent Flow", Annual Review of Fluid Mechanics, Edited by M. Van Dyke, J.V. Wehausen, and J.L. Lumley, Vol. 13, pg. 457-515. Palo Alto, CA: Annual Reviews, Inc., 1981.
19. Davies, P.O.A.L., and Yule, A.J., "Coherent Structures in Turbulence". Journal of fluid Mechanics, Vol. 69 (1975), pg. 513-537.
20. Yule, A.J., "Investigations of Eddy Coherence in Jet Flows", in The Role of Coherent Structures in Modelling Turbulence and Mixing, Lecture Notes in Physics, Edited by J. Jiminez, Vol. 136, pg. 188-207. Springer Verlag, Berlin/Heidelberg/New York, 1980.
21. Brown, G.L., and Roshko, A., "On Density Effects and Large Structure in Turbulent Mixing Layers", Journal of Fluid Mechanics, Vol. 64 (1974), pg. 775-816.
22. Winant, C., and Browand, F., "Vortex Pairing: The Mechanism of Turbulent Mixing - Layer Growth at Moderate Reynolds Number". Journal of Fluid Mechanics, Vol. 63 (1974), pg. 237-255.
23. Dimotakis, P., and Brown, G.L., "The Mixing Layer at High Reynolds Number: Large-Structure Dynamics and Entrainment". Journal of Fluid Mechanics, Vol. 78 (1976), pg. 535-560.

24. Blackwelder, R.F., and Kaplan, R.E., "On the Wall Structure of the Turbulent Boundary Layer". Journal of Fluid Mechanics, Vol. 76 (1976), pg. 89-112
25. Lu, S.S., and Willmarth, W.W., "Measurements of the Structure of the Reynolds Stress in a Turbulent Boundary Layer". Journal of Fluid Mechanics, Vol. 60 (1973), pg. 481-511.
26. Corino, E.R., and Brodkey, R.S., "A Visual Investigation of the Wall Region in Turbulent flow". Journal of Fluid Mechanics, Vol. 37 (1969), pg. 1-30.
27. Kovaszny, L.S.G., Kibens, V., and Blackwelder, R., "Large-Scale Motion in the Intermittent Region of a Turbulent Boundary Layer". Journal of Fluid Mechanics, Vol. 41 (1970), pg. 283-325.
28. Mathieu, J., and Charnay, G., "Experimental Methods in Turbulent Structure Research", in The Role of Coherent Structures in Modelling Turbulence and Mixing, Lecture Notes in Physics, Edited by J. Jiminez, Vol. 103, pg. 146-187. Springer Verlag, Berlin/Heidelberg/New York, 1980.
29. Schlichting, H., Boundary Layer Theory, Trans. by J. Kestin (New York: McGraw Hill, 1979), seventh edition, Ch. 24.
30. Riley, J.J., and Metcalfe, R.W., "Direct Simulations of Chemically Reacting Turbulent Mixing Layers", NASA Contractor Report 174640, March 1984.

APPENDIX A

HOLD,CV

```

0000100      DIMENSION V(1000),C(1000),VN(1000)
0000200      REAL*8 VEL
0000300      REAL NEWBAR,NEWRMS
0000400      INTEGER RUN,POINT,Z
0000500      VBAR=0.
0000600      VRMS=0.
0000700      N4=0
0000735 C    THIS PROGRAM PERFORMS CONDITIONAL SAMPLING ON RUNS OF CONCENTRATION-
0000770 C    VELOCITY DATA(METRIC UNITS)
0000790 C    READ INFO FROM HEADER
0000800      READ(11,10)RUN,POINT
0000900      10 FORMAT(26X,I2,10X,I2)
0001000      READ(11,15)N0
0001100      15 FORMAT(41X,I3)
0001150      NFIRST=N0
0001200      READ(11,20)Z,RR0
0001300      20 FORMAT(27X,I3,12X,F6.3)
0001400      READ(11,25)
0001500      READ(11,25)
0001600      25 FORMAT(5X)
0001700      READ(11,30)VEL
0001800      30 FORMAT(34X,1A8)
0001900      DO 40 N=1,4
0002000      READ(11,25)
0002100      40 CONTINUE
0002150 C    READ ALL DATA; CALCULATE INITIAL MEAN & RMS
0002200      DO 50 I=1,N0
0002300      READ(11,45)V(I),C(I)
0002400      45 FORMAT(33X,F6.3,7X,F6.3)
0002500      VBAR=VBAR+V(I)
0002600      VRMS=VRMS+V(I)**2
0002700      50 CONTINUE
0002800      VBAR=VBAR/FLOAT(N0)
0002900      VRMS=VRMS/FLOAT(N0)-VBAR**2
0003000      VRMS=SQRT(VRMS)
0003035 C    THROW OUT DATA FARTHER THAN 3*VRMS AWAY FROM VBAR & CALCULATE
0003070 C    NEW MEAN & RMS WITH DATA LEFT OVER.
0003100      DO 200 N=1,5
0003200      IF((FLOAT(N4)/FLOAT(N0)).GT.0.99)GO TO 200
0003300      IF(N.GT.1)N0=N4
0003400      NEWBAR=0.
0003500      NEWRMS=0.
0003600      N4=0
0003700      DO 100 I=1,N0
0003800      IF(ABS(V(I)-VBAR).GT.(3.0*VRMS))GO TO 100
0003900      N4=N4+1
0004000      NEWBAR=NEWBAR+V(I)
0004100      NEWRMS=NEWRMS+V(I)**2
0004200      V(N4)=V(I)
0004300      C(N4)=C(I)
0004400      100 CONTINUE
0004500      VBAR=NEWBAR/FLOAT(N4)
0004600      VRMS=NEWRMS/FLOAT(N4)-VBAR**2
0004700      VRMS=SQRT(VRMS)
0004800      200 CONTINUE
0005000      V1=0.
0005100      V2=0.
0005200      U3=0.
0005300      U4=0.
0005400      Q1=0.
0005500      Q2=0.
0005600      G1=0.
0005650 C    CALCULATE ASSORTED STATISTICAL PARAMETERS(MEAN,RMS,MOMENTS,ETC.)
0005700      DO 500 I=1,N4
0005800      V1=V1+V(I)
0005900      V2=V2+V(I)**2
0006000      U3=U3+V(I)**3
0006100      U4=U4+V(I)**4
0006200      Q1=Q1+C(I)
0006300      Q2=Q2+C(I)**2
0006400      G1=G1+V(I)*C(I)
0006500      500 CONTINUE
0006600      V1=V1/FLOAT(N4)
0006700      U4=U4/FLOAT(N4)-4.*V1*U3/FLOAT(N4)+6.*V1**2*V2/FLOAT(N4)-3.*V1**4
0006800      U3=U3/FLOAT(N4)-3.*V1*V2/FLOAT(N4)+2.*V1**3
0006900      V2=V2/FLOAT(N4)-V1**2
0007000      U2=SQRT(V2)
0007100      Q1=Q1/FLOAT(N4)
0007200      Q2=Q2/FLOAT(N4)-Q1**2
0007300      Q2=SQRT(Q2)

```



```

0007400      Q1=Q1/FLOAT(N4)-Q1*V1
0007500      N6=0
0007600      P8=0.
0007700      R9=0.
0007800      N7=0
0007900      R8=0.
0008000      809 WRITE(7,810)
0008100      810 FORMAT(/)
0008200      WRITE(7,815)RUN,POINT
0008300      815 FORMAT(5X,'DATA OUTPUT FOR RUN',I3,' POINT',I3)
0008400      WRITE(7,820)
0008500      820 FORMAT(/)
0008530      WRITE(7,822)VEL
0008560      822 FORMAT(1X,1A7,' VELOCITY VS CONCENTRATION')
0008590      WRITE(7,823)Z,RR0
0008595      823 FORMAT(1X,'Z=',I3,' MM AND R/R0=',F6.3)
0008600      WRITE(7,825)NFIRST,N4
0008700      825 FORMAT(1X,'NO='I4,' AND N4=',I3)
0008800      WRITE(7,830)V1
0008900      830 FORMAT(1X,'VBAR=',F9.4,' MPS')
0009000      WRITE(7,840)U2
0009100      840 FORMAT(1X,'VRMS=',F9.4,' MPS')
0009200      WRITE(7,850)U3
0009300      850 FORMAT(1X,'THIRD MOMENT OF TURBULENCE=',E12.5,' MPS**3')
0009400      R3=U3/U2**3
0009500      WRITE(7,860)R3
0009600      860 FORMAT(1X,'THIRD CORRELATION COEFFICIENT=',F9.4)
0009700      WRITE(7,870)U4
0009800      870 FORMAT(1X,'FOURTH MOMENT OF TURBULENCE=',E12.5,' MPS**4')
0009900      R4=U4/U2**4
0010000      WRITE(7,880)R4
0010100      880 FORMAT(1X,'FOURTH CORRELATION COEFFICIENT=',F9.4)
0010200      WRITE(7,881)Q1
0010300      881 FORMAT(1X,'CBAR=',F8.3,' X')
0010400      WRITE(7,882)Q2
0010500      882 FORMAT(1X,'CRM=',F8.3,' X')
0010600      WRITE(7,883)G1
0010700      883 FORMAT(1X,'CPVPBAR=',F10.6)
0010800      TT=G1/Q2/U2
0010900      WRITE(7,884)TT
0011000      884 FORMAT(1X,'OVERALL TRANSPORT COEFFICIENT=',F10.6)
0011100      WRITE(7,810)
0011150      C CONDITIONAL SAMPLING SECTION BEGINS HERE!
0011200      WRITE(7,890)
0011300      890 FORMAT(29X,'CONDITIONAL SAMPLING RESULTS')
0011400      WRITE(7,900)
0011500      900 FORMAT(/)
0011600      WRITE(7,910)
0011700      910 FORMAT(1X,'CONCENTRATION',4X,'NUMBER OF',15X,'RELATIVE',19X,'TRANSPORT',6X,'TRANSPORT')
0011800      WRITE(7,920)
0011900      920 FORMAT(2X,'FLUCTUATION',5X,'OCCURANCES',4X,'MEAN',8X,'MEAN',
0012000      110X,'RMS',7X,'COEFFICIENT',7X,'RATIO')
0012100      DO 925 K=1,20
0012200      A1=-1.0+(K-1)*0.1
0012300      A2=A1+.0999
0012400      W1=0.
0012500      NCOND=0
0012600      V3=0.
0012700      V4=0.
0012800      VR=0.
0012900      DO 925 N=1,N4
0013000      C TEST TO MAKE SURE C' IS IN THE DESIRED RANGE.
0013100      IF(V(N).EQ.-100.) GO TO 925
0013200      IF((C(N)-Q1).LT.A1) GO TO 925
0013300      IF((C(N)-Q1).GT.(A2)) GO TO 925
0013400      V3=V3+V(N)
0013500      V4=V4+V(N)**2
0013600      NCOND=NCOND+1
0013700      W1=W1+(C(N)-Q1)*(V(N)-V1)
0013800      925 CONTINUE
0014400      927 IF(NCOND.EQ.0) GO TO 950
0014500      C V3 IS CONDITIONAL MEAN VELOCITY.
0014600      V3=V3/FLOAT(NCOND)
0014700      C V4 IS CONDITIONAL RMS VELOCITY FLUCTUATION.
0014800      V4=V4/FLOAT(NCOND)-V3**2
0014900      V4=SQRT(V4)
0015000      C W1 IS CONDITIONAL MASS TRANSPORT COEFFICIENT.
0015100      W1=W1/FLOAT(NCOND)/U2/Q2
0015200      C VR IS RELATIVE MEAN VELOCITY(CONDITIONAL MEAN-OVERALL MEAN).
0015300      VR=V3-V1

```

```

0015400 C Y IS THE MASS TRANSPORT COEFFICIENT RATIO(CONDITIONAL/OVERALL).
0015500     Y=W1/TT
0015600     WRITE(7,930)A1,A2,NCOND,V3,VR,V4,W1,Y
0015700     930 FORMAT(1X,F4.1,' - ',F7.4,6X,I3,5X,F8.4,4X,F9.5,4X,F9.5,4X,F10.5,5X,F10.3)
0015800     GO TO 974
0015900     950 WRITE(7,960)A1,A2,NCOND
0016000     960 FORMAT(1X,F4.1,' - ',F7.4,6X,I3)
0016100 C X IS THE CENTER OF THE C' INTERVAL.
0016200     974 X=A1+.05
0016300 C 928 IS THE FORMAT STATEMENT USED FOR WRITING PLOT FILES.
0016400     928 FORMAT(F5.2,F10.3)
0016500     975 CONTINUE
0016600     WRITE(7,970)
0016700     965 WRITE(7,970)RUN,POINT
0016800     970 FORMAT(1X,'END OF RUN',I3,' -POINT',I3)
0016900     STOP
0017000     END

```

HOLD,COND3

```
0000100      DIMENSION N1(1000),N2(1000)
0000200      DIMENSION V(1000),C(1000),VN(1000)
0000300      REAL*8 VEL
0000400      REAL NEWBAR,NEWRMS
0000500      INTEGER RUN,POINT,Z
0000600      VBAR=0.
0000700      VRMS=0.
0000800      N4=0
0000900 C THIS PROGRAM PERFORMS CONDITIONAL SAMPLING ON RUNS OF CONCENTRATION-
0001000 C VELOCITY DATA(METRIC UNITS) AND CALCULATES PROBABILITY DENSITY DISTRIBUTIONS
0001100 C READ INFO FROM HEADER
0001200      READ(11,10)RUN,POINT
0001300      10 FORMAT(26X,I2,10X,I2)
0001400      READ(11,15)N0
0001500      15 FORMAT(41X,I3)
0001600      NFIRST=N0
0001700      READ(11,20)Z,RR0
0001800      20 FORMAT(27X,I3,12X,F6.3)
0001900      READ(11,25)
0002000      READ(11,25)
0002100      25 FORMAT(5X)
0002200      READ(11,30)VEL
0002300      30 FORMAT(34X,1A8)
0002400      DO 40 N=1,4
0002500      READ(11,25)
0002600      40 CONTINUE
0002700 C READ ALL DATA; CALCULATE INITIAL MEAN & RMS
0002800      DO 50 I=1,N0
0002900      READ(11,45)V(I),C(I)
0003000      45 FORMAT(33X,F6.3,7X,F6.3)
0003100      VBAR=VBAR+V(I)
0003200      VRMS=VRMS+V(I)**2
0003300      50 CONTINUE
0003400      VBAR=VBAR/FLOAT(N0)
0003500      VRMS=VRMS/FLOAT(N0)-VBAR**2
0003600      VRMS=SQRT(VRMS)
0003700 C THROW OUT DATA FARTHER THAN 3*VRMS AWAY FROM VBAR & CALCULATE
0003800 C NEW MEAN & RMS WITH DATA LEFT OVR.
0003900      DO 200 N=1,5
0004000      IF((FLOAT(N4)/FLOAT(N0)).GT.0.99)GO TO 200
0004100      IF(N.GT.1)N0=N4
0004200      NEWBAR=0.
0004300      NEWRMS=0.
0004400      N4=0
0004500      DO 100 I=1,N0
0004600      IF(ABS(V(I)-VBAR).GT.(3.0*VRMS))GO TO 100
0004700      N4=N4+1
0004800      NEWBAR=NEWBAR+V(I)
0004900      NEWRMS=NEWRMS+V(I)**2
0005000      V(N4)=V(I)
0005100      C(N4)=C(I)
0005200      100 CONTINUE
0005300      VBAR=NEWBAR/FLOAT(N4)
0005400      VRMS=NEWRMS/FLOAT(N4)-VBAR**2
0005500      VRMS=SQRT(VRMS)
0005600      200 CONTINUE
0005700      DO 500 I=1,N4
0005800      V1=V1+V(I)
0005900      V2=V2+V(I)**2
0006200      Q1=Q1+C(I)
0006500      500 CONTINUE
0006600      V1=V1/FLOAT(N4)
0006700      V2=V2/FLOAT(N4)-V1**2
0006800      U2=SQRT(V2)
0006900      Q1=Q1/FLOAT(N4)
0007000      809 WRITE(7,810)
0007100      810 FORMAT(/)
0007200      WRITE(7,815)RUN,POINT
0007300      815 FORMAT(5X,'DATA OUTPUT FOR RUN',I3,' POINT',I3)
0007400      WRITE(7,820)
0007500      820 FORMAT(/)
0007600      WRITE(7,822)VEL
0007700      822 FORMAT(1X,1A7,' VELOCITY VS CONCENTRATION')
0007800      WRITE(7,823)Z,RR0
0007900      823 FORMAT(1X,'Z=',I3,' MM AND R/RO=',F6.3)
0008000      WRITE(7,25)
0008100      WRITE(7,980)
0008200      980 FORMAT(3X,'SELECT MINIMUM POSITIVE AND NEGATIVE CONCENTRATION FLUCTUATION')
0008300      WRITE(7,981)
0008400      981 FORMAT(1X,'TO BE INCLUDED IN LARGE SCALE STRUCTURE USING F4.1 FURMA1')
```

C-2

```

0008500      WRITE(7,982)
0008600      982 FORMAT(2X,'CPPOS=')
0008700      READ(7,983)CPPOS
0008800      983 FORMAT(F4.1)
0008900      WRITE(7,984)
0009000      984 FORMAT(2X,'CPNEG=')
0009100      READ(7,983)CPNEG
0009200      N5=0
0009300      UBAR=0.
0009400      URMS=0.
0009500      DO 999 I=1,N4
0009600      N1(I)=0
0009700      N2(I)=0
0009800      999 CONTINUE
0009900      VMIN=UBAR-3.0*URMS
0010000      VMAX=UBAR+3.0*URMS
0010100      DO 1000 N=1,N4
0010200      IF(((C(N)-Q1).LT.CPPOS).AND.((C(N)-Q1).GE.CPNEG)) GO TO 950
0010300      N5=N5+1
0010400      UBAR=UBAR+V(N)
0010500      URMS=URMS+V(N)**2
0010600      I=INT(((V(N)-VMIN)/(VMAX-VMIN))*50)+1
0010700      IF(I.EQ.51)I=50
0010800 C      N1 IS THE NUMBER OF CONDITIONAL SAMPLES
0010900      N1(I)=N1(I)+1
0011000      950 I=INT(((V(N)-VMIN)/(VMAX-VMIN))*50)+1
0011100      IF (I.EQ.51)I=50
0011200 C      N2 IS THE NUMBER OF TOTAL SAMPLES
0011300      N2(I)=N2(I)+1
0011400      1000 CONTINUE
0011500 C      UBAR & URMS ARE CONDITIONAL(LARGE SCALE) MEAN & RMS VELOCITIES
0011600      UBAR=UBAR/FLOAT(N5)
0011700      URMS=(URMS/FLOAT(N5)-UBAR**2)**.5
0011800      WRITE(7,25)
0011900      WRITE(7,1010)NFIRST,N4,N5
0012000      1010 FORMAT(1X,'NUMBER OF SAMPLES; ORIGINAL=',I3,' GOOD DATA=',I3,' LARGE SCALE=',I3)
0012100      WRITE(7,25)
0012200      WRITE(7,1025)
0012300      1025 FORMAT(25X,'NUMBER OF SAMPLES')
0012400      WRITE(7,1050)
0012500      1050 FORMAT(5X,'I',5X,'VMID(M/S)',5X,'L.S.',5X,'OVERALL')
0012550      WRITE(7,25)
0012600      DO 1100 I=1,50
0012700      VMID=VMIN+4*(VMAX-VMIN)/50.*(I-.5)
0012800      WRITE(7,1075)I,VMID,N1(I),N2(I)
0012900      1075 FORMAT(4X,I2,6X,F6.3,7X,I3,7X,I3)
0013000      1100 CONTINUE
0013010      WRITE(7,25)
0013020      WRITE(7,1500)UBAR,UBAR
0013030      1500 FORMAT(1X,'MEAN VELOCITY(M/S); OVERALL=',F6.3,' & LARGE SCALE=',F6.3)
0013040      WRITE(7,1600)URMS,URMS
0013050      1600 FORMAT(1X,'RMS VELOCITY(M/S); OVERALL=',F6.3,' & LARGE SCALE=',F6.3)
0013060      WRITE(7,1700)Q1,CPPOS,CPNEG
0013070      1700 FORMAT(1X,'CBAR=',F6.3,' CPPOS=',F6.3,' CPNEG=',F6.3)
0013100      STOP
0013200      END

```

APPENDIX B

SAMPLE 63,17
 SUCCESSFUL (TEMP) RESTORE RUN63P17 AS (TP17)
 CANCELLED: DDNAME RMD5 UNKNOWN

DATA OUTPUT FOR RUN 63 POINT 17

AXIAL VELOCITY VS CONCENTRATION
 Z=152 MM AND R/R0= 0.025
 NO= 999 AND N4=995
 UBAR= 0.9244 MPS
 VRMS= 0.1916 MPS
 THIRD MOMENT OF TURBULENCE= 0.19140E-02 MPS**3
 THIRD CORRELATION COEFFICIENT= 0.2721
 FOURTH MOMENT OF TURBULENCE= 0.37374E-02 MPS**4
 FOURTH CORRELATION COEFFICIENT= 2.7726
 CRAR= 0.5042
 CRMS= 0.2632
 CPVPBAR= -0.022902
 OVERALL TRANSPORT COEFFICIENT= -0.454270

CONDITIONAL SAMPLING RESULTS

CONCENTRATION FLUCTUATION	NUMBER OF OCCURRENCES	MEAN	RELATIVE MEAN	RMS	TRANSPORT COEFFICIENT	TRANSPORT RATIO
-1.0 - -0.9001	0					
-0.9 - -0.8001	0					
-0.8 - -0.7001	0					
0.7 - -0.6001	0					
-0.6 - -0.5001	1	1.4450	0.52056	0.00000	-5.18168	11.407
-0.5 - -0.4001	43	1.1458	0.22137	0.17740	1.92815	4.244
-0.4 - -0.3001	85	1.0816	0.15712	0.19224	-1.09526	2.412
-0.3 - -0.2001	137	1.0153	0.09081	0.18916	-0.45393	0.999
-0.2 - -0.1001	124	0.9327	0.0923	0.18489	-0.04148	0.071
-0.1 - -0.0001	148	0.9411	0.01666	0.16404	-0.02478	0.055
-0.0 - 0.0999	115	0.8689	-0.03359	0.17576	-0.04960	0.109
0.1 - 0.1999	94	0.8373	-0.08713	0.15352	-0.27027	0.595
0.2 - 0.2999	77	0.8142	-0.11025	0.14144	-0.54529	1.200
0.3 - 0.3999	72	0.7975	-0.12693	0.09456	-0.80232	1.942
0.4 - 0.4999	71	0.8356	0.00883	0.12068	-0.77370	1.747
0.5 - 0.5999	24	0.8961	-0.02833	0.11139	-0.29574	0.651
0.6 - 0.6999	0					
0.7 - 0.7999	0					
0.8 - 0.8999	0					
0.9 - 0.9999	0					

END OF RUN 63 -POINT 17
 TERMINATED: STOP

SAMPLE 63,18
 SUCCESSFUL (TEMP) RESTORE KUN63P18 AS (TF18)
 CANCELLED: DDNAME KNDS UNKNOWN

DATA OUTPUT FOR RUN 63 POINT 18

AXIAL VELOCITY VS CONCENTRATION
 Z=152 MM AND R/R0=-0.025
 NO= 999 AND N4=997
 VBAR= 0.9180 MPS
 VRMS= 0.1948 MPS
 THIRD MOMENT OF TURBULENCE= 0.14629E-02 MFS**3
 THIRD CORRELATION COEFFICIENT= 0.1980
 FOURTH MOMENT OF TURBULENCE= 0.41790E-02 MFS**4
 FOURTH CORRELATION COEFFICIENT= 2.9033
 CBAR= 0.508Z
 CRMS= 0.267Z
 CPVPBAR= -0.021049
 OVERALL TRANSPORT COEFFICIENT= -0.405335

CONDITIONAL SAMPLING RESULTS

CONCENTRATION FLUCTUATION	NUMBER OF OCCURRENCES	MEAN	RELATIVE MEAN	RMS	TRANSPORT COEFFICIENT	TRANSPORT RAII0
-1.0 - -0.9001	0					
-0.9 - -0.8001	0					
-0.8 - -0.7001	0					
-0.7 - -0.6001	0					
-0.6 - -0.5001	0					
-0.5 - -0.4001	32	1.0863	0.16832	0.20598	-1.45983	3.602
-0.4 - -0.3001	102	1.0801	0.16209	0.18968	1.09105	2.192
-0.3 - -0.2001	128	0.9937	0.07569	0.20108	-0.39860	0.984
-0.2 - -0.1001	160	0.9354	0.01733	0.20236	-0.05051	0.125
-0.1 - -0.0001	121	0.9030	-0.01498	0.18355	-0.00481	0.012
0.0 - 0.0999	112	0.8861	-0.03191	0.17327	-0.03586	0.088
0.1 - 0.1999	92	0.8487	-0.06928	0.15151	-0.19860	0.490
0.2 - 0.2999	70	0.8391	-0.07890	0.14156	-0.39470	0.974
0.3 - 0.3999	90	0.8304	-0.08764	0.14393	0.59399	1.465
0.4 - 0.4999	54	0.7987	-0.11936	0.11972	-1.03118	2.544
0.5 - 0.5999	30	0.8341	0.08393	0.09709	0.87713	2.164
0.6 - 0.6999	4	0.8907	-0.02736	0.10235	-0.32556	0.806
0.7 - 0.7999	0					
0.8 - 0.8999	0					
0.9 - 0.9999	0					

END OF RUN 63 -POINT 18
 TERMINATED: STOP

SAMPLE 63119
 SUCCESSFUL (TEMP) RESTORE RUN63F19 AS (TF19)
 CANCELLED: UDNAME RMD5 UNKNOWN

DATA OUTPUT FOR RUN 63 POINT 19

AXIAL VELOCITY VS CONCENTRATION
 Z=152 MM AND R/R0=-0.075
 NO= 999 AND N4=998
 VBAR= 0.9728 MPS
 VRMS= 0.2004 MPS
 THIRD MOMENT OF TURBULENCE= 0.19636E-02 MFS##3
 THIRD CORRELATION COEFFICIENT= 0.2440
 FOURTH MOMENT OF TURBULENCE= 0.42067E-02 MFS##4
 FOURTH CORRELATION COEFFICIENT= 2.6087
 CBAR= 0.444X
 CRMS= 0.242X
 CPVBAR= -0.024204
 OVERALL TRANSPORT COEFFICIENT= -0.461109

CONDITIONAL SAMPLING RESULTS

CONCENTRATION FLUCTUATION	NUMBER OF OCCURRENCES	MEAN	RELATIVE MEAN	RMS	TRANSPORT COEFFICIENT	TRANSPORT RATIO
-1.0 - -0.9001	0					
-0.9 - -0.8001	0					
-0.8 - -0.7001	0					
-0.7 - -0.6001	0					
-0.6 - -0.5001	0					
-0.5 - -0.4001	31	1.1630	0.19020	0.18301	-1.7243	3.411
-0.4 - -0.3001	84	1.1489	0.19410	0.17428	1.30379	2.828
-0.3 - -0.2001	143	1.0656	0.09285	0.19000	-0.46430	1.007
-0.2 - -0.1001	157	0.9997	0.07890	0.19065	0.09028	0.196
-0.1 - -0.0001	138	0.9452	-0.02762	0.18217	0.01042	-0.023
0.0 - 0.0999	104	0.9351	-0.03767	0.19978	-0.03806	0.083
0.1 - 0.1999	95	0.9151	0.03772	0.17557	-0.17123	0.371
0.2 - 0.2999	78	0.9094	-0.06347	0.15909	-0.29565	0.641
0.3 - 0.3999	65	0.8238	-0.14903	0.11079	-0.97510	2.158
0.4 - 0.4999	62	0.8497	-0.12308	0.12264	-1.04662	2.270
0.5 - 0.5999	33	0.8445	-0.12832	0.09782	-1.31825	2.859
0.6 - 0.6999	4	0.8732	-0.09755	0.13103	-1.15456	2.504
0.7 - 0.7999	0					
0.8 - 0.8999	0					
0.9 - 0.9999	0					

END OF RUN 63 -POINT 19
 TERMINATED: STOP

ORIGINAL PAGE IS
OF POOR QUALITY

SAMPLE 63.20
SUCCESSFUL (TEMP) RESTORE RUN63P20 AS (1P20)
CANCELLED: DNAME KNBS UNKNOWN

DATA OUTPUT FOR RUN 63 POINT 20

AXIAL VELOCITY VS CONCENTRATION
Z=152 MM AND R/R0=-0.125
N0= 999 AND N4=998
VBAR= 1.0689 MPS
VRMS= 0.2352 MPS
THIRD MOMENT OF TURBULENCE= 0.22793E-02 MFS##3
THIRD CORRELATION COEFFICIENT= 0.1751
FOURTH MOMENT OF TURBULENCE= 0.76303E-02 MFS##4
FOURTH CORRELATION COEFFICIENT= 2.4727
CBAR= 0.401X
CRM= 0.253X
CPVBAR= -0.032587
OVERALL TRANSPORT COEFFICIENT= -0.546930

CONDITIONAL SAMPLING RESULTS

CONCENTRATION FLUCTUATION	NUMBER OF OCCURRENCES	MEAN	RELATIVE MEAN	RMS	TRANSPORT COEFFICIENT	TRANSPORT RATIO
-1.0 - -0.9001	0			0.11547	2.79736	5.115
-0.9 - -0.8001	0			0.19080	-1.45902	2.668
-0.8 - -0.7001	0			0.20854	-0.59798	1.093
-0.7 - -0.6001	0			0.22356	-0.19097	0.349
-0.6 - -0.5001	0			0.19925	0.00200	-0.004
-0.5 - -0.4001	7	1.4759	0.40698	0.18982	0.08426	0.134
-0.4 - -0.3001	82	1.3162	0.24728	0.17666	-0.26370	0.485
-0.3 - -0.2001	141	1.2069	0.13804	0.17437	-0.60496	1.106
-0.2 - -0.1001	171	1.1418	0.07294	0.17570	1.05817	1.735
-0.1 - -0.0001	171	1.0737	0.00461	0.13553	-1.46891	2.722
0.0 - 0.0999	120	0.9938	-0.07304	0.13159	1.87688	3.432
0.1 - 0.1999	87	0.9622	-0.10671	0.12500	-2.09072	3.823
0.2 - 0.2999	69	0.9213	-0.14761	0.07705	-2.51419	4.401
0.3 - 0.3999	47	0.8876	-0.18129	0.00000	-1.17460	2.148
0.4 - 0.4999	46	0.8678	-0.20110			
0.5 - 0.5999	26	0.8617	0.70719			
0.6 - 0.6999	17	0.8739	-0.19494			
0.7 - 0.7999	4	0.8685	-0.20036			
0.8 - 0.8999	1	0.9830	-0.08588			
0.9 - 0.9999	0					

END OF RUN 63 -POINT 20
TERMINATED: STOP

SAMPLE 6J,21
 SUCCESSFUL (TEMP) RESTORE RUN63F21 AS (FP21)
 CANCELLED: BNAME KMDS UNKNOWN

DATA OUTPUT FOR RUN 63 POINT 21

AXIAL VELOCITY VS CONCENTRATION
 Z=152 MM AND R/R0=-0.175
 M0= 999 AND M4=998
 VBAR= 1.1634 MPS
 VRMS= 0.2386 MPS
 THIRD MOMENT OF TURBULENCE=-0.14229E-02 MFS***3
 THIRD CORRELATION COEFFICIENT= -0.1048
 FOURTH MOMENT OF TURBULENCE= 0.85964E-02 MFS***4
 FOURTH CORRELATION COEFFICIENT= 2.6343
 CBAR= 0.3152
 CRMS= 0.2332
 CPVBAR=-0.029299
 OVERALL TRANSPORT COEFFICIENT= -0.527584

CONDITIONAL SAMPLING RESULTS

CONCENTRATION FLUCTUATION	NUMBER OF OCCURRENCES	MEAN	RELATIVE MEAN	RMS	TRANSPORT COEFFICIENT	TRANSPORT RATIO
-1.0 - -0.9001	0					
-0.9 - -0.8001	0					
-0.8 - -0.7001	0					
-0.7 - -0.6001	0					
-0.6 - -0.5001	0					
-0.5 - -0.4001	0					
-0.4 - -0.3001	40	1.3532	0.18984	0.22964	-1.07672	2.041
-0.3 - -0.2001	175	1.3249	0.16151	0.20354	0.72917	1.302
-0.2 - -0.1001	189	1.2696	0.10622	0.17378	-0.28248	0.235
-0.1 - 0.0001	167	1.1440	0.09027	0.24519	0.01400	0.027
0.0 - 0.0999	143	1.0955	-0.04789	0.19480	-0.05420	0.103
0.1 - 0.1999	98	1.0617	0.10163	0.20368	-0.25831	0.490
0.2 - 0.2999	75	0.9877	-0.17571	0.17375	-0.78189	1.482
0.3 - 0.3999	37	0.9888	0.17461	0.16513	-1.14599	2.134
0.4 - 0.4999	29	0.9268	-0.10663	0.16281	-1.51163	2.865
0.5 - 0.5999	25	0.9251	0.24827	0.16771	2.36309	4.479
0.6 - 0.6999	14	0.8964	-0.26703	0.11330	-3.17737	6.022
0.7 - 0.7999	6	0.9098	-0.23355	0.11807	-3.31135	6.276
0.8 - 0.8999	0					
0.9 - 0.9999	0					

END OF RUN 63 -POINT 21
 TERMINATED: STOP

SAMPLE 63,22
 SUCCESSFUL (TEMP) RESTORE RUN63P22 AS (TP22)
 CANCELLED: DDNAME RMD5 UNKNOWN

DATA OUTPUT FOR RUN 63 POINT 22

AXIAL VELOCITY VS CONCENTRATION
 Z=152 MM AND R/R0=-0.275
 N0= 999 AND N4=994
 UBAR= 1.3404 MPS
 VRMS= 0.2348 MPS
 THIRD MOMENT OF TURBULENCE=-0.77915E-02 MFS**3
 THIRD CORRELATION COEFFICIENT= -0.6018
 FOURTH MOMENT OF TURBULENCE= 0.94004E-02 MFS**4
 FOURTH CORRELATION COEFFICIENT= 3.0922
 CBAR= 0.136X
 CRMS= 0.153X
 CPU/PBAR= -0.011062
 OVERALL TRANSPORT COEFFICIENT= -0.308312

CONDITIONAL SAMPLING RESULTS

CONCENTRATION FLUCTUATION	NUMBER OF OCCURRENCES	MEAN	RELATIVE MEAN	RMS	TRANSPORT COEFFICIENT	TRANSPORT RATIO
-1.0 - -0.9001	0					
-0.9 - -0.8001	0					
-0.8 - -0.7001	0					
-0.7 - -0.6001	0					
-0.6 - -0.5001	0					
-0.5 - -0.4001	0					
-0.4 - -0.3001	0					
-0.3 - -0.2001	0					
-0.2 - -0.1001	350	1.3994	0.03925	0.23583	-0.22204	0.720
-0.1 - -0.0001	268	1.3730	0.03258	0.20309	-0.03678	0.184
0.0 - 0.0999	154	1.3087	-0.03171	0.22686	-0.07870	0.235
0.1 - 0.1999	110	1.2733	0.06703	0.21056	0.28768	0.933
0.2 - 0.2999	59	1.2181	-0.12224	0.25093	0.92278	2.991
0.3 - 0.3999	31	1.1369	-0.20345	0.23616	-2.01097	4.523
0.4 - 0.4999	11	1.2433	0.07711	0.20968	1.74042	4.023
0.5 - 0.5999	9	1.0910	-0.24930	0.20791	-3.78054	12.262
0.6 - 0.6999	1	1.1610	-0.17938	0.00000	3.02255	9.804
0.7 - 0.7999	1	1.2060	-0.13430	0.00000	-2.76619	8.972
0.8 - 0.8999	0					
0.9 - 0.9999	0					

END OF RUN 63 -POINT 22
 TERMINATED: STOP

SAMPLE 63.26
 SUCCESSFUL (TEMP) RESTORE RUN63P26 AS (TF26)
 CANCELLED: DNAME RND5 UNKNOWN

DATA OUTPUT FOR RUN 63 POINT 26

AXIAL VELOCITY VS CONCENTRATION
 Z=152 MM AND R/R0=-0.674
 NO= 499 AND N4=498
 VBAR= 0.1676 MPS
 VRMS= 0.3987 MPS
 THIRD MOMENT OF TURBULENCE= 0.16914E-01 MFS**3
 THIRD CORRELATION COEFFICIENT= 0.2669
 FOURTH MOMENT OF TURBULENCE= 0.64401E-01 MFS**4
 FOURTH CORRELATION COEFFICIENT= 2.5488
 CBAR= 0.017X
 CRMS= 0.020X
 CPVPBAR= -0.001629
 OVERALL TRANSPORT COEFFICIENT= -0.207616

CONDITIONAL SAMPLING RESULTS

CONCENTRATION FLUCTUATION	NUMBER OF OCCURRENCES	MEAN	RELATIVE MEAN	RMS	TRANSPORT COEFFICIENT	TRANSPORT RATIO
-1.0 - -0.9001	0					
-0.9 - -0.8001	0					
-0.8 - -0.7001	0					
-0.7 - -0.6001	0					
-0.6 - -0.5001	0					
-0.5 - -0.4001	0					
-0.4 - -0.3001	0					
-0.3 - -0.2001	0					
-0.2 - -0.1001	0					
-0.1 - -0.0001	268	0.2332	0.06565	0.40282	-0.14239	0.782
-0.0 - 0.0999	230	0.0911	0.07650	0.37978	0.26034	1.254
0.1 - 0.1999	0					
0.2 - 0.2999	0					
0.3 - 0.3999	0					
0.4 - 0.4999	0					
0.5 - 0.5999	0					
0.6 - 0.6999	0					
0.7 - 0.7999	0					
0.8 - 0.8999	0					
0.9 - 0.9999	0					

END OF RUN 63 -POINT 26
 TERMINATED: STOP

SAMPLE 63.27
 SUCCESSFUL (TEMP) RESTORE RUN63P27 AS (1P27)
 CANCELLED: DDNAME RMD5 UNKNOWN

DATA OUTPUT FOR RUN 63 POINT 27

AXIAL VELOCITY VS CONCENTRATION
 Z=152 MM AND R/R0= 0.025
 NO= 999 AND M4=994
 VBAR= 0.9195 MPB
 VBAR= 0.1969 MPB
 THIRD MOMENT OF TURBULENCE= 0.29316E-02 MPB**3
 THIRD CORRELATION COEFFICIENT= 0.1840
 FOURTH MOMENT OF TURBULENCE= 0.42467E-02 MPB**4
 FOURTH CORRELATION COEFFICIENT= 2.8251
 CBAR= 0.5372
 CRMS= 0.2672
 CPVBAR= -0.022243
 OVERALL TRANSPORT COEFFICIENT= -0.423246

CONDITIONAL SAMPLING RESULTS

CONCENTRATION FLUCTUATION	NUMBER OF OCCURRENCES	MEAN	RELATIVE MEAN	RMS	TRANSPORT COEFFICIENT	TRANSPORT RATIO
-1.0 - -0.9001	0					
-0.9 - -0.8001	0					
-0.8 - -0.7001	0					
-0.7 - -0.6001	0					
-0.6 - -0.5001	6	1.2780	0.35852	0.09241	-3.57417	8.327
-0.5 - -0.4001	40	1.2007	0.78124	0.16525	2.18064	5.625
-0.4 - -0.3001	90	1.0528	0.13334	0.19419	-0.86785	2.050
-0.3 - -0.2001	127	0.9982	0.07876	0.21224	-0.37539	0.887
-0.2 - -0.1001	150	0.9576	0.03814	0.18466	-0.11254	0.266
-0.1 - -0.0001	134	0.8786	-0.04085	0.17856	0.03930	-0.093
0.0 - 0.0999	95	0.9544	0.06511	0.16338	-0.03538	0.131
0.1 - 0.1999	95	0.8453	-0.07413	0.16232	-0.21722	0.513
0.2 - 0.2999	87	0.8035	-0.11595	0.13633	-0.56315	1.331
0.3 - 0.3999	74	0.8326	-0.08690	0.13035	-0.58210	1.128
0.4 - 0.4999	74	0.8605	-0.05901	0.11445	-0.50259	1.187
0.5 - 0.5999	23	0.8590	0.06048	0.10770	-0.41866	1.462
0.6 - 0.6999	1	0.8500	-0.06947	0.00000	-0.80356	1.899
0.7 - 0.7999	0					
0.8 - 0.8999	0					
0.9 - 0.9999	0					

END OF RUN 63 -POINT 27
 TERMINATED: STOP

SAMPLE 63,28
 SUCCESSFUL (TEMP) RESTORE RUN63P28 AS (TF28)
 CANCELLED! DDNAME RND5 UNKNOWN

DATA OUTPUT FOR RUN 63 POINT 28

AXIAL VELOCITY VS CONCENTRATION
 Z=152 MM AND R/R0= 0.075
 NO= 999 AND N4=996
 VBAR= 0.9769 MPS
 VKMS= 0.2154 MPS
 THIRD MOMENT OF TURBULENCE= 0.37899E-02 MFS**3
 THIRD CORRELATION COEFFICIENT= 0.3791
 FOURTH MOMENT OF TURBULENCE= 0.62628E-02 MFS**4
 FOURTH CORRELATION COEFFICIENT= 2.9082
 CBAR= 0.466Z
 CRMS= 0.266Z
 CPVPBAR= -0.027163
 OVERALL TRANSPORT COEFFICIENT= -0.473547

CONDITIONAL SAMPLING RESULTS

CONCENTRATION FLUCTUATION	NUMBER OF OCCURANCES	MEAN	RELATIVE MEAN	RMS	TRANSPORT COEFFICIENT	TRANSPORT RATIO
-1.0 - -0.9001	0					
-0.9 - -0.8001	0					
-0.8 - -0.7001	0					
-0.7 - -0.6001	0					
-0.6 - -0.5001	0					
-0.5 - -0.4001	31	1.2321	0.25525	0.24829	-1.94549	4.108
-0.4 - -0.3001	95	1.2052	0.27830	0.21101	1.40306	2.963
-0.3 - -0.2001	127	1.0866	0.10971	0.20767	-0.49345	1.042
-0.2 - -0.1001	180	0.9931	0.01624	0.19245	-0.06144	0.130
-0.1 - -0.0001	118	0.9546	-0.02222	0.19422	0.01847	-0.039
0.0 - 0.0999	117	0.9058	0.07108	0.18028	-0.07063	0.149
0.1 - 0.1999	87	0.8655	-0.11134	0.16644	-0.28664	0.605
0.2 - 0.2999	61	0.830	-0.09384	0.13054	-0.40863	0.363
0.3 - 0.3999	69	0.8606	-0.11631	0.12400	-0.70546	1.490
0.4 - 0.4999	74	0.8598	-0.11712	0.12384	-0.72789	1.959
0.5 - 0.5999	31	0.8831	-0.09378	0.14141	-0.88245	1.863
0.6 - 0.6999	6	0.9062	-0.07070	0.08127	-0.75330	1.591
0.7 - 0.7999	0					
0.8 - 0.8999	0					
0.9 - 0.9999	0					

END OF RUN 63 -POINT 28
 TERMINATED: STOP

SAMPLE 63,29
 SUCCESSFUL (TEMP) RESTORE RUM63P29 AS (1P29)
 CANCELLED: DDNAME RMD5 UNKNOWN

DATA OUTPUT FOR RUN 63 POINT 29

AXIAL VELOCITY VS CONCENTRATION
 Z=152 MM AND R/R0= 0.125
 NO= 999 AND M4=998
 VBAR= 1.0449 MPB
 VRMS= 0.2190 MPB
 THIRD MOMENT OF TURBULENCE= 0.22058E-02 MFS883
 THIRD CORRELATION COEFFICIENT= 0.2099
 FOURTH MOMENT OF TURBULENCE= 0.57974E-02 MFS884
 FOURTH CORRELATION COEFFICIENT= 2.5181
 CBAR= 0.4117
 CRMS= 0.255X
 CPUPBAR= -0.028794
 OVERALL TRANSPORT COEFFICIENT= -0.515516

CONDITIONAL SAMPLING RESULTS

CONCENTRATION FLUCTUATION	NUMBER OF OCCURRENCES	MEAN	RELATIVE MEAN	RMS	TRANSPORT COEFFICIENT	TRANSPORT RATIO
-1.0 - -0.9001	0					
-0.9 - -0.8001	0					
-0.8 - -0.7001	0					
-0.7 - -0.6001	0					
-0.6 - -0.5001	0					
-0.5 - -0.4001	3	1.2290	0.18411	0.19559	-1.38565	2.688
-0.4 - -0.3001	99	1.2580	0.17113	0.18172	1.29885	2.520
-0.3 - -0.2001	134	1.2016	0.15668	0.18996	-0.72182	1.400
-0.2 - -0.1001	191	1.1037	0.05877	0.19858	-0.16814	0.726
-0.1 - -0.0001	140	0.9928	-0.05212	0.19452	0.04397	-0.085
0.0 - 0.0999	129	0.9971	-0.04777	0.19840	-0.03937	0.076
0.1 - 0.1999	81	0.9392	0.01571	0.17666	0.24324	0.472
0.2 - 0.2999	49	0.8880	-0.15886	0.14674	-0.73269	1.421
0.3 - 0.3999	60	0.9084	-0.13847	0.16569	-0.86407	1.676
0.4 - 0.4999	37	0.8974	-0.14746	0.13798	-1.19425	2.317
0.5 - 0.5999	40	0.8704	-0.17446	0.09376	-1.49724	3.792
0.6 - 0.6999	15	0.9235	-0.12135	0.07988	-1.36790	2.653
0.7 - 0.7999	0					
0.8 - 0.8999	0					
0.9 - 0.9999	0					

END OF RUN 63 -POINT 29
 TERMINATED: STOP

SAMPLE 63,30
 SUCCESSFUL (TEMP) RESTORE RUN63F30 AS (TF30)
 CANCELLED: DDNAME RMD5 UNKNOWN

DATA OUTPUT FOR RUN 63 POINT 30

AXIAL VELOCITY VS CONCENTRATION
 Z=152 MM AND R/RO= 0.175
 NO= 999 AND N4=998
 VBAR= 1.1652 MPS
 VRMS= 0.2307 MPS
 THIRD MOMENT OF TURBULENCE=-0.14648E-02 MFS**3
 THIRD CORRELATION COEFFICIENT= -0.1192
 FOURTH MOMENT OF TURBULENCE= 0.71544E-02 MFS**4
 FOURTH CORRELATION COEFFICIENT= 2.5246
 CBAR= 0.2762
 CRMS= 0.1972
 CPVPBAR= -0.024480
 OVERALL TRANSPORT COEFFICIENT= -0.537532

CONDITIONAL SAMPLING RESULTS

CONCENTRATION FLUCTUATION	NUMBER OF OCCURANCES	MEAN	RELATIVE MEAN	RMS	TRANSPORT COEFFICIENT	TRANSPORT RATIO
-1.0 - -0.9001	0					
-0.9 - -0.8001	0					
-0.8 - -0.7001	0					
-0.7 - -0.6001	0					
-0.6 - -0.5001	0					
-0.5 - -0.4001	0					
-0.4 - -0.3001	2	1.4635	0.29832	0.06851	-2.01484	3.748
-0.3 - -0.2001	140	1.3500	0.10487	0.20949	-1.02391	1.705
-0.2 - -0.1001	196	1.2780	0.11278	0.16765	-0.37885	0.705
-0.1 - -0.0001	224	1.1847	0.01953	0.21010	-0.04877	0.091
0.0 - 0.0999	179	1.1180	-0.04715	0.18819	-0.02301	0.117
0.1 - 0.1999	106	1.0331	-0.13211	0.21002	-0.41830	0.815
0.2 - 0.2999	70	0.9728	-0.19237	0.19492	-1.04965	1.953
0.3 - 0.3999	37	0.9789	-0.10523	0.15566	-1.42606	2.633
0.4 - 0.4999	18	0.9613	-0.20384	0.13970	-1.99683	3.715
0.5 - 0.5999	11	0.9483	-0.1690	0.10704	-2.49833	4.648
0.6 - 0.6999	14	0.8874	-0.22775	0.13630	-3.93111	7.313
0.7 - 0.7999	1	1.0430	0.12218	0.00000	1.93742	3.604
0.8 - 0.8999	0					
0.9 - 0.9999	0					

END OF RUN 63 -POINT 30
 TERMINATED: STOP

SAMPLE 63J1
 SUCCESSFUL (TEMP) RESTORE KUN63J1 AS (TF31)
 CANCELLED: DNAME RMD5 UNKNOWN

DATA OUTPUT FOR RUN 63 POINT 31

AXIAL VELOCITY VS CONCENTRATION
 Z=132 MM AND R/RQ= 0.225
 M= 999 AND N4=997
 VBAR= 1.2683 MPS
 VRMS= 0.2422 MPS
 THIRD MOMENT OF TURBULENCE=-0.52404E-02 MFS**3
 THIRD CORRELATION COEFFICIENT= -0.3690
 FOURTH MOMENT OF TURBULENCE= 0.90446E-02 MFS**4
 FOURTH CORRELATION COEFFICIENT= 2.3300
 CBAR= 0.197X
 CRMS= 0.171X
 CPVPBAR= -0.021122
 OVERALL TRANSPORT COEFFICIENT= -0.510441

CONDITIONAL SAMPLING RESULTS

CONCENTRATION FLUCTUATION	NUMBER OF OCCURRENCES	MEAN	RELATIVE MEAN	RMS	TRANSPORT COEFFICIENT	TRANSPORT RATIO
-1.0 - -0.9001	0					
-0.9 - -0.8001	0					
-0.8 - -0.7001	0					
-0.7 - -0.6001	0					
-0.6 - -0.5001	0					
-0.5 - -0.4001	0					
-0.4 - -0.3001	0					
-0.3 - -0.2001	60	1.432H	0.16446	0.21294	-0.82973	1.626
-0.2 - -0.1001	280	1.3884	0.12014	0.21635	0.43350	0.049
-0.1 - -0.0001	225	1.3185	0.05024	0.19989	-0.06231	0.161
-0.0 - 0.0999	192	1.2157	-0.07265	0.21256	0.07853	0.134
0.1 - 0.1999	111	1.1282	-0.14007	0.20355	-0.51467	1.008
0.2 - 0.2999	64	1.0785	0.10976	0.18299	-1.10108	2.157
0.3 - 0.3999	36	1.0466	-0.23173	0.22466	-1.81941	3.565
0.4 - 0.4999	13	0.9582	0.31215	0.15726	3.46937	6.797
0.5 - 0.5999	3	0.9677	-0.30061	0.11614	-3.96355	7.765
0.6 - 0.6999	0					
0.7 - 0.7999	0					
0.8 - 0.8999	0					
0.9 - 0.9999	0					
		0.9413	0.37697	0.03797	-4.97792	9.752

END OF RUN 63 -POINT 31
 TERMINATED: STOP

SAMPLE 63J2
 SUCCESSFUL (ITEM) RESTORE KUN63J2 AS (1F32)
 CANCELLED: DDNAME RMS UNKNOWN

DATA OUTPUT FOR RUN 63 POINT J2

AXIAL VELOCITY VS CONCENTRATION
 Z=152 MM AND R/KO= 0.325
 NO= 999 AND N4=974
 UBAR= 1.3713 MPS
 VRMS= 0.2231 MPS
 THIRD MOMENT OF TURBULENCE=-0.86908E-02 MPS**3
 THIRD CORRELATION COEFFICIENT= -0.7829
 FOURTH MOMENT OF TURBULENCE= 0.80614E-02 MPS**4
 FOURTH CORRELATION COEFFICIENT= 3.2355
 CBAR= 0.0732
 CRMS= 0.1142
 CPUFBAR= -0.005959
 OVERALL TRANSPORT COEFFICIENT= -0.230130

CONDITIONAL SAMPLING RESULTS

CONCENTRATION FLUCTUATION	NUMBER OF OCCURRENCES	MEAN	RELATIVE MEAN	RMS	TRANSPORT COEFFICIENT	TRANSPORT RATIO
-1.0 - -0.9001	0					
-0.9 - -0.8001	0					
-0.8 - -0.7001	0					
-0.7 - -0.6001	0					
-0.6 - -0.5001	0					
-0.5 - -0.4001	0					
-0.4 - -0.3001	0					
-0.3 - -0.2001	0					
-0.2 - -0.1001	19	1.4574	0.08602	0.19955	-0.34965	1.519
-0.1 - -0.0001	646	1.3856	0.01424	0.22648	0.02969	0.129
0.0 - 0.0999	160	1.4143	0.04300	0.17252	0.04505	-0.196
0.1 - 0.1999	76	1.3165	-0.05481	0.17902	-0.35660	1.550
0.2 - 0.2999	34	1.1926	-0.17870	0.24405	-1.78822	7.770
0.3 - 0.3999	24	1.2007	-0.17060	0.23666	-2.28260	9.919
0.4 - 0.4999	11	1.2186	-0.15271	0.17507	2.58150	11.218
0.5 - 0.5999	3	0.9260	-0.44534	0.13437	-9.00262	39.120
0.6 - 0.6999	1	1.0550	0.31634	0.00000	-7.80620	33.721
0.7 - 0.7999	0					
0.8 - 0.8999	0					
0.9 - 0.9999	0					

END OF RUN 63 -POINT J2
 TERMINATED: STOP

SAMPLE 63J3
 SUCCESSFUL (TEMP) KESTORE RUN63P33 AS (TP33)
 CANCELLED: DDNAME RMD5 UNKNOWN

DATA OUTPUT FOR RUN 63 POINT 33

AXIAL VELOCITY VS CONCENTRATION
 Z=152 MM AND R/R0= 0.425
 NO= 999 AND N4=982
 VBAR= 1.2108 MFS
 URMS= 0.2943 MFS
 THIRD MOMENT OF TURBULENCE=-0.18863E-01 MFS**3
 THIRD CORRELATION COEFFICIENT= -0.7398
 FOURTH MOMENT OF TURBULENCE= 0.24559E-01 MFS**4
 FOURTH CORRELATION COEFFICIENT= 3.2725
 CBAR= 0.0172
 CRMS= 0.0532
 CPVBAR= 0.00044
 OVERALL TRANSPORT COEFFICIENT= 0.028279

CONDITIONAL SAMPLING RESULTS

CONCENTRATION FLUCTUATION	NUMBER OF OCCURANCES	MEAN	RELATIVE MEAN	RMS	TRANSPORT COEFFICIENT	TRANSPORT RATIO
-1.0 - -0.9001	0					
-0.9 - -0.8001	0					
-0.8 - -0.7001	0					
-0.7 - -0.6001	0					
-0.6 - -0.5001	0					
-0.5 - -0.4001	0					
-0.4 - -0.3001	0					
-0.3 - -0.2001	0					
-0.2 - -0.1001	0					
-0.1 - -0.0001	485	1.2133	0.00245	0.29197	-0.02270	-0.803
0.0 - 0.0999	234	1.1993	-0.01152	0.30915	0.06888	2.436
0.1 - 0.1999	28	1.3410	0.11018	0.19807	1.20554	42.630
0.2 - 0.2999	10	1.1928	-0.01802	0.16546	-0.42700	-15.099
0.3 - 0.3999	5	1.1140	0.02682	0.17451	2.54077	-82.773
0.4 - 0.4999	1	1.3190	0.10818	0.00000	3.06063	108.228
0.5 - 0.5999	0					
0.6 - 0.6999	0					
0.7 - 0.7999	0					
0.8 - 0.8999	0					
0.9 - 0.9999	0					

END OF RUN 63 -POINT 33
 TERMINATED: STOP

SAMPLE 63.34
 SUCCESSFUL (TEMP) RESTORE RUN63P34 AS (IF34)
 CANCELLED: DDNAME RMS UNKNOWN

DATA OUTPUT FOR RUN 63 POINT 34

AXIAL VELOCITY VS CONCENTRATION
 Z=152 MM AND R/R0= 0.025
 NO= 999 AND N4=996
 VBAR= 0.9075 MPS
 VRMS= 0.1888 MPS
 THIRD MOMENT OF TURBULENCE= 0.22865E-02 MFS883
 THIRD CORRELATION COEFFICIENT= 0.3396
 FOURTH MOMENT OF TURBULENCE= 0.37632E-07 MFS884
 FOURTH CORRELATION COEFFICIENT= 2.9575
 CBAR= 0.5502
 CRMS= 0.2732
 CPVPBAR= -0.021361
 OVERALL TRANSPORT COEFFICIENT= -0.414777

CONDITIONAL SAMPLING RESULTS

CONCENTRATION FLUCTUATION	NUMBER OF OCCURRENCES	MEAN	RELATIVE MEAN	RMS	TRANSPORT COEFFICIENT	TRANSPORT RATIO
-1.0 - -0.9001	0					
-0.9 - -0.8001	0					
-0.8 - -0.7001	0					
-0.7 - -0.6001	0					
-0.6 - -0.5001	5	1.1706	0.26312	0.15440	-2.70662	6.523
-0.5 - -0.4001	34	1.1185	0.21104	0.15158	-1.84638	4.452
-0.4 - -0.3001	105	1.0790	0.17150	0.19885	1.20077	2.395
-0.3 - -0.2001	143	0.9634	0.05587	0.19596	-0.28276	0.682
-0.2 - -0.1001	127	0.9331	0.02564	0.17618	-0.08198	0.198
-0.1 - -0.0001	106	0.8734	-0.03411	0.19100	0.02660	-0.064
0.0 - 0.0999	127	0.8455	-0.04194	0.16067	-0.04809	0.116
0.1 - 0.1999	89	0.8442	-0.06328	0.16521	-0.18760	0.452
0.2 - 0.2999	79	0.8001	-0.10734	0.11691	-0.31699	1.246
0.3 - 0.3999	72	0.8425	-0.06507	0.11705	-0.44230	1.066
0.4 - 0.4999	86	0.8433	-0.06418	0.10371	-0.57038	1.351
0.5 - 0.5999	20	0.8228	0.08468	0.10318	-0.09086	2.148
0.6 - 0.6999	3	0.8490	-0.05648	0.05067	-0.70457	1.699
0.7 - 0.7999	0					
0.8 - 0.8999	0					
0.9 - 0.9999	0					

END OF RUN 63 -POINT 34
 TERMINATED: STOP

SAMPL 51.8
 SUCCESSFUL (TEMP) RESTORE RUNSIPB AS (TFB)
 CANCELLED: DNAME RMS UNKNOWN

DATA OUTPUT FOR RUN 51 POINT 8

RAJIAL VELOCITY VS CONCENTRATION
 Z=152 MM AND R/R0= 0.025
 NO. 999 AND M4=982
 VRMS= -0.0012 MFS
 THIRD MOMENT OF TURBULENCE= 0.20424E-03 MFS**3
 THIRD CORRELATION COEFFICIENT= 0.0986
 FOURTH MOMENT OF TURBULENCE= 0.98762E-03 MFS**4
 FOURTH CORRELATION COEFFICIENT= 3.2010
 CBAR= 0.548Z
 CRMS= 0.265Z
 CPUFBAR= -0.001080
 OVERALL TRANSPORT COEFFICIENT= -0.030756

CONDITIONAL SAMPLING RESULTS

CONCENTRATION FLUCTUATION	NUMBER OF OCCURRENCES	MEAN	RELATIVE MEAN	RMS	TRANSPORT COEFFICIENT	TRANSPORT RATIO
-1.0 - -0.9001	0					
-0.9 - -0.8001	0					
-0.8 - -0.7001	0					
-0.7 - -0.6001	0					
-0.6 - -0.5001	6	0.0467	0.0478	0.18330	-0.62957	20.469
-0.5 - -0.4001	39	-0.0282	-0.02700	0.18836	0.36850	-12.631
-0.4 - -0.3001	78	0.0345	0.03566	0.18482	-0.36267	11.124
-0.3 - -0.2001	140	-0.0023	-0.00110	0.16783	-0.00316	0.168
-0.2 - -0.1001	133	0.0084	0.00958	0.13447	-0.04415	1.416
-0.1 - -0.0001	138	-0.0121	-0.01081	0.12704	0.01661	-0.605
0.0 - 0.0999	118	-0.0119	-0.01076	0.12464	-0.01405	0.452
0.1 - 0.1999	62	0.0123	0.01344	0.09079	0.01097	-1.782
0.2 - 0.2999	72	-0.0051	-0.00396	0.08590	-0.02749	0.894
0.3 - 0.3999	81	-0.0145	-0.01334	0.07768	-0.13071	4.250
0.4 - 0.4999	73	-0.0079	-0.00669	0.08937	-0.08344	2.713
0.5 - 0.5999	20	0.0133	0.01453	0.06537	0.22293	-7.148
0.6 - 0.6999	2	0.0470	0.04818	0.02100	0.84476	-27.141
0.7 - 0.7999	0					
0.8 - 0.8999	0					
0.9 - 0.9999	0					

END OF RUN 51 -POINT 8
 TERMINATED: STOP

SAMPLE 51.9
 SUCCESSFUL (TEMP) RESTORE KUN51F9 AS (TF9)
 CANCELLED: (DNAME RMD5 UNKNOWN

DATA OUTPUT FOR RUN 51 POINT 9

RADIAL VELOCITY VS CONCENTRATION
 Z=152 MM AND K/RO= 0.075
 NO= 999 AND N4=990
 UBAR= -0.0129 MPS
 VRMS= 0.1360 MPS
 THIRD MOMENT OF TURBULENCE=-0.87412E-03 MFS**3
 THIRD CORRELATION COEFFICIENT= -0.1473
 FOURTH MOMENT OF TURBULENCE= 0.11120E-02 MFS**4
 FOURTH CORRELATION COEFFICIENT= 3.2484
 CBAR= 0.510X
 CRMS= 0.256X
 CVPVBAR= 0.011591
 OVERALL TRANSPORT COEFFICIENT= 0.332705

CONDITIONAL SAMPLING RESULTS

CONCENTRATION FLUCTUATION	NUMBER OF OCCURRENCES	MEAN	RELATIVE MEAN	RMS	TRANSPORT COEFFICIENT	TRANSPORT RATIO
-1.0 - -0.9001	0					
-0.9 - -0.8001	0					
-0.8 - -0.7001	0					
-0.7 - -0.6001	0					
-0.6 - -0.5001	3	-0.3003	-0.28744	0.04224	4.20971	12.653
-0.5 - -0.4001	37	-0.1334	-0.12076	0.17973	1.57153	4.723
-0.4 - -0.3001	83	-0.0924	-0.07952	0.19612	0.74825	2.369
-0.3 - -0.2001	127	-0.0643	-0.05141	0.14166	0.37102	1.115
-0.2 - -0.1001	147	-0.0198	-0.00493	0.13609	0.03440	0.103
-0.1 - -0.0001	137	-0.0093	0.00359	0.11738	-0.00784	-0.024
0.0 - 0.0999	106	0.0195	0.03244	0.10833	0.05193	0.156
0.1 - 0.1999	109	0.0083	0.02115	0.11133	0.09531	0.186
0.2 - 0.2999	83	0.0522	0.06501	0.08491	0.45506	1.368
0.3 - 0.4999	77	0.0439	0.05676	0.07209	0.36326	1.093
0.4 - 0.4999	55	0.0289	0.04182	0.09190	0.52975	1.592
0.5 - 0.5999	26	0.0323	0.04523	0.07382	0.67765	2.037
0.6 - 0.6999	0					
0.7 - 0.7999	0					
0.8 - 0.8999	0					
0.9 - 0.9999	0					

END OF RUN 51 -POINT 9
 TERMINATED: STOP

SAMPLE 51,10
 SUCCESSFUL / TEMP, RESIDUE KUN51F10 AS (TF10)
 CANCELLED: UNKNOWN

DATA OUTPUT FOR KUN 51 POINT 10

RADIAL VELOCITY VS CONCENTRATION
 Z=152 MM AND R/R0= 0.125
 NO= 999 AND N4=991
 VBAR= -0.0215 MPS
 VRMS= 0.1509 MPS
 THIRD MOMENT OF TURBULENCE=-0.98048E-03 MFS**3
 THIRD CORRELATION COEFFICIENT= -0.2853
 FOURTH MOMENT OF TURBULENCE= 0.16024E-02 MFS**4
 FOURTH CORRELATION COEFFICIENT= 3.0701
 CBAR= 0.401Z
 CRMS= 0.236Z
 CUPBAR= 0.016350
 OVERALL TRANSPORT COEFFICIENT= 0.458312

CONDITIONAL SAMPLING RESULTS

CONCENTRATION FLUCTUATION	NUMBER OF OCCURRENCES	MEAN	RELATIVE MEAN	RMS	TRANSPORT COEFFICIENT	TRANSPORT RATIO
-1.0 - -0.9001	0					
-0.9 - -0.8001	0					
-0.8 - -0.7001	0					
-0.7 - -0.6001	0					
-0.6 - -0.5001	0					
-0.5 - -0.4001	7	-0.1844	-0.16289	0.14217	1.87018	4.081
-0.4 - -0.3001	62	-0.1898	0.11830	0.17977	1.4485	3.174
-0.3 - -0.2001	128	-0.1013	-0.07974	0.17016	0.57672	1.258
-0.2 - -0.1001	209	-0.0708	-0.04525	0.13847	0.22689	0.495
-0.1 - -0.0001	169	-0.0126	0.00891	0.13698	-0.00087	-0.002
-0.0 - 0.0999	126	0.0155	0.01704	0.12841	0.06687	0.146
0.1 - 0.1999	83	0.0521	0.07367	0.10364	0.29254	0.638
0.2 - 0.2999	62	0.0644	0.08196	0.08374	0.59441	1.197
0.3 - 0.3999	68	0.0626	0.08415	0.09015	0.82475	1.800
0.4 - 0.4999	46	0.0707	0.07219	0.04815	1.18191	2.379
0.5 - 0.5999	26	0.0869	0.10847	0.08139	1.62240	3.540
0.6 - 0.6999	5	0.0656	0.08714	0.05642	1.53457	3.348
0.7 - 0.7999	0					
0.8 - 0.8999	0					
0.9 - 0.9999	0					

END OF RUN 51 - POINT 10
 TERMINATED: STOP

SAMPLE 81.11
 SUCCESSFUL (TEMP) RESTOKE RUNSIF11 AS (TF11)
 CANCELLED: BOMME ANDS UNANIMM

DATA OUTPUT FOR RUN 51 POINT 11

RADIAL VELOCITY VS CONCENTRATION
 Z=152 MH AND R/R0= 0.175
 NO= 999 AND N4=993
 UBAR= -0.0371 MFS
 VRMS= 0.1608 MFS
 THIRD MOMENT OF TURBULENCE=-0.6720JK-03 MF5883
 THIRD CORRELATION COEFFICIENT= -0.1617
 FOURTH MOMENT OF TURBULENCE= 0.18304E-02 MFS884
 FOURTH CORRELATION COEFFICIENT= 2.7404
 CBAR= 0.321X
 CRMS= 0.216X
 CPVFBAR= 0.017106
 OVERALL TRANSPORT COEFFICIENT= 0.492046

CONDITIONAL SAMPLING RESULTS

CONCENTRATION FLUCTUATION	NUMBER OF OCCURANCES	MEAN	RELATIVE %LAN	RMS	TRANSPORT COEFFICIENT	TRANSPORT RATIO
-1.0 - -0.9001	0	-0.1651	-0.12801	0.12956	1.18328	2.465
-0.9 - -0.8001	0	-0.1439	-0.10480	0.14701	0.77300	1.571
-0.8 - -0.7001	0	-0.0958	-0.05869	0.16571	0.35254	0.513
-0.7 - -0.6001	0	-0.0556	-0.01854	0.14607	0.03399	0.054
-0.6 - -0.5001	0	-0.0014	0.03571	0.13051	0.05761	0.117
-0.5 - -0.4001	0	0.0643	0.07919	0.17418	0.44489	0.701
-0.4 - -0.3001	31	0.1001	0.10144	0.10283	0.70436	1.431
-0.3 - -0.2001	152	0.0862	0.13719	0.09531	1.37533	2.755
-0.2 - -0.1001	197	0.1384	0.17325	0.09846	1.59463	3.241
-0.1 - -0.0001	187	0.0922	0.12924	0.08843	2.74419	5.577
0.0 - 0.0999	141	0.0830	0.12924	0.08843	2.38544	4.848
0.1 - 0.1999	111	0.0830	0.12924	0.08843	2.48664	4.976
0.2 - 0.2999	69	0.1001	0.13719	0.09531	1.37533	2.755
0.3 - 0.3999	47	0.0862	0.12325	0.09846	1.59463	3.241
0.4 - 0.4999	30	0.0862	0.12325	0.09846	1.59463	3.241
0.5 - 0.5999	14	0.1384	0.17325	0.11674	2.74419	5.577
0.6 - 0.6999	13	0.0922	0.12924	0.08843	2.38544	4.848
0.7 - 0.7999	1	0.0830	0.12924	0.08843	2.38544	4.848
0.8 - 0.8999	0	0.0830	0.12924	0.08843	2.38544	4.848
0.9 - 0.9999	0	0.0830	0.12924	0.08843	2.38544	4.848

END OF RUN 51 -POINT 11
 TERMINATED: STOP

ORIGINAL PAGE IS
OF POOR QUALITY

SAMPLE 51.1.
SUCCESSFUL (TEMP) RESTORE RUNSIP12 AS (TF12)
CANCELLED: UNKNOWN UNKNONN

DATA OUTPUT FOR RUN 51 POINT 12

RADIAL VELOCITY VS CONCENTRATION
Z=152 MM AND R/R0= 0.235
N0= 999 AND N4=993
VBAR= -0.0143 MFS
VRMS= 0.1679 MFS
THIRD MOMENT OF TURBULENCE=-0.92308E-03 MFS**3
THIRD CORRELATION COEFFICIENT= -0.1950
FOURTH MOMENT OF TURBULENCE= 0.22956E-02 MFS**4
FOURTH CORRELATION COEFFICIENT= 2.8885
CBAR= 0.2502
CRMS= 0.2092
CPVBAR= 0.016107
OVERALL TRANSPORT COEFFICIENT= 0.458471

CONDITIONAL SAMPLING RESULTS

CONCENTRATION FLUCTUATION	NUMBER OF OCCURANCES	MEAN	RELATIVE MEAN	RMS	TRANSPORT COEFFICIENT	TRANSPORT RATIO
-1.0 - -0.9001	0					
-0.9 - -0.8001	0					
-0.8 - -0.7001	0					
-0.7 - -0.6001	0					
-0.6 - -0.5001	0					
-0.5 - -0.4001	0					
-0.4 - -0.3001	0					
-0.3 - -0.2001	189	-0.1058	-0.09153	0.15423	0.59311	1.298
-0.2 - -0.1001	177	-0.0727	-0.05841	0.13311	0.25980	0.567
-0.1 - -0.0001	212	-0.0346	-0.02030	0.15859	0.03441	0.072
0.0 - 0.0999	170	0.0048	0.01909	0.14367	0.07341	0.055
0.1 - 0.1999	91	0.0604	0.07470	0.14014	0.37057	0.899
0.2 - 0.2999	53	0.1032	0.11747	0.13470	0.44002	1.832
0.3 - 0.3999	45	0.1290	0.14378	0.10903	1.40861	3.072
0.4 - 0.4999	25	0.1487	0.16296	0.10326	2.08485	4.552
0.5 - 0.5999	15	0.1409	0.15515	0.10452	2.47207	5.392
0.6 - 0.6999	10	0.1264	0.14068	0.05536	2.59859	5.668
0.7 - 0.7999	3	0.1743	0.18861	0.02073	3.94406	8.503
0.8 - 0.8999	3	0.2697	0.28395	0.07759	7.01706	15.305
0.9 - 0.9999	0					

END OF RUN 51 -POINT 12
TERMINATED: STOP

SAMPLE 51,14
 SUCCESSFUL (TEMP) NESTORE KUN51P14 AS (TF14)
 CANCELLED: UNKNOWN RMS UNKNOWN

DATA OUTPUT FOR RUN 51 POINT 14

RADIAL VELOCITY VS CONCENTRATION
 Z=152 MM AND R/R0= 0.275
 NO= 999 AND N4=990
 VBAR= -0.0134 MFS
 VRMS= 0.1768 MFS
 THIRD MOMENT OF TURBULENCE=-0.1735E 02 MF.443
 THIRD CORRELATION COEFFICIENT= -0.3130
 FOURTH MOMENT OF TURBULENCE= 0.30041E-02 MFS**4
 FOURTH CORRELATION COEFFICIENT= 3.0715
 CBAR= 0.1692
 CRMS= 0.1733
 CPUFBAR= 0.012604
 OVERALL TRANSPORT COEFFICIENT= 0.412194

CONDITIONAL SAMPLING RESULTS

CONCENTRATION FLUCTUATION	NUMBER OF OCCURRENCES	MEAN	RELATIVE MEAN	RMS	TRANSPORT COEFFICIENT	TRANSPORT RATIO
-1.0 - -0.9001	0					
-0.9 - -0.8001	0					
-0.8 - -0.7001	0					
-0.7 - -0.6001	0					
-0.6 - -0.5001	0					
-0.5 - -0.4001	0					
-0.4 - -0.3001	0					
-0.3 - -0.2001	2	-0.0050	0.00840	0.04200	-0.05513	-0.134
-0.2 - -0.1001	378	-0.0837	0.07039	0.18107	0.34857	0.446
-0.1 - -0.0001	213	-0.0314	-0.01797	0.16066	0.02661	0.065
0.0 - 0.0999	160	0.0236	0.01700	0.15339	0.07001	0.170
0.1 - 0.1999	120	0.0376	0.05098	0.12868	0.26512	0.643
0.2 - 0.2999	53	0.1205	0.11387	0.13312	1.09814	2.664
0.3 - 0.3999	28	0.1421	0.15547	0.14350	1.78440	4.329
0.4 - 0.4999	16	0.1922	0.20559	0.10523	2.99292	7.261
0.5 - 0.5999	12	0.1481	0.16146	0.08864	2.91831	7.080
0.6 - 0.6999	4	0.2650	0.27840	0.04467	3.75303	13.937
0.7 - 0.7999	3	0.1190	0.13240	0.08916	3.08397	7.482
0.8 - 0.8999	1	0.1460	0.15940	0.00000	4.41731	10.717
0.9 - 0.9999	0					

END OF RUN 51 -POINT 14
 TERMINATED: STOP

SAMPLE 5115
 SUCCESSFUL (TEMP, KESTUKE KUNSHIP15 AS (TF15)
 CANCELLED: DNAME KNDS UNKNOWN

DATA OUTPUT FOR RUN 51 POINT 15

RADIAL VELOCITY VS CONCENTRATION
 Z=152 MM AND R/R0= 0.324
 NO= 999 AND N4=984
 UBAR= 0.0177 MFS
 VRMS= 0.1837 MFS
 THIRD MOMENT OF TURBULENCE=-0.11389E-02 MFS**3
 THIRD CORRELATION COEFFICIENT= -0.1838
 FOURTH MOMENT OF TURBULENCE= 0.34364E-02 MFS**4
 FOURTH CORRELATION COEFFICIENT= 3.0195
 CBAR= 0.086X
 CRMS= 0.127X
 CPUPBAR= 0.007435
 OVERALL TRANSPORT COEFFICIENT= 0.317890

CONDITIONAL SAMPLING RESULTS

CONCENTRATION FLUCTUATION	NUMBER OF OCCURANCES	MEAN	RELATIVE MEAN	RMS	TRANSPORT COEFFICIENT	TRANSPORT RATIO
-1.0 - -0.9001	0					
-0.9 - -0.8001	0					
-0.8 - -0.7001	0					
-0.7 - -0.6001	0					
-0.6 - -0.5001	0					
-0.5 - -0.4001	0					
-0.4 - -0.3001	0					
-0.3 - -0.2001	0					
-0.2 - -0.1001	70	-0.0308	-0.04852	0.13920	0.21957	0.691
-0.1 - -0.0001	587	-0.0147	-0.03234	0.18553	0.10116	0.110
0.0 - 0.0999	166	0.0519	0.03474	0.15623	0.08644	0.272
0.1 - 0.1999	85	0.0621	0.04444	0.14496	0.30277	0.752
0.2 - 0.2999	36	0.1730	0.15231	0.16782	1.67483	5.269
0.3 - 0.3999	21	0.1800	0.16232	0.14754	2.14363	7.487
0.4 - 0.4999	8	0.2357	0.21807	0.07744	4.13511	13.008
0.5 - 0.5999	8	0.2014	0.13370	0.10173	4.27196	13.501
0.6 - 0.6999	3	0.2530	0.23537	0.03476	6.31431	19.863
0.7 - 0.7999	0					
0.8 - 0.8999	0					
0.9 - 0.9999	0					

END OF RUN 51 -POINT 15
 TERMINATED: STOP

SAMPLE 51.16
 SUCCESSFUL (TEMP) RESTORE RUNS16 AS (TF13)
 CANCELLED: DNAME RMS UNKNOWN

DATA OUTPUT FOR RUN 51 POINT 16

RADIAL VELOCITY VS CONCENTRATION
 Z=152 MM AND R/R0= 0.175
 N0= 999 AND N4=991
 VBAR= 0.0141 MFS
 VRMS= 0.2063 MPS
 THIRD MOMENT OF TURBULENCE=-0.24825E-02 MFS**3
 THIRD CORRELATION COEFFICIENT= -0.2827
 FOURTH MOMENT OF TURBULENCE= 0.59804E-02 MFS**4
 FOURTH CORRELATION COEFFICIENT= 3.3015
 CBAR= 0.045X
 CRMS= 0.091X
 CPUPBAR= 0.004325
 OVERALL TRANSPORT COEFFICIENT= 0.231336

CONDITIONAL SAMPLING RESULTS

CONCENTRATION FLUCTUATION	NUMBER OF OCCURRENCES	MEAN	RELATIVE MEAN	RMS	TRANSPORT COEFFICIENT	TRANSPORT RATIO
-1.0 - -0.9001	0	-0.0104	-0.02454	0.20708	0.05304	0.229
-0.9 - -0.8001	0	0.0485	0.03434	0.20017	0.14858	0.442
-0.8 - -0.7001	0	0.1020	0.08787	0.14338	0.65101	2.814
-0.7 - -0.6001	0	0.1249	0.11079	0.14966	1.35809	5.071
-0.6 - -0.5001	0	0.1645	0.15236	0.12214	2.81257	12.158
-0.5 - -0.4001	0	0.2609	0.24676	0.19204	5.69401	24.822
-0.4 - -0.3001	0	0.2740	0.26186	0.00201	7.64486	33.047
-0.3 - -0.2001	0	0.1740	0.11986	0.00000	5.17428	23.137
-0.2 - -0.1001	0					
-0.1 - -0.0001	718					
-0.0 - 0.0999	175					
0.1 - 0.1999	60					
0.2 - 0.2999	15					
0.3 - 0.3999	10					
0.4 - 0.4999	10					
0.5 - 0.5999	2					
0.6 - 0.6999	1					
0.7 - 0.7999	0					
0.8 - 0.8999	0					
0.9 - 0.9999	0					

END OF RUN 51 -POINT 16
 TERMINATED: STOP

SAMPLE 51,17
 SUCCESSFUL (TEMP) NESTOR KUNSI17 AS (T17)
 CANCELLED: UNKNOWN

DATA OUTPUT FOR RUN 51 POINT 17

RADIAL VELOCITY VS CONCENTRATION
 Z=152 MM AND R/R0= 0.425
 N0= 999 AND N4=990
 VBAR= 0.0401 MPS
 VRMS= 0.2194 MPS
 THIRD MOMENT OF TURBULENCE=-0.42006E-02 MFS**3
 THIRD CORRELATION COEFFICIENT= -0.3979
 FOURTH MOMENT OF TURBULENCE= 0.74492E-02 MFS**4
 FOURTH CORRELATION COEFFICIENT= 3.2166
 CBAR= 0.023X
 CRMS= 0.054X
 CPVPBAR= 0.002122
 OVERALL TRANSPORT COEFFICIENT= 0.171592

CONDITIONAL SAMPLING RESULTS

CONCENTRATION FLUCTUATION	NUMBER OF OCCURRENCES	MEAN	RELATIVE MEAN	RMS	TRANSPORT COEFFICIENT	TRANSPORT RATIO
-1.0 - -0.9001	0					
-0.9 - -0.8001	0					
-0.8 - -0.7001	0					
-0.7 - -0.6001	0					
-0.6 - -0.5001	0					
-0.5 - -0.4001	0					
-0.4 - -0.3001	0					
-0.3 - -0.2001	0					
-0.2 - -0.1001	0					
-0.1 - -0.0001	692	0.0267	-0.01335	0.21606	0.00440	0.026
0.0 - 0.0999	240	0.0403	0.09023	0.22886	0.07017	0.292
0.1 - 0.1999	40	0.1752	0.13511	0.15020	1.65402	9.639
0.2 - 0.2999	15	0.2375	0.17747	0.11400	3.88145	22.520
0.3 - 0.3999	1	0.2610	0.22093	0.00000	6.50590	37.915
0.4 - 0.4999	2	0.3392	0.29943	0.04850	11.95493	69.670
0.5 - 0.5999	0					
0.6 - 0.6999	0					
0.7 - 0.7999	0					
0.8 - 0.8999	0					
0.9 - 0.9999	0					

END OF RUN 51 -POINT 17
 TERMINATED: STOP

SAMPLE 51,21
 SUCCESSFUL (TEMP) RESTOKE RUNSIF21 AS (TF21/
 CANCELLED: DNAME RMS UNKNOWN

DATA OUTPUT FOR RUN 51 POINT 21

RADIAL VELOCITY VS CONCENTRATION
 Z=152 MM AND R/KO= 0.624
 NO= 999 AND N4=991
 UBAR= 0.0405 MFS
 VRMS= 0.2339 MFS
 THIRD MOMENT OF TURBULENCE= 0.16932E-02 MFS**3
 THIRD CORRELATION COEFFICIENT= 0.1324
 FOURTH MOMENT OF TURBULENCE= 0.10379E-01 MFS**4
 FOURTH CORRELATION COEFFICIENT= 3.4689
 CBAR= 0.0132
 CRMS= 0.0222
 CPVPRAR= -0.000354
 OVERALL TRANSPORT COEFFICIENT= -0.068616

CONDITIONAL SAMPLING RESULTS

CONCENTRATION FLUCTUATION	NUMBER OF OCCURRENCES	MEAN	RELATIVE MEAN	RMS	TRANSPORT COEFFICIENT	TRANSPORT RATIO
-1.0 - -0.9001	0					
-0.9 - -0.8001	0					
-0.8 - -0.7001	0					
-0.7 - -0.6001	0					
-0.6 - -0.5001	0					
-0.5 - -0.4001	0					
-0.4 - -0.3001	0					
-0.3 - -0.2001	0					
-0.2 - -0.1001	0					
-0.1 - -0.0001	522	0.0576	0.01710	0.22337	-0.07901	1.151
-0.0 - 0.0999	469	0.0215	-0.01903	0.24366	-0.05707	0.832
0.1 - 0.1999	0					
0.2 - 0.2999	0					
0.3 - 0.3999	0					
0.4 - 0.4999	0					
0.5 - 0.5999	0					
0.6 - 0.6999	0					
0.7 - 0.7999	0					
0.8 - 0.8999	0					
0.9 - 0.9999	0					

END OF RUN 51 -POINT 21
 TERMINATED: STOP

SAMPLE 51.27
 SUCCESSFUL (TEMP) RESTORE KUN51F07 M5 (TF 7)
 CANCELLED: DDNAME AMDS UNF/MGMH

DATA OUTPUT FOR KUN 51 POINT 27

RADIAL VELOCITY VS CONCENTRATION
 Z=152 MM AND R/R0= 0.025
 NO= 999 AND NA=991
 VBAR= -0.0126 MPS
 VRMS= 0.1430 MPS
 THIRD MOMENT OF TURBULENCE=-0.40891E-03 MFS**3
 THIRD CORRELATION COEFFICIENT= -0.1397
 FOURTH MOMENT OF TURBULENCE= 0.14709E-02 MFS**4
 FOURTH CORRELATION COEFFICIENT= 3.5145
 CBAR= 0.5502
 CRMS= 0.2752
 CPVPBAR= 0.004814
 OVERALL TRANSPORT COEFFICIENT= 0.122495

CONDITIONAL SAMPLING RESULTS

CONCENTRATION FLUCTUATION	NUMBER OF OCCURRENCES	MEAN	RELATIVE MEAN	RMS	TRANSPORT COEFFICIENT	TRANSPORT RATIO
-1.0 - -0.9001	0					
-0.9 - -0.8001	0					
-0.8 - -0.7001	0					
-0.7 - -0.6001	0					
-0.6 - -0.5001	11	-0.0353	-0.02263	0.28142	0.31005	2.531
-0.5 - -0.4001	54	-0.0401	0.07746	0.21717	0.32881	2.884
-0.4 - -0.3001	75	-0.0335	-0.07084	0.18454	0.18560	1.517
-0.3 - -0.2001	123	-0.0386	-0.03598	0.14912	0.17968	1.467
-0.2 - -0.1001	133	-0.0244	-0.01177	0.15898	0.05197	0.424
-0.1 - -0.0001	136	0.0029	0.03554	0.11980	-0.02128	-0.174
0.0 - 0.0999	99	-0.0154	-0.00278	0.12126	-0.00789	-0.064
0.1 - 0.1999	95	-0.0080	0.09461	0.11021	0.01739	0.142
0.2 - 0.2999	83	0.0073	0.01994	0.10624	0.12593	1.028
0.3 - 0.3999	75	0.0075	0.02017	0.08644	0.17825	1.455
0.4 - 0.4999	65	0.0213	0.03394	0.07392	0.40442	3.302
0.5 - 0.5999	33	0.0023	0.01492	0.08903	0.20286	1.656
0.6 - 0.6999	2	-0.0545	-0.04185	0.03250	-0.67197	-5.486
0.7 - 0.7999	0					
0.8 - 0.8999	0					
0.9 - 0.9999	0					

END OF RUN 51 -POINT 27
 TERMINATED: STOP

ORIGINAL PAGE IS
 OF POOR QUALITY

SAMPLE 51.28
 SUCCESSFUL (ITEM) RESTORE RUN51P28 AS (1F28)
 CANCELLED: UNKNOWN NAME UNKNOWN

DATA OUTPUT FOR RUN 51 POINT 28

RADIAL VELOCITY VS CONCENTRATION
 Z=152 MM AND R/R0=-0.025
 N0= 999 AND N4=986
 VBAK= -0.0033 MFS
 VRMS= 0.1440 MFS
 THIRD MOMENT OF TURBULENCE=-0.63230E-03 MFS**3
 THIRD CORRELATION COEFFICIENT= -0.2117
 FOURTH MOMENT OF TURBULENCE= 0.13094E-02 MFS**4
 FOURTH CORRELATION COEFFICIENT= 3.0439
 CRAR= 0.578Z
 CRMS= 0.288Z
 CFVBAR= 0.01083B
 OVERALL TRANSPORT COEFFICIENT= 0.261394

CONDITIONAL SAMPLING RESULTS

CONCENTRATION FLUCTUATION	NUMBLK OF OCCURRENCES	MEAN	RELATIVE MEAN	RMS	IMPORT COEFFICIENT	TRANSPORT RATIO
-1.0 - -0.9001	0					
-0.9 - -0.8001	0					
-0.8 - -0.7001	0					
-0.7 - -0.6001	9	-0.1730	-0.16974	0.18174	2.17482	8.320
-0.6 - -0.5001	0					
-0.5 - -0.4001	44	0.0845	0.08124	0.20060	0.31176	3.259
-0.4 - -0.3001	109	-0.0616	-0.05837	0.19559	0.48301	1.848
-0.3 - -0.2001	136	-0.0260	-0.02272	0.16002	0.13482	0.592
-0.2 - -0.1001	121	-0.0379	-0.03461	0.15017	0.11689	0.447
-0.1 - -0.0001	114	0.0189	0.02214	0.11763	0.02017	-0.072
-0.0 - 0.0999	102	0.0315	0.03475	0.11180	0.04810	0.184
0.1 - 0.1999	78	0.0096	0.01286	0.12191	0.04198	0.161
0.2 - 0.2999	84	0.0343	0.03950	0.10218	0.23963	0.878
0.3 - 0.3999	57	0.0412	0.04444	0.06902	0.38079	1.457
0.4 - 0.4999	92	0.0476	0.05088	0.08786	0.55434	2.121
0.5 - 0.5999	40	0.0248	0.02811	0.08539	0.37441	1.432
0.6 - 0.6999	0					
0.7 - 0.7999	0					
0.8 - 0.8999	0					
0.9 - 0.9999	0					

END OF RUN 51 -POINT 28
 TERMINATED: STOP

SAMPLE 51.29
 SUCCESSFUL (TEMP) RESTORE RUNS1P29 AS (1F29)
 CANCELLED: USERNAME UNKNOWN

DATA OUTPUT FOR RUN 51 POINT 29

RAJIAL VELOCITY VS CONCENTRATION
 Z=152 MH AND R/R0=-0.075
 NO= 999 AND M4=980
 VBAR= -0.0074 MPS
 VRMS= 0.1460 MPS
 THIRD MOMENT OF TURBULENCE=-0.1105E-02 MFS**3
 THIRD CORRELATION COEFFICIENT= -0.3569
 FOURTH MOMENT OF TURBULENCE= 0.14492E-02 MFS**4
 FOURTH CORRELATION COEFFICIENT= 3.1909
 CBAR= 0.510Z
 CRMS= 0.288Z
 CVPBAR= 0.01624Z
 OVERALL TRANSPORT COEFFICIENT= 0.386500

CONDITIONAL SAMPLING RESULTS

CONCENTRATION FLUCTUATION	NUMBER OF OCCURRENCES	MEAN	RELATIVE MEAN	RMS	TRANSPORT COEFFICIENT	TRANSPORT RATIO
-1.0 - -0.9001	0					
-0.9 - -0.8001	0					
-0.8 - -0.7001	0					
-0.7 - -0.6001	0					
-0.6 - -0.5001	5	-0.1952	-0.18775	0.09425	2.29057	5.926
-0.5 - -0.4001	57	-0.1481	-0.14066	0.13368	1.48452	3.841
-0.4 - -0.3001	91	-0.0992	-0.09173	0.16993	0.75201	1.946
-0.3 - -0.2001	129	-0.0549	-0.04742	0.16459	0.79357	0.760
-0.2 - -0.1001	135	-0.0265	-0.01900	0.14487	0.07027	0.182
-0.1 - -0.0001	120	0.0090	0.01645	0.15040	-0.01064	-0.028
0.0 - 0.0999	98	0.0466	0.03406	0.10974	0.06949	0.180
0.1 - 0.1999	93	0.0256	0.03306	0.11737	0.10677	0.276
0.2 - 0.2999	72	0.0464	0.03384	0.08684	0.33413	0.465
0.3 - 0.3999	62	0.0525	0.06000	0.10360	0.52177	1.350
0.4 - 0.4999	53	0.0797	0.01719	0.04854	0.91474	2.418
0.5 - 0.5999	49	0.0453	0.05280	0.08075	0.68717	1.778
0.6 - 0.6999	14	0.0474	0.03488	0.05592	0.02968	2.147
0.7 - 0.7999	0					
0.8 - 0.8999	0					
0.9 - 0.9999	0					

END OF RUN 51 -POINT 29
 TERMINATED: STOP

SAMPLE 51.30
 SUCCESSFUL (TEMP) RESTORE RUNSIF30 AS (IF30)
 CANCELLED: DNAME RMS UNKNOWN

DATA OUTPUT FOR RUN 51 POINT 30

RADIAL VELOCITY VS CONCENTRATION
 Z=152 MM AND R/R0=-0.125
 NO. 999 AND N4=993
 VBAR= -0.0059 MPS
 VRMS= 0.1526 MPS
 THIRD MOMENT OF TURBULENCE=-0.63993E-03 MFS**3
 THIRD CORRELATION COEFFICIENT= -0.1800
 FOURTH MOMENT OF TURBULENCE= 0.15618E-02 MFS**4
 FOURTH CORRELATION COEFFICIENT= 2.8777
 CBAR= 0.410X
 CRMS= 0.258X
 CVPBAR= 0.016842
 OVERALL TRANSPORT COEFFICIENT= 0.427718

CONDITIONAL SAMPLING RESULTS

CONCENTRATION FLUCTUATION	NUMBER OF OCCURRANCES	MEAN	RELATIVE MEAN	RMS	TRANSPORT COEFFICIENT	TRANSPORT RATIO
-1.0 - -0.9001	0	-0.1455	-0.13962	0.14079	1.44858	3.434
-0.9 - -0.8001	0	-0.0936	0.08767	0.15426	0.75554	1.766
-0.8 - -0.7001	0	-0.0903	-0.08441	0.16366	0.53749	1.257
-0.7 - -0.6001	0	-0.0378	0.03187	0.14871	0.10998	0.757
-0.6 - -0.5001	0	-0.0199	-0.01407	0.13552	0.02015	0.047
-0.5 - -0.4001	17	0.0309	0.03679	0.14561	0.07540	0.176
-0.4 - -0.3001	83	0.0540	0.05994	0.11775	0.25478	0.596
-0.3 - -0.2001	138	0.0837	0.08965	0.10855	0.37089	0.867
-0.2 - -0.1001	164	0.0809	0.08681	0.09484	0.77300	1.807
-0.1 - -0.0001	171	0.1217	0.12763	0.09669	1.46247	3.419
0.0 - 0.0999	127	0.1044	0.11034	0.09560	1.53321	3.631
0.1 - 0.1999	77	0.1124	0.11836	0.05730	1.96129	4.715
0.2 - 0.2999	68	0.0680	0.07391	0.10726	1.42281	3.327
0.3 - 0.3999	59					
0.4 - 0.4999	39					
0.5 - 0.5999	27					
0.6 - 0.6999	18					
0.7 - 0.7999	5					
0.8 - 0.8999	0					
0.9 - 0.9999	0					

END OF RUN 51 -POINT 30
 TERMINATED: STOP

SAMPLE 51.31
 SUCCESSFUL (TEMP) RESTORE RUNSIP31 AS (TF31)
 CANCELLED! IDNAME RADS UNKNOWN

DATA OUTPUT FOR RUN 51 POINT 31

RADIAL VELOCITY VS CONCENTRATION
 Z=152 MM AND R/R0=-0.175
 NO= 999 AND N4=992
 UBAR= 0.0003 MFS
 VRMS= 0.1558 MFS
 THIRD MOMENT OF TURBULENCE=-0.97946E-03 MFS**3
 THIRD CORRELATION COEFFICIENT= -0.2589
 FOURTH MOMENT OF TURBULENCE= 0.17766E-02 MFS**4
 FOURTH CORRELATION COEFFICIENT= 3.0139
 CBAR= 0.329%
 CRMS= 0.239%
 CPVBAR= 0.016425
 OVERALL TRANSPORT COEFFICIENT= 0.440394

CONDITIONAL SAMPLING RESULTS

CONCENTRATION FLUCTUATION	NUMBER OF OCCURRENCES	MEAN	RELATIVE MEAN	RMS	TRANSPORT COEFFICIENT	TRANSPORT RATIO
-1.0 - -0.9001	0					
-0.9 - -0.8001	0					
-0.8 - -0.7001	0					
-0.7 - -0.6001	0					
-0.6 - -0.5001	0					
-0.5 - -0.4001	0					
-0.4 - -0.3001	63	-0.0998	-0.10009	0.14419	0.84180	1.957
-0.3 - -0.2001	159	-0.0892	-0.08954	0.17458	0.10622	1.177
-0.2 - -0.1001	174	-0.0338	-0.03417	0.14848	0.15194	0.345
-0.1 - -0.0001	162	-0.0165	0.01680	0.13329	0.03614	0.082
0.0 - 0.0999	151	0.0298	0.02947	0.14549	0.04386	0.100
0.1 - 0.1999	99	0.0463	0.04596	0.10797	0.18710	0.425
0.2 - 0.2999	64	0.1003	0.10000	0.12770	0.69159	1.570
0.3 - 0.3999	53	0.0889	0.08834	0.10224	0.83705	1.901
0.4 - 0.4999	29	0.1146	0.11426	0.10233	1.31801	3.038
0.5 - 0.5999	15	0.1595	0.15914	0.06916	2.35268	5.342
0.6 - 0.6999	13	0.1453	0.14498	0.06086	2.50372	5.685
0.7 - 0.7999	4	0.1510	0.15068	0.07156	2.95614	6.712
0.8 - 0.8999	5	0.1478	0.14748	0.04726	3.43373	7.796
0.9 - 0.9999	1	0.1830	0.18268	0.00000	4.50817	10.337

END OF RUN 51 -POINT 31
 TERMINATED: STOP

SAMPLE 51.32
 SUCCESSFUL (TEMP) RESTOKE KUN51P32 AS (TF32)
 CANCELLED: DUNAKE RMD5 UNKNOWN

DATA OUTPUT FOR RUN 51 POINT 32

RADIAL VELOCITY VS CONCENTRATION
 Z=152 MM AND R/R0=-0.225
 N0= 999 AND N4=991
 VBAR= 0.0151 MPS
 VARNS= 0.1795 MPS
 THIRD MOMENT OF TURBULENCE=-0.68932E-03 MFS**3
 THIRD CORRELATION COEFFICIENT= -0.1192
 FOURTH MOMENT OF TURBULENCE= 0.32729E-02 MFS**4
 FOURTH CORRELATION COEFFICIENT= 3.1532
 CBAR= 0.2372
 CRMS= 0.2142
 CPVPBAR= 0.016870
 OVERALL TRANSPORT COEFFICIENT= 0.439960

CONDITIONAL SAMPLING RESULTS

CONCENTRATION FLUCTUATION	NUMBER OF OCCURRENCES	MEAN	RELATIVE MEAN	RMS	TRANSPORT COEFFICIENT	TRANSPORT RATIO
-1.0 - -0.9001	0	-0.0768	-0.09197	0.19744	0.53364	1.213
-0.9 - -0.8001	0	-0.0430	-0.04010	0.17019	0.24565	0.538
-0.8 - -0.7001	0	-0.0028	-0.01798	0.15219	0.03985	0.091
-0.7 - -0.6001	0	0.0459	0.03072	0.13672	0.03778	0.131
-0.6 - -0.5001	0	0.0694	0.05430	0.14685	0.21981	0.500
-0.5 - -0.4001	0	0.1229	0.10771	0.13376	0.71971	1.436
-0.4 - -0.3001	0	0.1521	0.13692	0.11788	1.25570	2.854
-0.3 - -0.2001	184	0.1887	0.17357	0.12958	1.93597	4.194
-0.2 - -0.1001	208	0.1960	0.18085	0.08210	2.58491	5.875
-0.1 - -0.0001	186	0.1965	0.10131	0.12100	3.12991	7.114
0.0 - 0.0999	135	0.1965	0.22725	0.05032	4.40830	10.020
0.1 - 0.1999	125	0.2424	0.22725	0.00000	5.61926	12.772
0.2 - 0.2999	65	0.2300	0.21485	0.03100	5.20261	11.825
0.3 - 0.3999	30					
0.4 - 0.4999	21					
0.5 - 0.5999	18					
0.6 - 0.6999	11					
0.7 - 0.7999	5					
0.8 - 0.8999	1					
0.9 - 0.9999	2					

END OF RUN 51 -POINT 32
 TERMINATED: STOP

ORIGINAL PAGE IS
OF POOR QUALITY

SAMPLE 51,JJ
SUCCESSFUL (TEMP) RESTOKE KUNSF33 AS (TF33)
CANCELLED; DNAME RMD5 UNKNOWN

DATA OUTPUT FOR RUN 51 POINT 33

RADIAL VELOCITY VS CONCENTRATION
Z=152 MM AND R/R0=-0.275
NO= 999 AND N4=990
UBAR= 0.0343 MPS
VRMS= 0.1776 MPS
THIRD MOMENT OF TURBULENCE=-0.54516E-03 MFS**3
THIRD CORRELATION COEFFICIENT= -0.0973
FOURTH MOMENT OF TURBULENCE= 0.31653E-02 MFS**4
FOURTH CORRELATION COEFFICIENT= 3.1803
CBAR= 0.159%
CRMS= 0.185%
CPVPPBAR= 0.01237%
OVERALL TRANSPORT COEFFICIENT= 0.376874

CONDITIONAL SAMPLING RESULTS

CONCENTRATION FLUCTUATION	NUMBER OF OCCURANCES	MEAN	RELATIVE MEAN	RMS	TRANSPORT COEFFICIENT	TRANSPORT RATIO
-1.0 - -0.9001	0	-0.0197	-0.05399	0.17267	0.23771	0.631
-0.9 - -0.8001	0	0.0079	-0.02639	0.16743	0.04646	0.123
-0.8 - -0.7001	0	0.0558	0.02144	0.15291	0.03033	0.080
-0.7 - -0.6001	0	0.0905	0.05616	0.16972	0.25726	0.683
-0.6 - -0.5001	0	0.1477	0.11335	0.15813	0.91348	2.424
-0.5 - -0.4001	0	0.1564	0.12209	0.13704	1.24971	3.316
-0.4 - -0.3001	0	0.2300	0.19567	0.12846	2.69590	7.153
-0.3 - -0.2001	411	0.2206	0.18625	0.13035	3.13865	8.328
-0.2 - -0.1001	199	0.2412	0.20687	0.14030	4.14299	10.993
-0.1 - -0.0001	154	0.3230	0.28867	0.04900	6.65189	17.650
0.0 - 0.0999	95	0.1707	0.13634	0.08367	3.44102	9.130
0.1 - 0.1999	50	0.2190	0.18467	0.00000	5.06840	13.449
0.2 - 0.2999	36					
0.3 - 0.3999	22					
0.4 - 0.4999	12					
0.5 - 0.5999	5					
0.6 - 0.6999	2					
0.7 - 0.7999	3					
0.8 - 0.8999	1					
0.9 - 0.9999	1					

END OF RUN 51 -POINT 33
TERMINATED; STOP

SAMPLE 51, J4
 SUCCESSFUL (TEMP) RESTORE RUNSIF34 AS (TF34)
 CANCELLED: UNKNOWN ANDS UNKNOWN

DATA OUTPUT FOR RUN 51 POINT 34

RADIAL VELOCITY VS CONCENTRATION
 Z=152 MM AND R/R0=-0.325
 NO= 999 AND N4=994
 VBAR= 0.0410 MPS
 VRMS= 0.2030 MPS
 THIRD MOMENT OF TURBULENCE=-0.19230E-02 MF***
 THIRD CORRELATION COEFFICIENT= -0.2299
 FOURTH MOMENT OF TURBULENCE= 0.51567E-02 MFS***
 FOURTH CORRELATION COEFFICIENT= 3.0379
 CBAR= 0.101X
 CRMS= 0.146X
 CPVFBAR= 0.008284
 OVERALL TRANSPORT COEFFICIENT= 0.280485

CONDITIONAL SAMPLING RESULTS

CONCENTRATION FLUCTUATION	NUMBER OF OCCURRENCES	MEAN	RELATIVE MEAN	RMS	TRANSPORT COEFFICIENT	TRANSPORT RATIO
-1.0 - -0.9001	0	0.0383	-0.00273	0.17407	0.00887	0.032
-0.9 - -0.8001	0	-0.0002	0.04125	0.21527	0.11573	0.411
-0.8 - -0.7001	0	0.0623	0.02127	0.16709	0.03163	0.113
-0.7 - -0.6001	0	0.1036	0.06758	0.16616	0.34618	1.234
-0.6 - -0.5001	0	0.1883	0.14727	0.15694	1.24473	4.478
-0.5 - -0.4001	0	0.1528	0.11178	0.17292	1.36348	4.861
-0.4 - -0.3001	0	0.1954	0.15433	0.15990	2.79087	8.168
-0.3 - -0.2001	0	0.3380	0.29495	0.10591	5.44098	20.112
-0.2 - -0.1001	162	0.2712	0.23015	0.06351	4.98682	17.779
-0.1 - -0.0001	526	0.2662	0.22520	0.11280	5.96094	21.252
0.0 - 0.0999	124					
0.1 - 0.1999	86					
0.2 - 0.2999	41					
0.3 - 0.3999	35					
0.4 - 0.4999	8					
0.5 - 0.5999	3					
0.6 - 0.6999	5					
0.7 - 0.7999	4					
0.8 - 0.8999	0					
0.9 - 0.9999	0					

END OF RUN 51 -POINT 34
 TERMINATED: STOP

SAMPLE 51,35
 SUCCESSFUL (TEMP) KESTOKE KUN51F35 AL (1F35)
 CANCELLED: UNKNOWN RMS UNKNOWN

DATA OUTPUT FOR RUN 51 POINT 35

RADIAL VELOCITY VS CONCENTRATION
 Z=152 MM AND R/R0=-0.375
 N0= 999 AND N4=994
 UBAR= 0.0633 MPS
 URMS= 0.2114 MPS
 THIRD MOMENT OF TURBULENCE=-0.12811E-02 MFS**3
 THIRD CORRELATION COEFFICIENT= -0.1357
 FOURTH MOMENT OF TURBULENCE= 0.63522E-02 MFS**4
 FOURTH CORRELATION COEFFICIENT= 3.1830
 CBAR= 0.045X
 CRMS= 0.091X
 CFVFBAR= 0.003890
 OVERALL TRANSPORT COEFFICIENT= 0.202920

CONDITIONAL SAMPLING RESULTS

CONCENTRATION FLUCTUATION	NUMBER OF OCCURRENCES	MEAN	RELATIVE MEAN	RMS	TRANSPORT COEFFICIENT	TRANSPORT RATIO
-1.0 - -0.9001	0					
-0.9 - -0.8001	0					
-0.8 - -0.7001	0					
-0.7 - -0.6001	0					
-0.6 - -0.5001	0					
-0.5 - -0.4001	0					
-0.4 - -0.3001	0					
-0.3 - -0.2001	0					
-0.2 - -0.1001	0					
-0.1 - -0.0001	742	0.0399	-0.02334	0.20536	0.03489	0.172
0.0 - 0.0999	149	0.0932	0.02989	0.21901	0.11623	0.371
0.1 - 0.1999	58	0.1928	0.13249	0.20798	0.96715	4.766
0.2 - 0.2999	24	0.1589	0.07563	0.18007	1.00235	4.740
0.3 - 0.3999	13	0.2378	0.17456	0.16155	3.16566	15.600
0.4 - 0.4999	4	0.1322	0.06896	0.10879	1.61432	7.955
0.5 - 0.5999	3	0.2360	0.17271	0.03544	4.59791	22.659
0.6 - 0.6999	0					
0.7 - 0.7999	0					
0.8 - 0.8999	1	0.3660	0.30271	0.00000	13.95503	68.771
0.9 - 0.9999	0					

END OF RUN 51 -POINT 35
 TERMINATED: STOP

SAMPLE 51.36
 SUCCESSFUL (TEMP) RESTORE KUN5IP36 AS (TF36)
 CANCELLED: ROMAME RMD5 UNKNOWN

DATA OUTPUT FOR RUN 51 POINT 36

RADIAL VELOCITY VS CONCENTRATION
 Z=152 MM AND R/RO=-0.425
 NO= 999 AND N4=995
 VBAK= 0.0478 MPS
 VRMS= 0.2325 MPS
 THIRD MOMENT OF TURBULENCE=-0.34786E-02 MFS**3
 THIRD CORRELATION COEFFICIENT= -0.2767
 FOURTH MOMENT OF TURBULENCE= 0.84200E-02 MFS**4
 FOURTH CORRELATION COEFFICIENT= 2.8797
 CBAR= 0.028X
 CRMS= 0.047X
 CFVBAR= 0.002330
 OVERALL TRANSPORT COEFFICIENT= 0.150439

CONDITIONAL SAMPLING RESULTS

CONCENTRATION FLUCTUATION	NUMBER OF OCCURANCES	MEAN	RELATIVE MEAN	RMS	TRANSPORT COEFFICIENT	TRANSPORT RATIO
-1.0 - -0.9001	0					
-0.9 - -0.8001	0					
-0.8 - -0.7001	0					
-0.7 - -0.6001	0					
-0.6 - -0.5001	0					
-0.5 - -0.4001	0					
-0.4 - -0.3001	0					
-0.3 - -0.2001	0					
-0.2 - -0.1001	0					
-0.1 - -0.0001	726	0.0538	-0.01397	0.22602	0.01159	0.07
0.0 - 0.0999	206	0.0758	0.00800	0.23293	0.08273	0.550
0.1 - 0.1999	38	0.1849	0.11710	0.19293	1.09573	7.284
0.2 - 0.2999	14	0.2060	0.13820	0.20051	1.88663	12.541
0.3 - 0.3999	6	0.2677	0.19987	0.18156	4.24673	28.329
0.4 - 0.4999	2	0.2380	0.17020	0.04200	5.11706	34.014
0.5 - 0.5999	2	0.2960	0.27820	0.00600	7.73012	52.711
0.6 - 0.6999	1	0.1860	0.11870	0.00000	4.59791	30.564
0.7 - 0.7999	0					
0.8 - 0.8999	0					
0.9 - 0.9999	0					

END OF RUN 51 -POINT 36
 TERMINATED: STOP

1 Report No NASA CR-175035	2 Government Accession No	3 Recipient's Catalog No	
4 Title and Subtitle Influence of Large-Scale Motion on Turbulent Transport for Confined Coaxial Jets. Volume I - Analytical Analysis of the Experimental Data Using Conditional Sampling		5 Report Date January 1986	6 Performing Organization Code
		8 Performing Organization Report No None	10 Work Unit No
7 Author(s) David C. Brondum and John C. Bennett		11 Contract or Grant No NAG 3-350	13 Type of Report and Period Covered Contractor Report
		9 Performing Organization Name and Address The University of Connecticut P.O. Box U-139 Storrs, Connecticut 06268	
12 Sponsoring Agency Name and Address National Aeronautics and Space Administration Washington, D.C. 20546		14 Sponsoring Agency Code 505-31-42	
		15 Supplementary Notes Final report. Project Manager, C. John Marek, Altitude Wind Tunnel Project Office, NASA Lewis Research Center, Cleveland, Ohio 44135.	
16 Abstract The existence of large-scale coherent structures in turbulent shear flows has been well documented. Discrepancies between experimental and computational data suggest a necessity to understand the roles they play in mass and momentum transport. Using conditional sampling and averaging on coincident two-component velocity and concentration-velocity experimental data for swirling and nonswirling coaxial jets, triggers for identifying the structures were examined. Concentration fluctuation was found to be an adequate trigger or indicator for the concentration-velocity data, but no suitable detector was located for the two-component velocity data. The large-scale structures are found in the region where the largest discrepancies exist between model and experiment. The traditional gradient transport model does not fit in this region as a result of these structures. The large-scale motion was found to be responsible for a large percentage of the axial mass transport. The large-scale structures were found to convect downstream at approximately the mean velocity of the overall flow in the axial direction. The radial mean velocity of the structures was found to be substantially greater than that of the overall flow.			
17 Key Words (Suggested by Author(s)) Shear layers; Coaxial jets; Large scale coherent structures		18 Distribution Statement Unclassified - unlimited STAR Category 07	
19 Security Classif (of this report) Unclassified	20 Security Classif (of this page) Unclassified	21 No of pages 133	22 Price* A07